SOUTH CAROLINA DEPARTMENT OF NATURAL RESOURCES
MARINE RESOURCES RESEARCH INSTITUTE

Nuclear Magnetic Resonance (NMR) Metabolomics Developed Biomarkers for Rapid Evaluation of Fish Health and Feed Responses Using Transcriptomics

---

Final Report to the Soy Aquaculture Alliance

Executive Summary

Nuclear Magnetic Resonance (NMR) Metabolomics Developed Biomarkers for Rapid Evaluation of Fish Health and Feed Responses Using Transcriptomics

Aaron M. Watson[1], John W. Leffler[1], Dan Bearden[2], Gibson T. Gaylord[3], Frederic T. Barrows[4], Paul A. Sandifer[5], Michael R. Denson[1]

[1]South Carolina Department of Natural Resources, Marine Resources Research Institute, Charleston, SC
[2]National Institute of Standards and Technology, Hollings Marine Laboratory, Charleston, SC
[3]United States Fish and Wildlife Service, Fish Technology Center, Bozeman, MT
[4]United States Department of Agriculture – Agriculture Research Service, Fish Technology Center, Bozeman, MT
[5]National Oceanographic and Atmospheric Administration (retired, current – College of Charleston, Charleston, SC)

This study was designed to identify biomarkers that help determine the maximum level of soybean meal (SBM) that should be included in pelleted diets for red drum (*Sciaenops ocellatus)* before deleterious effects are detected. The hypothesis was that if increasing soy use results in decreasing performance or decreasing health indices, there would be corresponding changes in metabolite concentrations and changes in gene expression levels that could be used to determine optimum levels to be included in diets. We also hypothesized that the changes in metabolites and gene expression levels would occur before gross differences in weight or feed consumption were detected between experimental groups, allowing us to shorten the duration of future trials. To test these hypotheses we initiated two 12-week feeding trials with juvenile red drum. The first trial compared a commercial diet to 5 experimental diets containing increasing levels of SBM (0%, 15%, 30%, 45%, 60%). Over the course of the study, we sampled plasma, liver, intestine, and muscle tissue weekly from 6 individual fish from each treatment. We also analyzed feed consumption, final weight, feed conversion ratios, growth rate, condition factor, intestinal histology, and the metabolomes of plasma, intestine, liver, and muscle. We detected a statistically significant effect of SBM level on feed consumption, weight gain, and final weight. All experimental diets performed equivalently to the commercial reference diet, a noteworthy result since all experimental diets were 100% fishmeal free. Another important finding of the first trial was the significant decrease in hepatosomatic index (% liver weight to body weight) as SBM inclusion increased. These tissues were also used for nuclear magnetic resonance (NMR) metabolomics, an emerging technique for identifying and quantifying small, polar metabolites. During the first feeding trial, 1,872 individual samples were analyzed. This represents one of the largest and most extensive metabolomics studies ever reported on fish nutrition.

We compared all metabolites generated from nuclear magnetic resonance scans from tissues of fish fed the various diets and identified metabolites that were significantly different between diets. Neither plasma nor intestinal tissues revealed differences in overall metabolite concentrations over time during the 12-week trial, or between the graded levels of soy included in the diets. Liver and muscle tissues, however, do show significant differences over time and between dietary treatments. This might suggest that the overall metabolomes (concentration of various metabolites) were different in these tissues at the conclusion of the feeding trial, and

correlated with the traditional performance measures (growth, FCR etc.) which also showed negative effects as SBM inclusion increased.

Using publicly available software (MetaboAnalyst) and databases (KEGG) we were able to identify the serine, glycine, and threonine metabolic pathway as being the most affected, both through the number of affected metabolites and the importance of those metabolites within the pathway. Choline, betaine, and sarcosine were identified as three of the affected metabolites that all fell within a sequential portion of the metabolic pathway, with single enzymatic steps between 3-4 metabolites prior to the synthesis of glycine. This is critical as glycine is one of the primary inputs for gluconeogenesis, a process animals enter into during starvation, fasting, or periods of unbalanced nutrition. Knowing that all of our feeds meet the known protein, lipid, and amino acids requirements for red drum, this is a clear indication that diets with increasing levels of SBM still lacked some essential nutrient(s) or some unknown component was introduced with the SBM that prevented optimal ingestion, digestion, absorption, or utilization of an essential component. These metabolites and affected pathways were identified in both trials for liver tissues, and muscle analysis revealed evidence of catabolic processes, which corroborates the metabolomics results and confirms the hypothesis that these animals have entered into a non-growth optimal metabolic state where they are breaking down muscle tissue to acquire the needed components for energy production.

These findings confirm our hypothesis that a metabolic signature can be identified that indicates catabolism of muscle tissue at a threshold level of SBM inclusion. We were also able to determine that the metabolomes of these tissues stabilizes, or reaches an equilibrium after about 9 weeks into the feeding trial, much earlier than the conclusion of the feeding trial at 12 weeks. This provides a useful guideline for future studies of when to sample for dietary effects on metabolism under similar conditions. Prior to nine weeks, fish are still adjusting to the diet change and altering their metabolism based on the test diets and the metabolome earlier than this point may not be indicative of the final trajectory of changes caused by the treatment.

Utilizing the results of a separate red drum transcriptome sequencing project, we were able to design and test several sets of quantitative PCR probes and primers. Although more genes are discussed in the full report, choline dehydrogenase, dimethylglycine dehydrogenase, apolipoprotein IV, lanosterol 14-alpha demethylase, glucose-6-phosphate isomerase, and breast cancer anti-estrogen resistance all showed significant differences in expression level with increasing soybean level. These represent potential transcript biomarkers for SBM exposure with some beginning to show divergent expression levels only four weeks into the trial, several weeks before growth differences were detected and five weeks before the metabolomes began to stabilize.

From the performance indices at the conclusion of the first trial, we were able to determine that for the second feeding trial to examine practical dietary formulations, we could effectively include high levels (40-55%) of individual commercial soy products. We did observe a drop-off in performance when approaching 60% of the diet as SBM, however this level may not be practical for inclusion of a single ingredient to obtain balanced formulations. In light of this, for the second trial, we were able to examine four practical dietary formulations, each based on a commercially available soy protein concentrate. Pro-Fine VF, Nutraferma SPC, Nutrivance SPC, and HP 300 SPC were all included in individual experimental diets so that each ingredient supplied equivalent protein to the diet. We again used the 60% SBM diet as a reference for performance to compare to

the first trial. During this second trial we also included a reference diet of red drum's natural feed items fish, squid, and shrimp. This natural diet served as a positive control to represent the theoretical maximum performance possible as red drum grow very quickly. Comparing this treatment's tissue metabolomes and performance to high quality pelleted, experimental feeds will begin to help us close the gap and potentially begin to reverse engineer formulated feeds to better meet the optimal nutritional needs of juvenile red drum.

The second 12-week feeding trial was carried out with a different sampling regime based on the results from the first feeding trial. Analysis of the results showed that the fish fed the Nutraferma diet consumed significantly more pellets than the Pro-Fine treatment, although these two were not significantly different than the other 3 experimental treatments. Although there were significant differences observed in some whole body and fillet composition parameters, none were correlated to the differences observed in performance and are most likely representative of differences in the test ingredients. Gene expression assays from the second trial revealed no significant differences in gene expression between the experimental soy feeds, as expected for genes affected by soy level since the soy protein levels of the second experiment were very similar. There were some significant differences in gene expression between the experimental soy diets and the natural diet, further confirming the effect of soy on the metabolism of these fish.

Red drum appear to be highly tolerant to SBM inclusion, performing equivalently to a commercial diet from 0-60% inclusion levels in the first trial. The formulations for this study were also 100% fishmeal free, in itself a major step forward for increasing the sustainability and viability of aquaculture. Although feed consumption and growth were low, feed conversion ratios were comparable to or better than what has been reported in the literature, indicating that more success may be observed simply by improving the palatability of feeds that contain such high levels of plant ingredients.

Both the metabolomics and gene expression assay work identified candidate biomarkers for soy exposure, and further work with these datasets and tools that have been developed will assist in identifying the maximum amount of different soy proteins (meal, concentrate, etc) red drum can tolerate and will assist in identifying specific metabolites and dietary components that can be supplemented to prevent red drum from entering into the non-growth optimal gluconeogenic processes observed here that are apparent from levels of soy protein above 40%.

List of Tables

List of Figures

Final Report

Nuclear Magnetic Resonance (NMR) Metabolomics Developed Biomarkers for Rapid Evaluation of Fish Health and Feed Responses Using Transcriptomics

Aaron M. Watson[1], John W. Leffler[1], Dan Bearden[2], Gibson T. Gaylord[3], Frederic T. Barrows[4], Paul A. Sandifer[5], Michael R. Denson[1]

[1]South Carolina Department of Natural Resources, Marine Resources Research Institute, Charleston, SC
[2]National Institute of Standards and Technology, Hollings Marine Laboratory, Charleston, SC
[3]United States Fish and Wildlife Service, Fish Technology Center, Bozeman, MT
[4]United States Department of Agriculture – Agriculture Research Service, Fish Technology Center, Bozeman, MT
[5]National Oceanographic and Atmospheric Administration (retired, current – College of Charleston, Charleston, SC)

1.0 Introduction

Expansion of the soy industry into aquaculture feeds and the transition away from fishmeal-based proteins requires the aquaculture feed industry to accelerate testing of soy-based diets. Quantitative techniques that quickly characterize the physiological effects of fish diets are necessary to address this challenge. The objective of our proposed research is to use NMR-based metabolomics to identify diet-induced metabolic changes for which quick and cost-effective transcriptomic assays can be applied to efficiently address diet development.

Metabolomics is a systems approach of analyzing the biochemical profile of small metabolites (Samuelsson and Larsson, 2008; Schock et al., 2012). NMR-based metabolomic profiling is highly reproducible and allows for the analysis of complex bio-fluids and multiple tissue types. Since profiles between treatments can be compared to identify differences, metabolomics has potential as a powerful diagnostics tool, and is already being used as such in human medicine (Duarte et al., 2013). NMR metabolomics have been applied to aquaculture to examine the effects of pathogen challenges (Solanky et al., 2005), sewage exposure (Samuelsson et al., 2011), dietary manipulations (Schock et al., 2012; Watanabe et al., 2013 abstract), shrimp health (Schock et al., 2013), and fate of bioactive compounds (Martinez et al., 2005). Determining the physiological relevance of observed differences will reveal targets for simpler assay methods for early detection of future performance.

Transcriptomics, the study of gene expression profiles, is well suited to complement NMR metabolomics in the effort to identify suitable biomarkers and assay techniques. One such transcriptomic method, multiplexed quantitative PCR (q-PCR), is a rapid and cost effective tool for early identification of the relevant differences observed in transcriptomic profiles due to physiological responses and changes and can be used to confirm metabolomic observations. Multiplexed q-PCR allows for the simultaneous quantification of multiple gene targets within a single pathway or multiple pathways in response to dietary manipulations. These two techniques already have been combined with promising results in the medical and entomology fields (Knolhoff et al., 2013; Teets et al., 2012).

Differences in NMR-generated metabolomic profiles may be attributable to physiological responses to stress, dietary insufficiency, synthesis activity, or inflammatory processes as has been observed in the intestines of Atlantic salmon and carp when fed (vegetable-based) plant protein

diets (Chikwati et al., 2013; Sahlmann et al., 2013; Urán et al., 2008). Specific pathways that are up- or down-regulated in poor performing fish can be identified based on the metabolite differences observed in NMR profiles. Genes responsible for the regulation of those pathways can be targeted with q-PCR methods. In a similar fashion and based upon the pathways identified by the NMR method of determining changes in metabolite concentrations, q-PCR could rapidly determine the changes in gene transcript abundance that will be indicative of a specific metabolic trajectory, potentially weeks before observing growth or health differences (Figure 1). Similarly, the World Health Organization (WHO) utilizes PCR and q-PCR based techniques for the rapid identification of multiple pathogen types in humans including HIV, malaria, and influenza (WHO, 2013), well before physical symptoms arise.

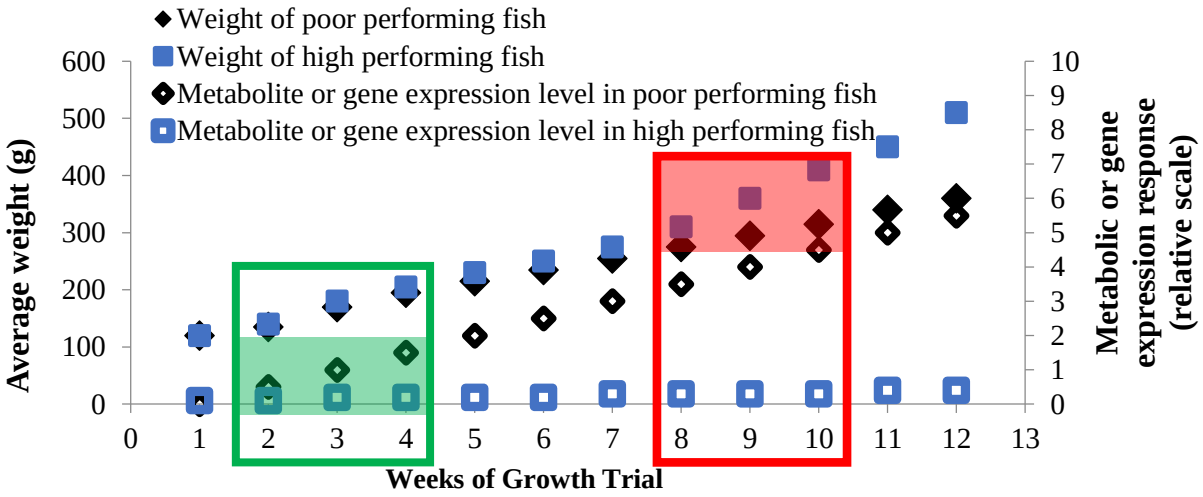

Figure 1. Conceptual diagram illustrating combined metabolomic and transcriptomic approaches. Green box represents the potential window of detection when utilizing metabolomic and transcriptomic approaches to identify metabolite and gene expression profiles. Red box represents the window of detection with traditional aquaculture measures (growth rate, feed conversion ratio, etc.). Shaded areas represent potentially significant differences detectable by the different methods. NMR metabolomic and transcriptomic profiles permit much earlier detection of deviations in performance trajectories.

For example, using NMR metabolomics Schock et al. (2013) observed a 314% increase in the concentration of nicotinate in the whole body tissue of shrimp following an ammonia spike in an intensive culture setting. Searching the KEGG (Kyoto Encyclopedia of Genes and Genomes) open-access database reveals four enzymes that can be responsible for nicotinate production; nicotinamidase, purine-nucleoside phosphorylase, uridine nucleosidase, and nicotinate phosphoribosyltransferase. The NCBI database can then be utilized to find species-specific mRNA sequences for those genes, and the open-access software Primer3 can be used to design multiplexed q-PCR probes and primers for all four genes. Such an approach would allow expression levels for all four genes to be monitored in tandem with nicotinate concentrations to both confirm the NMR profile data and potentially observe the very beginning stages of increasing expression of one or more of the four genes responsible, indicating an early response to increasing ammonia levels, prior to a potentially catastrophic spike. A similar process could be used to identify genes and design primers in stress response, inflammatory, or anabolic/catabolic pathways based on what is observed during the first phase of the study proposed here.

Several studies of liver and intestines have shown differences in gene expression in ion and amino acid transporters as well as immune responses in fish fed alternative protein source diets (Lilleeng et al., 2007; Luo et al., 2012; Sahlmann et al., 2013; Wacyk et al., 2012). Atlantic salmon,

Salmo salar, rapidly develop intestinal enteritis when fed diets containing soybean meal (SBM). Morphological and gene expression changes (fatty acid binding protein, regulators of T and B cell function, and other immune-related responses) in the intestines of Atlantic salmon have been documented after only a few days (Sahlmann et al., 2013; Venold et al., 2013) on diets with ~20% SBM. If these differences are indicative of future performance and the change in transcript abundance can be detected before gross physiological differences emerge, an early detection method could prove a valuable tool in diet and fish evaluation. Responses may differ significantly between fish within a treatment, which may indicate stronger genetic responses to stimuli, thus representing a potential selection tool for broodstock development as well.

Part of this project has been to attempt to identify genes that change in expression rapidly in relation to the overall changes in growth observed as soybean meal inclusion level increased. Quantitative PCR (q-PCR) is a very rapid, cost effective technique that can measure 1-4 target gene expression levels per reaction and analyze up to 30 samples on a single plate which can be prepped and run in just over an hour once all RNA samples have been extracted, quantified, and reverse transcribed to cDNA. Overall, even when dealing with hundreds of samples, gene expression can be analyzed over the course of a few days as opposed to weeks to months to analyze the total metabolome. We are aiming to use the untargeted, lengthy NMR metabolomics approach to assist in identifying what metabolites, metabolic pathways, and ultimately individual genes may be the keys to the overall physiological changes that occur. Identifying specific target genes that can be analyzed weeks into a feeding trial, as opposed to gross growth metrics potentially months into a feeding trial, could speed up diet and ingredient evaluations. Paired with the overall metabolomics derived from multiple tissues, gene expression assays will assist in understanding the physiology and why different diets perform differently so that targeted approaches to improve feeds can be designed.

The biggest drawback to gene expression analysis is having access to the messenger RNA (mRNA) sequence to design the needed primers and probes from for each gene. These are species specific sequences and the largest publicly accessible databases rarely have more than a handful of sequences for non-model species. Although genome sequencing and transcriptome sequencing are becoming more popular, cheaper, and more accessible, at the time this project was undertaken, there was not a large sequence database for red drum. We were able to sequence the transcriptome of liver, intestine, and brain tissue of red drum from the first trial of this project through separately acquired funding. This has not only given us the sequence database of thousands of genes we need to complete targeted gene expression assays, but since the samples for sequencing came from our 0% SBM and 60% SBM treatments, we were able to conduct some preliminary transcript abundance measurements to assess any gross differences in transcript abundance (potentially directly related to expression levels) between these two treatments as one way to identify target genes.

We proposed red drum as an excellent model species because of its relatively high tolerance to SBM and accompanying anti-nutritional factors (ANFs). Identifying responses to ANFs has challenged NMR metabolomics to identify subtle physiological responses that are more readily observed in species with a much lower tolerance like salmon. In addition, NMR spectra have been established by our research team for juvenile red drum on a variety of diets and feeding regimes through previous studies. Samples were taken weekly to permit high resolution metabolomic trajectories to be plotted and the earliest possible detection of potentially negative impacts as

trajectories diverge. We have utilized these profiles as benchmarks for early detection of changes in concentrations of various metabolites that, when compared to the known trajectories, will provide indicators of future performance. Identification and characterization of such indicators could significantly shorten the time required for growth trials, allowing more rapid analysis of any number of dietary variables once the longer-term profiles are established. Drawbacks to wide implementation of NMR screening include the capital costs of equipment and facilities, specialized scientific expertise required, and extended data processing time. These limit availability of this methodology to NMR-equipped laboratories which are generally not available to diet evaluators and aquaculture operations. However, utilizing NMR metabolomics technology to discover and identify biomarkers that would otherwise go undetected can be exceptionally useful. Therefore, coupling NMR-generated metabolomic trajectories with specific biomarkers that can be assayed with the faster and cost-effective methods, such as q-PCR, to detect early performance potential will become an invaluable tool-set for the research and production efforts of the global aquaculture community, resulting in reduced time and costs of diet evaluation.

Growth trials to evaluate dietary formulations can be time consuming and expensive especially as the inclusion rates and varieties of expensive, highly processed ingredients for aquaculture feeds continue to increase. Methods need to be developed to lower the costs and durations of feed trials. NMR-based metabolomic profiles and trajectories from growth trials provide insights into which metabolites and pathways are indicators of poor performance of fish fed experimental diets (i.e. effects of ANFs), and with weekly sampling, the timeframe of departures from desired performance trajectories can be identified. The ability of the NMR technique to quantify and profile dozens of metabolites simultaneously will identify compounds as biomarkers that would otherwise go undetected in traditional sampling techniques. Simpler, faster and more cost-effective q-PCR methods can be developed from the NMR data to significantly reduce the time and costs of diet evaluation. The first phase of this study worked towards identifying the threshold and responses of red drum to standard solvent extracted soybean meal. The second phase developed rapid transcriptomic (multiplexed q-PCR) assays for the early detection gene expression changes indicative of future performance. The third phase evaluated the transcriptomic approach as well as an evaluation of practical feeds for juvenile red drum containing high quantities of more refined soy protein concentrate ingredients.

2.0 Material and Methods for first trial

2.1 Diets

A 12 week feeding trial was conducted with juvenile red drum (47g) utilizing five levels of standard hexane extracted SBM (0-59g $100g^{-1}$ diet) and a standard commercial diet (45% protein, 16% lipids) which has been used in previous SCDNR-NIST collaborative metabolomic studies as a reference for comparison between experiments. Formulations of the diets are provided in table 1. Wheat flour, corn protein concentrate and poultry meal were decreased as SBM increased to keep diets isonitrogenous and menhaden oil increased with increased SBM to ensure isolipidic diets. Lysine and Threonine supplementation were gradually reduced with elevating SBM to account for higher concentrations of these amino acids in SBM.

Table 1. Composition of experimental diets for juvenile red drum fed varying levels of soybean meal (Trial 1).

Grams 100 grams^{-1}	SBM 0%	SBM 15%	SBM 30%	SBM 45%	SBM 60%
Soybean meal (SBM) [a]	0.00	14.75	29.50	44.25	59.00
Corn protein conc. [b]	18.10	13.57	9.04	4.51	0.00
Poultry meal [c]	18.10	13.57	9.04	4.51	0.00
Wheat flour [d]	36.42	30.36	24.28	18.10	12.00
Menhaden oil [e]	10.20	11.00	11.75	12.50	13.25
Squid meal [f]	4.08	4.08	4.08	4.08	4.08
Blood meal [g]	5.00	5.00	5.00	5.00	5.00
Lysine HCl	2.40	2.05	1.80	1.55	1.30
DL-Methionine	0.60	0.64	0.68	0.72	0.75
Threonine	0.80	0.68	0.58	0.48	0.38
Mono-Dical phosphate	2.40	2.40	2.40	2.40	2.40
Vitamin premix [h]	1.00	1.00	1.00	1.00	1.00
Choline CL	0.60	0.60	0.60	0.60	0.60
Vitamin C [i]	0.20	0.20	0.20	0.20	0.20
Trace min premix [j]	0.10	0.10	0.10	0.10	0.10
Formulated Composition, % as-is					
Crude Protein	40.6	40.4	40.3	40.2	40.1
Lipid	14.0	14.0	14.0	14.0	14.0
Phosphorus	0.92	0.91	0.91	0.91	0.91

[a] ADM, 468 g/kg crude protein.
[b] Cargill, Empyreal 75, 756 g/kg crude protein.
[c] IDF Inc., 832 g/kg protein.
[d] Manildra Milling, 120 g/kg crude protein.
[e] Omega Proteins Inc., Virginia Prime menhaden oil .
[f] Wilbur-Ellis, 813 g/kg protein.
[g] Wilbur-Ellis, 892 g/kg protein.
[h] ARS 702; contributed, per kg diet; vitamin A 9650 IU; vitamin D 6600 IU; vitamin E 132 IU; vitamin K3 1.1 gm: thiamin mononitrate 9.1 mg; riboflavin 9.6 mg; pyridoxine hydrochloride 13.7 mg; pantothenate DL-calcium 46.5 mg; cyancobalamin 0.03 mg; nicotinic acid 21.8 mg; biotin 0.34 mg; folic acid 2.5 mg; inostitol 600 mg.
[i] Stay-C, 35%, DSM Nutritional Products.
j Contributed in mg/kg of diet; manganese 13; iodine 5; copper 9; zinc 40.

2.2 Fish and Experimental Design

Captive, wild red drum broodstock were volitionally spawned at the Marine Resources Research Institute (MRRI) in Charleston, South Carolina by South Carolina Department of Natural Resources (SCDNR) personnel. Larval fish from a single unique genetic family were transported and stocked into earthen ponds at the Waddell Mariculture Center (WMC) in Bluffton, South Carolina in the fall of 2013. Fish were then transported back to the MRRI in the spring of 2014 and cultured in a recirculating aquaculture system consisting of twenty-four, 1,600 liter tanks utilizing sand filters, fluidized bed filters, and protein fractionation for mechanical and biological filtration and UV sterilizers. Fish were fed to apparent satiation twice daily with a standard commercial feed containing 40% protein and 10% lipids and excess feed was removed from tanks after ten minutes of no visible feeding. Fish were acclimated to 25°C over a period of one week at 1°C day^{-1} and held at a salinity of 30-32 mg L^{-1}. These conditions remained constant until a 45g per fish mean was obtained to begin the feeding trial.

At the beginning of the feeding trial (May 25, 2014), ten fish were euthanized using tricaine methanesulfonate (MS-222,Argent Labs) at a concentration of 500 mg L^{-1} buffered with sodium bicarbonate for subsequent analysis of whole-body and fillet composition (DM, CP, lipids, ash, gross energy, minerals). Twenty-five fish per tank were stocked into each tank with a mean weight of 46.88 ± 1.82g. The six diets were randomly assigned to four tanks per treatment. Treatments were split into 2 groups (A and B), which were alternated for sampling every week to minimize handling stress. All tanks were batch weighed on Day 0 and three fish per tank were randomly selected and sacrificed from group A-tanks for initial body and eviscerated weights and lengths. Using a syringe with a 22 gauge needle, 1 to 2 ml of blood from the fish caudal vasculature were collected into Li heparin collection tubes and gently inverted 8 times. The collection tubes were rapidly placed on ice. Blood samples were then centrifuged at 2000xg at 4°C for 6 min. The top layer (plasma) was transferred into 2 ml cryovials, flash frozen in liquid nitrogen and stored at -80°C. After blood was drawn fish were euthanized with an overdose of MS-222 for 3 min prior to dissection. Intestine tissue extended from just posterior to the pyloric caeca to just anterior to the anus was excised, sliced lengthwise to open, and rinsed clean with cold 3% saline solution. The entire liver was excised and similarly rinsed. These two tissues were placed into separate, labeled 5 ml cryovials, flash frozen in liquid nitrogen, and stored at -80°C. The fish were then fully eviscerated, weighed again for carcass weight, and the one consistent fillet removed. Muscle punch samples removed from the fillet, 4-6 per individual, were collected, placed in 5 ml cryovials, flash frozen in liquid nitrogen, and stored at -80°C.

Tank batch weights and tissue sampling the following week (Day 7) only included the B-tanks. This pattern continued every week until the conclusion of the 12-week feeding trial. On Day 0, fish were transitioned to experimental diets and fed to apparent satiation twice daily or once daily on weekends and total weight consumed recorded. Any excess feed was removed from the system after 10 minutes by siphon and a 25% water exchange was completed weekly after tank cleaning using settled, polished water from Charleston Harbor. Water temperature, dissolved oxygen, pH and salinity were recorded three times per week on a subset of tanks (n= 12 tanks/sampling) and ammonia, nitrite and nitrate measured weekly (n= 12 tanks/week) using Hach spectrophotometer reagents. Additional fish (n=10 fish/treatment) were sacrificed at the conclusion of the 12-week growth trial for whole-body and fillet composition. Proximate analysis of the whole body and fillet samples was performed by Clemson University Feed and Forage Laboratory, Clemson, South Carolina.

2.3 Histological Sampling

The distal section of the small intestine was removed from three fish per tank (n=6 fish/treatment) during weekly sampling events and preserved in 10% neutral buffered formalin. Preserved samples were processed using standard histological techniques before being embedded in paraffin wax (Humanson 1972). Three cross sections per sample were mounted on glass slides and stained using hematoxylin and eosin-y. Two replicates per tank (n=4 fish/treatment) from weeks 0, 3, 6, 9 and 12 were randomly chosen and images were obtained using Jenoptik ProgRes SpeedXT core 5 digital camera mounted on a Nikon Eclipse 55i compound microscope at 10x. Mucosal fold height (n=4 fish/treatment/time point) and area of the lamina propria (LP) within the

mucosal fold (n=2 fish/treatment/time point) were measured using I-Solution imaging software. Ten measurements of each parameter per fish were obtained. Qualitative assessment of intestinal morphology was used to determine signs and severity of inflammation. Intestinal morphology was determined using criteria developed by Baeverfjord and Krogdahl (1996): 1) widening and shortening of the mucosal fold 2) loss of supranuclear vacuolization within the enterocytes of the epithelium 3) widening of lamina propria and increase in connective tissue of the intestinal fold 4) infiltration of inflammatory cells primarily lymphocytes and granulocytes in the mucosal folds.

2.4 NMR Metabolomics Sample Preparation, Data Collection and Spectroscopy

Frozen plasma samples were thawed on ice for ~ 2 hours. 350 µl of plasma per sample were loaded onto spin filters (3 kDa molecular weight cutoff) that were previously washed in DI water overnight. Filters were then centrifuged at 10,000xg, at 4°C for 90 min and for up to two times an additional 30 min for samples that provided less than 200 µl of filtrate. 200 µl of filtrate was transferred into Eppendorf tubes and 400 µl of NMR buffer was added to each sample to a final volume of 600 µl. The samples were then vortexed for a few seconds and centrifuged. 550 µl of the resulting solution was transferred into 5 mm NMR tubes.

The total water content of each tissue (liver, muscle, intestine) was determined prior to this experiment to determine appropriate solvent volumes. The average weights of wet tissues were used to calculate the solvent volumes used for extraction. In each extraction set, seven or eight experimental samples along with QC materials were extracted using a slightly modified Bligh-Dyer bi-phasic solvent system. The QC samples used during tissue preparation were appropriate pooled tissues: control materials and NIST SRM 1946 – Lake Superior Fish Tissue. A cold polar solvent mixture, methanol (4 mL g^{-1} wet weight, henceforth 'gww') (Honeywell) and Millipore water (1.6 mL g^{-1} ww), was added to the frozen homogenate sample in the ceramic bead tube. The tissues/polar solvents were mixed using a Precellys 24 homogenizer (Bertin Technologies) in two cycles of 15 s at 6500 rpm. The whole homogenate was transferred to a glass vial containing cold chloroform (4 mL g^{-1} ww) (Fisher Scientific) and Millipore water (2 mL g^{-1} ww) for a final solvent volume ratio of 2 chloroform: 2 methanol: 1.8 water. The mixture was vortexed for 30 s and incubated on ice for 10 min. The solvent phases were partitioned by centrifugation at 2000 x g_n at 4 °C for 5 min. The upper polar phase was collected into a 1.5 mL Eppendorf tube, and dried by vacuum centrifuge for 2 hours at room temperature (Eppendorf, Vacufuge). Dried polar extracts were re-hydrated with 600 µL of NMR buffer, and 550 µL of each sample was then transferred into 5 mm NMR tubes for analysis.

Approximately 1760 samples (5 experimental diets with graded SBM inclusion plus a pelleted reference diet; intestine, liver, plasma, muscle, quality control) were prepared and analyzed by NMR. Preliminary analysis of these results advised the sample collection and analysis protocols for trial 2. In addition, NMR spectra such as ^{13}C-HSQC and TOCSY experiments were collected on selected samples to aid compound identification.

All spectra were obtained at a temperature of 298 K on a Bruker Advance II 700 MHz NMR spectrometer (Bruker Biospin, Inc., Billerica, MA) equipped with a cryoprobe (TCI 5 mm triple-resonance, z-gradient). Spectra were collected under full automation using ICON-NMR with a standard 1D pulse sequence (noesygppr1d). The NMR protocol included 10 minutes for

temperature equilibration, automated shimming with on-axis and off-axis shims, automated probe tuning and pulse calibration on each individual sample. ^{1}H spectra were acquired with 65536 real data points across a spectral width of 20 ppm with 8 steady state scans, 80 transients, a 3 s relaxation delay, a 60 ms mixing period and an acquisition time of 2.34 s for a total repetition time (D1 + AQ) of 5.34 s. The spectra were Fourier transformed after multiplying the free induction decay by an exponential line broadening function of 0.3 Hz and zero-filling to 65536 complex points. The spectra were manually phased, and the baseline was automatically corrected with a fifth order polynomial. For the trial 1 samples, additional spectra were acquired under similar parameters including CPMG, 2D JRES and PURGE water suppression, giving an NMR protocol duration of approximately 60 minutes per sample.

Two-dimensional edited ^{13}C heteronuclear single quantum correlation (HSQC) spectra with adiabatic ^{13}C decoupling (hsqcedetgpsisp2.2) were collected on selected samples to enable improved metabolite identification. In general, 128 scans and 2048 data points with 512 increments were acquired with spectral widths of 11 ppm in F2 and 180 ppm in F1 (^{13}C). A relaxation delay equal to 1.5 s was used between acquisitions, and a refocusing delay corresponding to a 145 Hz $^{1}J_{C\text{-}H}$ coupling was used. The FIDs were weighted using a shifted sine-square function in both dimensions. Manual two-dimensional phasing was applied; all spectra were referenced to the TMSP internal standard at 0.00 ppm for ^{1}H and ^{13}C.

Selected samples were also used for 2-dimensional Total Correlation Spectroscopy (TOCSY) analysis to elaborate the ^{1}H-^{1}H coupling networks for compound identification. A phase-sensitive TOCSY with a DIPSI2 mixing sequence (90 ms duration) and water suppression via pre-saturation and excitation sculpting (dipsi2esgpph) was used for this. In general, 48 scans and 2048 data points with 256 increments were acquired with spectral widths of 10 ppm in F1 and F2. A relaxation delay equal to 1.5 s was used between acquisitions. The FIDs were weighted using a shifted sine-squared function in both dimensions, and the data was Fourier transformed to 4096 by 1024 complex points by zero filling. Manual two-dimensional phasing was applied; all spectra were referenced to the TMSP internal standard at 0.00 ppm for ^{1}H.

2.5 NMR Spectral Analysis, Multivariate Analysis and Quality Control

Metabolites were identified based on 1D ^{1}H, 2D ^{1}H-^{1}H TOCSY and 2D ^{1}H-^{13}C HSQC NMR experiments. Identities were based on comparison of chemical shifts and spin-spin couplings with reference spectra and tables noted in published reports, the Human Metabolome Database (HMDB), the Biological Magnetic Resonance data bank (BMRB), an in-house compiled spectrabase and Chenomx® NMR Suite profiling software (version 8.1). Metabolite identification most often was achieved at a Level 2, putative identification level (Sumner et al. 2007).

For multivariate analysis, the spectra were binned with a bin size of 0.005 ppm between 0.2 ppm and 10.0 ppm and certain spectral regions were excluded because of spectral artifacts due to water suppression or because of contaminants that appeared in our blank sample spectra. Spectra were checked for uniform referencing and baseline condition and normalized to constant total spectral intensity after binning and exclusions. Generally, principal component analysis (PCA) was conducted on appropriate subsets of the data with appropriate class labeling of the subsets to aid in visual pattern recognition. Pareto normalization with mean centering of the bins was used

in all cases to account for the sometimes wide dynamic range of spectral feature intensity. PCA scores plots were assessed for meaningful groupings and groups were assessed for significant differences using ± 1 standard error of the mean (SEM) error bars and Student's t-tests.

Quality control materials were used during this study to ensure the reproducibility of the sample processing method. Red Drum Fillet Control Material (RD-FCM) and Liver Control Material (LCM) were prepared by pooling homogenized fillet or liver samples collected during the preliminary studies. NIST SRM 1946– Lake Superior Fish Tissue and pooled tissue control materials were extracted along with both liver and muscle test samples. Along with the test plasma samples, NIST standard reference materials SRM 1950–Human plasma and Red Drum Control Plasma (RDCP) were processed. Control plasma was prepared by pooling the extra red drum plasma samples collected during the previous studies. In addition to SRM and pooled control materials, experimental samples were prepared in triplicates or duplicates as technical replicates. Blanks which do not contain any tissue were prepared to test for contamination during sample processing.

2.6 Gene Expression Assays

Sub-samples of tissue from sample preparation for the metabolomics analyses were utilized for gene expression assays. These consisted of aliquots of homogenized liver stored at -80°C. Four of six individual fish sampled at each time point for each dietary treatment from the first trial were used for gene expression analyses and samples from the even numbered weeks were analyzed. RNA was extracted via a standard phenol/chloroform extraction, dried and reconstituted in 50 µl water, and quantified using a Qbit™ fluorometer. 1000 ng of RNA from each sample was used in a reverse transcription reaction (iScript RT Supermix, Bio-Rad, Hercules, CA, USA) and diluted to 10 ng μl^{-1}. Genes selected based on the metabolomics results (Table 2.) were analyzed individually using Sso Advanced SYBR Green (Bio-Rad, Hercules, CA, USA) with 800 µmolar primer concentrations in 10 µl reaction volumes. Genes selected based on the transcriptomic sequencing were analyzed in two multiplexed reaction sets using iQ Multiplex Powermix (Bio-Rad, Hercules, CA, USA) with 800 µmolar primer and 400 µmolar probe concentrations in 10 µl reaction volumes (Tables 3 and 4). Elongation factor 1-alpha (EF1A) was used as a common reference gene across all q-PCR panels. All samples were run with 10 ng total RNA in triplicate on a Bio-Rad CFX96 Touch Real Time PCR Detection system (Bio-Rad, Hercules, CA, USA). Currently all plots and statistics have been run solely within the Bio-Rad CFX manager software.

Table 2. Genes selected based on comparative metabolomics results.

Gene Name	Primer Sequence	Tm (°C)
Lactate Deydrogenase (LacDh) Forward	5'-CGATCTTGGAGGTCTTGAGG-3'	59.80
Lactate Dehydrogenase (LacDh) Reverse	5'-CCCAGGAACAAGGTGACTGT-3'	60.00
Sarcosine Dehydrogenase (SarDh) Forward	5'-GAGTCGAGAGGTGCTTCAGG-3'	60.14
Sarcosine Dehydrogenase (SarDh) Reverse	5'-GGTAGACTGGCAGGCAAGAG-3'	60.01
Dimethylglycine Dehydrogenase (DmgDh) Forward	5'-ATATCCGCGACATTTTGGAG-3'	59.92
Dimethylglycine Dehydrogenase (DmgDh) Reverse	5'-ACTTGGGTCTTGACCTGTGG-3'	60.00
Betaine Homocysteine Methyltransferase (BHMT) Forward	5'-CAGCACAAAGAAGCAACCAG-3'	59.63
Betaine Homocysteine Methyltransferase (BHMT) Reverse	5'-CCAAACGTAACTGGGGAAGA-3'	59.96
Choline Dehydrogenase (ChDh) Forward	5'-CGGGGATGTCAAGTTGTTTT-3'	59.83
Choline Dehydrogenase (ChDh) Reverse	5'-GATCCTGTTTGATGGCAACC-3'	60.33
Elongation Factor 1-alpha (EF1A) Forward	5'-GCTCGTTTCGAGGAAATCAC-3'	59.82
Elongation Factor 1-alpha (EF1A) Reverse	5'-CATCCCTTGAACCAGCTCAT-3'	60.07

Table 3. Genes selected for multiplexed q-PCR panel #1 based on transcriptome sequencing and comparative abundance between 0% SBM and 60% SBM diets.

Gene Name	Primer Sequence	Tm (°C)
Lanosterol 14-alpha Demethylase (L14AD) Forward	5'-TCTTTGGTCTCTGCCTCGAT-3'	59.95
Lanosterol 14-alpha Demethylase (L14AD) Reverse	5'-GACTGACCACTCCGGTGTTT-3'	60.01
Lanosterol 14-alpha Demethylase (L14AD) Probe	5'-Cy55-AAAGACGGGGTTGGGGACAT-IAbrQSp-3'	64.87
Apolipoprotein A-IV (APOA4) Forward	5'-TGAGGCAAGGTGACAACAAG-3'	59.87
Apolipoprotein A-IV (APOA4) Reverse	5'-CAGCAAGGACCTTCATGGTT-3'	60.11
Apolipoprotein A-IV (APOA4) Probe	5'-6-FAM-CCAAGTGCTCCCAGGTGGAC-IABkFQ-3'	65.30
Elongation of Very Long Chain Fatty Acids 1 (EVLOV1) Forward	5'-CTTCGTGCTGAGGAAAAAGC-3'	60.13
Elongation of Very Long Chain Fatty Acids 1 (EVLOV1) Reverse	5'-CATGATCACGTGGACGGTAG-3'	59.98
Elongation of Very Long Chain Fatty Acids 1 (EVLOV1) Probe	5'-HEX-TTCCTATGCCCCTGGTGGAA-IABkFQ-3'	64.81
Squalene Synthase (SQS) Forward	5'-CACCCGGAGGAGATACTCAA-3'	60.07
Squalene Synthase (SQS) Reverse	5'-GCTTGAATCACAGCTGCAAA-3'	60.14
Squalene Synthase (SQS) Probe	5'-TYE665-CCAAACCAGCCGGAGTTTTG-IAbRQSp-3'	64.90
Elongation Factor 1-alpha (EF1A) Forward	5'-GCTCGTTTCGAGGAAATCAC-3'	59.82
Elongation Factor 1-alpha (EF1A) Reverse	5'-CATCCCTTGAACCAGCTCAT-3'	60.07
Elongation Factor 1-alpha (EF1A) Probe	5'-TEX615-ATGGCACGGAGACAACATGC-IAbRQSp-3'	64.80

Table 4. Genes selected for multiplexed q-PCR panel #2 based on transcriptome sequencing and comparative abundance between 0% SBM and 60% SBM diets.

Gene Name	Primer Sequence	Tm (°C)
Thioredoxin (TXN) Forward	5'-CAAAGCACTGAAGCCCAAAT-3'	60.25
Thioredoxin (TXN) Reverse	5'-GGGATCGAGGAAAAGAATCC-3'	59.84
Thioredoxin (TXN) Probe	5'-6-FAM-AAGCCTACAGCCCCGATGGT-IABkFQ-3'	65.22
Glucose-6-Phosphate Isomerase (G6PI) Forward	5'-GGAACGTTCTGATCCAGAGG-3'	59.65
Glucose-6-Phosphate Isomerase (G6PI) Reverse	5'-GACTGGGTTGGAGGTCGTTA-3'	59.97
Glucose-6-Phosphate Isomerase (G6PI) Probe	5'-HEX-ACGTGCAGAGCGATGGACAG-IABkFQ-3'	64.94
Breast Cancer Anti-Estrogen Resistance (BCAR) Forward	5'-CTGGCAACCGTCTCAAGATT-3'	60.25
Breast Cancer Anti-Estrogen Resistance (BCAR) Reverse	5'-AGGTGTTGGTTTGGCGTAAG-3'	60.03
Breast Cancer Anti-Estrogen Resistance (BCAR) Probe	5'-Cy55-CGGATCCAGTCGCTTCCTGT-IAbRQSp-3'	64.90
Lysozyme (LYZ) Forward	5'-CACCAGAGCCACCAACTACA-3'	59.74
Lysozyme (LYZ) Reverse	5'-ATCGCCACACTGACATCATC-3'	59.51
Lysozyme (LYZ) Probe	5'-TYE665-CACATCCAGTGCAGCCAGCT-IAbRQSp-3'	64.94
Elongation Factor 1-alpha (EF1A) Forward	5'-GCTCGTTTCGAGGAAATCAC-3'	59.82
Elongation Factor 1-alpha (EF1A) Reverse	5'-CATCCCTTGAACCAGCTCAT-3'	60.07
Elongation Factor 1-alpha (EF1A) Probe	5'-TEX615-ATGGCACGGAGACAACATGC-IAbRQSp-3'	64.80

2.7 Calculations and Statistical Analyses

Standard performance parameters utilized in this feeding trial to compare treatments were:

- Weight gain, % = (final weight − initial weight) / initial weight ∗ 100
- Specific growth rate, SGR = ln (final weight − initial weight) / days ∗ 100)
- Protein efficiency ratio, PER = grams weight gained / grams protein fed
- Feed conversion ratio, FCR = grams fed / grams weight gained
- Condition factor, K = (weight (g) ∗ 100) / (length $(cm)^3$)
- Hepatosomatic index, HSI = (liver weight / body weight) * 100

The effects of experimental treatments were compared using a linear regression model within R statistical software (v3.0.2, R Core Team, 2013) to examine the effects of the graded levels of SBM with significance set to P = 0.05.

3.0 Results from first trial

3.1 Diets

Proximate composition of the experimental diets as well as the commercial reference are shown in table 5.

Table 5. Proximate composition of diets for first feeding trial (Clemson University analyses).

	SBM 0%	**SBM 15%**	**SBM 30%**	**SBM 45%**	**SBM 60%**	**Commercial**
Crude protein (g $100g^{-1}$)	46.3	45.1	44.4	43.5	42.5	44.5
Fiber (ADF) (g $100g^{-1}$)	5.5	4.6	6.7	6.5	9.5	4.4
Crude fiber (g $100g^{-1}$)	4.4	3.7	5.3	5.2	7.6	3.5
Crude fat (g $100g^{-1}$)	11.9	12.4	12.8	12.6	13.8	15
Ash (g $100g^{-1}$)	4.9	5.1	6.1	6.2	6.8	8.5
Dry matter (g $100g^{-1}$)	94.7	96.1	96.2	97.4	96.3	97.6
Energy (Kcal Kg^{-1})	3724	3783	3736	3743	3704	3893
Phosphorous (g $100g^{-1}$)	0.99	0.97	0.94	1.05	1.01	1.25
Potassium (g $100g^{-1}$)	0.2	0.5	0.74	1.13	1.35	0.65
Calcium (g $100g^{-1}$)	1.03	0.98	0.9	0.94	0.87	2
Magnesium (g $100g^{-1}$)	0.08	0.12	0.15	0.21	0.23	0.16
Sulfur (g $100g^{-1}$)	0.64	0.62	0.58	0.61	0.54	0.58
Zinc (ppm)	155	146	137	202	140	124
Copper (ppm)	26	28	27	45	31	53
Manganese (ppm)	50	52	53	21	66	92
Iron (ppm)	615	593	558	729	617	872

3.2 Feeding Trial

Water quality parameters as monitored during the 12 week feeding trial are show in table 6, all parameters were maintained within optimal ranges for juvenile red drum.

Table 6. Water quality parameters during the first trial.

Parameter	Average ± S.D.
Temperature (°C)	24.8 ± 0.1
Dissolved Oxygen (mg L^{-1})	6.25 ± 0.23
Salinity (ppt)	31.71 ± 0.55
pH	7.85 ± 0.06
NH_3 (mg L^{-1})	0.04 ± 0.03
NO_2 (mg L^{-1})	0.014 ± 0.008
No_3 (mg L^{-1})	2.1 ± 0.6

Production characteristics from the first feeding trial are shown in table 7. Increasing SBM within the diet resulted in a significant reduction in feed consumption (P=0.0003), weight gain in grams gained per fish (P=0.029), and final weight in grams (P=0.022). No significant effects of SBM level were observed in weight gain as a percent of initial weight (P=0.09), final length (P=0.062), feed conversion ratio (P=0.926), specific growth rate (P=0.084), or condition factor at the conclusion of the trial (P=0.143). Results from the commercial diet were not included in statistical comparisons, however, all results from this treatment fell within the ranges observed on the SBM diets except for feed consumption and feed conversion ratio, which were both slightly higher than any SBM experimental treatments.

Table 7. Production characteristics from the first feeding trial. Linear regression model to test for significant effect of SBM (Commercial diet excluded), P<0.05 indicates significant effect of SBM level.

Treatment	Feed Consumption (g fish)	Weight gain (g fish)	Weight gain (% initial)	Final Weight (g)	Final Length (mm)	FCR	PER	SGR	Condition Factor
Commercial	223.90 ± 27.17	121.04 ± 11.56	261.74 ± 20.57	163.66 ± 12.90	242.38 ± 17.13	1.85 ± 0.17	1.18 ± 0.13	1.46 ± 0.1	1.15 ± 0.07
0% SBM	219.69 ± 13.97	133.78 ± 23.07	277.11 ± 51.71	173.15 ± 15.19	247.40 ± 21.57	1.69 ± 0.38	1.23 ± 0.22	1.51 ± 0.2	1.15 ± 0.07
15% SBM	216.30 ± 7.85	120.88 ± 11.39	255.25 ± 26.55	166.33 ± 10.08	240.64 ± 17.08	1.80 ± 0.16	1.22 ± 0.11	1.52 ± 0.1	1.17 ± 0.07
30% SBM	199.78 ± 11.91	112.02 ± 19.79	242.63 ± 40.49	157.46 ± 13.89	237.64 ± 21.46	1.83 ± 0.37	1.26 ± 0.20	1.50 ± 0.1	1.16 ± 0.07
45% SBM	197.52 ± 18.66	117.60 ± 6.92	249.80 ± 20.52	163.63 ± 12.07	242.41 ± 16.13	1.69 ± 0.19	1.36 ± 0.21	1.50 ± 0.1	1.14 ± 0.06
60% SBM	187.48 ± 5.06	104.31 ± 19.62	226.22 ± 35.75	149.60 ± 13.31	233.57 ± 20.60	1.84 ± 0.29	1.30 ± 0.15	1.36 ± 0.1	1.13 ± 0.07
Pooled S.E.	0.1234	0.1258	0.2599	0.1322	0.0896	0.0025	0.0018	0.0012	0.0003
P	0.0003	0.029	0.09	0.022	0.062	0.926	0.316	0.084	0.143

Table 8. Proximate analyses for whole body. Linear regression model to test for significant effect of SBM, *P*<0.05 indicates significant effect of SBM level.

Treatment	Dry matter (%)	Protein (%)	Ash (%)	Fat (%)	P (ppm)	K (ppm)	Ca (ppm)	Mg (ppm)	Zn (ppm)	Cu (ppm)	Mn (ppm)	Fe (ppm)	S (ppm)	Na (ppm)
0% SBM	28.40 ± 0.01	71.08 ± 6.25	14.52 ± 2.71	17.89 ± 2.61	23351.46 ± 4540.34	10913.82 ± 700.60	39005.17 ± 9699.10	1322.63 ± 270.96	44.78 ± 4.51	2.34 ± 0.52	8.61 ± 2.83	43.95 ± 9.26	6765.00 ± 472.09	4722.36 ± 533.44
15% SBM	28.88 ± 0.01	65.84 ± 5.18	14.33 ± 1.26	18.77 ± 1.94	18960.93 ± 2811.81	11411.83 ± 944.68	31438.74 ± 9896.25	1136.73 ± 142.59	42.39 ± 3.25	1.98 ± 0.38	8.06 ± 1.76	32.57 ± 10.94	6740.10 ± 534.79	4451.32 ± 369.88
30% SBM	29.44 ± 0.02	64.86 ± 8.79	13.41 ± 1.02	19.41 ± 3.54	23083.15 ± 1598.13	10343.54 ± 1083.86	39654.90 ± 6328.64	1288.00 ± 67.81	48.56 ± 5.07	1.76 ± 0.28	10.30 ± 2.06	33.46 ± 7.58	6123.17 ± 634.23	4547.56 ± 448.62
45% SBM	29.15 ± 0.01	66.48 ± 3.84	15.10 ± 2.54	17.67 ± 1.38	23814.03 ± 2644.72	11279.29 ± 798.61	39609.78 ± 7414.96	1355.18 ± 103.49	49.92 ± 4.31	2.16 ± 0.43	10.28 ± 2.46	28.76 ± 3.43	6455.81 ± 454.71	4707.49 ± 380.35
60% SBM	28.92 ± 0.02	69.85 ± 8.29	15.41 ± 1.82	19.78 ± 3.51	23571.99 ± 3485.06	10686.72 ± 993.31	45528.11 ± 9927.61	1334.84 ± 171.41	49.70 ± 6.32	1.90 ± 0.29	11.97 ± 3.53	32.81 ± 4.03	5763.20 ± 496.18	4627.42 ± 599.67
Pooled S.E.	.0001	0.0637	0.0143	0.0244	26.33	7.283	71.92	1.339	0.0358	0.0035	0.0223	0.0554	4.084	3.864
P	0.514	0.851	0.247	0.473	0.193	0.596	0.061	0.239	0.004	0.193	0.014	0.005	0.001	0.910

Table 9. Proximate analyses for fillets. Linear regression model to test for significant effect of SBM, $P<0.05$ indicates significant effect of SBM level.

Treatment	Dry matter (%)	Protein (%)	Ash (%)	Fat (%)	P (ppm)	K (ppm)	Ca (ppm)	Mg (ppm)	Zn (ppm)	Cu (ppm)	Mn (ppm)	Fe (ppm)	S (ppm)	Na (ppm)
0% SBM	23.51 ± 0.01	90.26 ± 1.12	4.84 ± 0.22	2.36 ± 0.64	8845.78 ± 258.36	18159.20 ± 442.95	509.29 ± 85.83	1371.07 ± 49.71	19.79 ± 1.09	1.56 ± 0.12	0.69 ± 0.10	11.09 ± 2.41	8917.08 ± 161.46	1690.34 ± 333.06
15% SBM	20.64 ± 0.04	89.5 ± 0.83	5.00 ± 0.19	2.70 ± 0.84	9090.87 ± 277.18	17345.96 ± 815.52	1113.06 ± 467.65	1407.34 ± 43.72	22.37 ± 0.99	1.99 ± 0.46	1.51 ± 1.34	67.36 ± 99.55	8997.71 ± 143.25	1803.16 ± 69.00
30% SBM	25.83 ± 0.02	88.11 ± 0.96	5.21 ± 0.11	2.86 ± 0.86	9191.51 ± 637.66	17234.52 ± 500.98	994.77 ± 723.10	1362.36 ± 126.61	22.31 ± 1.01	1.79 ± 0.26	1.01 ± 0.84	27.62 ± 45.21	8870.18 ± 168.26	1755.92 ± 171.71
45% SBM	21.98 ± 0.04	90.37 ± 0.92	5.32 ± 0.23	2.79 ± 0.53	9251.72 ± 601.88	17751.96 ± 431.41	1142.37 ± 817.75	1333.46 ± 109.40	22.72 ± 1.78	1.46 ± 0.16	0.91 ± 0.33	13.07 ± 5.31	8876.04 ± 107.34	1873.52 ± 302.15
60% SBM	22.86 ± 0.07	89.36 ± 0.85	5.27 ± 0.12	2.13 ± 0.50	9191.10 ± 1086.60	16628.65 ± 1489.52	1356.11 ± 637.25	1410.81 ± 168.23	22.21 ± 2.46	1.49 ± 0.21	0.92 ± 0.23	13.5 ± 4.43	8435.30 ± 870.07	1727.92 ± 236.81
Pooled S.E.	0.0003	0.0114	0.002	0.0066	4.025	6.694	5.083	0.7815	0.1435	0.003	0.0057	0.3642	2.718	2.411
P	0.995	0.589	0.001	0.712	0.067	0.054	0.022	0.682	0.029	0.075	0.908	0.375	0.074	0.576

Proximate and mineral compositions for the whole body and fillet tissues are shown in tables 8 and 9, respectively. There were no significant effects of SBM level on dry matter, protein, ash, or fat in the whole body tissues. There was a significant effect of SBM on several minerals concentrations in the whole body tissues. Zinc increased with increasing SBM (P=0.004), manganese increased with increasing SBM (P=0.014) and iron (P=0.005) and sulfur (P=0.001) both decreased in whole body concentration as dietary SBM increased.

There were no significant effects of SBM level on dry matter, protein, or fat, however fillet ash significantly increased with increasing dietary SBM (P=0.001). Fillet calcium (P=0.022) and zinc (P=0.029) concentrations were significantly affected by dietary SBM level with both increasing with increasing dietary SBM.

At the conclusion of the 12-week trial, eviscerated body (carcass) weights were compared across treatments. Livers were also weighed and the hepatosomatic index was calculated for each treatment. There was no significant effect of dietary SBM level observed on eviscerated weights (P=0.906), however there was a significant decrease in hepatosomatic index as dietary SBM increased (P=0.0002) (Table 10). Again, although not included in the statistical comparisons, results for the commercial diet for both measurements fell within the ranges observed in the experimental treatments.

Table 10. Eviscerated fish weight (g) and hepatosomatic index (HSI) at final sampling. Linear regression model to test for significant effect of SBM (Commercial diet excluded), P<0.05 indicates significant effect of SBM level.

Treatment	Eviscerated Weight (g)	Hepatosomatic Index
Commercial	135.83 ± 24.94	2.94 ± 0.63
0% SBM	138.67 ± 18.01	3.4 ± 0.38
15% SBM	145.50 ± 30.28	3.25 ± 0.71
30% SBM	131.00 ± 15.19	2.69 ± 0.64
45% SBM	142.17 ± 47.30	2.62 ± 0.19
60% SBM	138.00 ± 36.11	2.39 ± 0.42
Pooled S.E.	2.611	0.0042
P	0.906	0.0002

3.3 Intestinal Histology

Representative examples of the intestinal histology for the SBM 0% and SBM 60% treatments at the mid-point and conclusion of the trial are shown in figure 2. A qualitative assessment revealed similar levels of mild supranuclear vacuolization, thickness of the lamina propria, lymphocyte infiltration, and eosinophilic granulocytes. These were all qualitatively more severe than the initial samples. At the conclusion of the 12-week trial, qualitative assessment again revealed similar levels of these intestinal health markers between the treatments, and all were qualitatively more severe than the 6-week assessment. Throughout the trial the intestinal samples from the commercial diet treatment were qualitatively similar to the experimental diets.

A quantitative assessment was carried out on weekly intestinal histology samples to measure mucosal fold height (µm) and the proportion of mucosal fold area to lamina propria area (%), both markers for potential inflammation and intestinal enteritis. Figure 3A shows the average mucosal fold height throughout the trial for each treatment. As expected the average length increases through time with increasing body weight and length, however at the conclusion of the trial there was no significant difference observed between treatments as an effect of dietary SBM level (P=0.052, Table 11). Figure 3B shows the proportion of mucosal fold area to lamina propria for each treatment throughout the 12-week trial. There was no significant effect of dietary SBM level (P=0.208, Table 11).

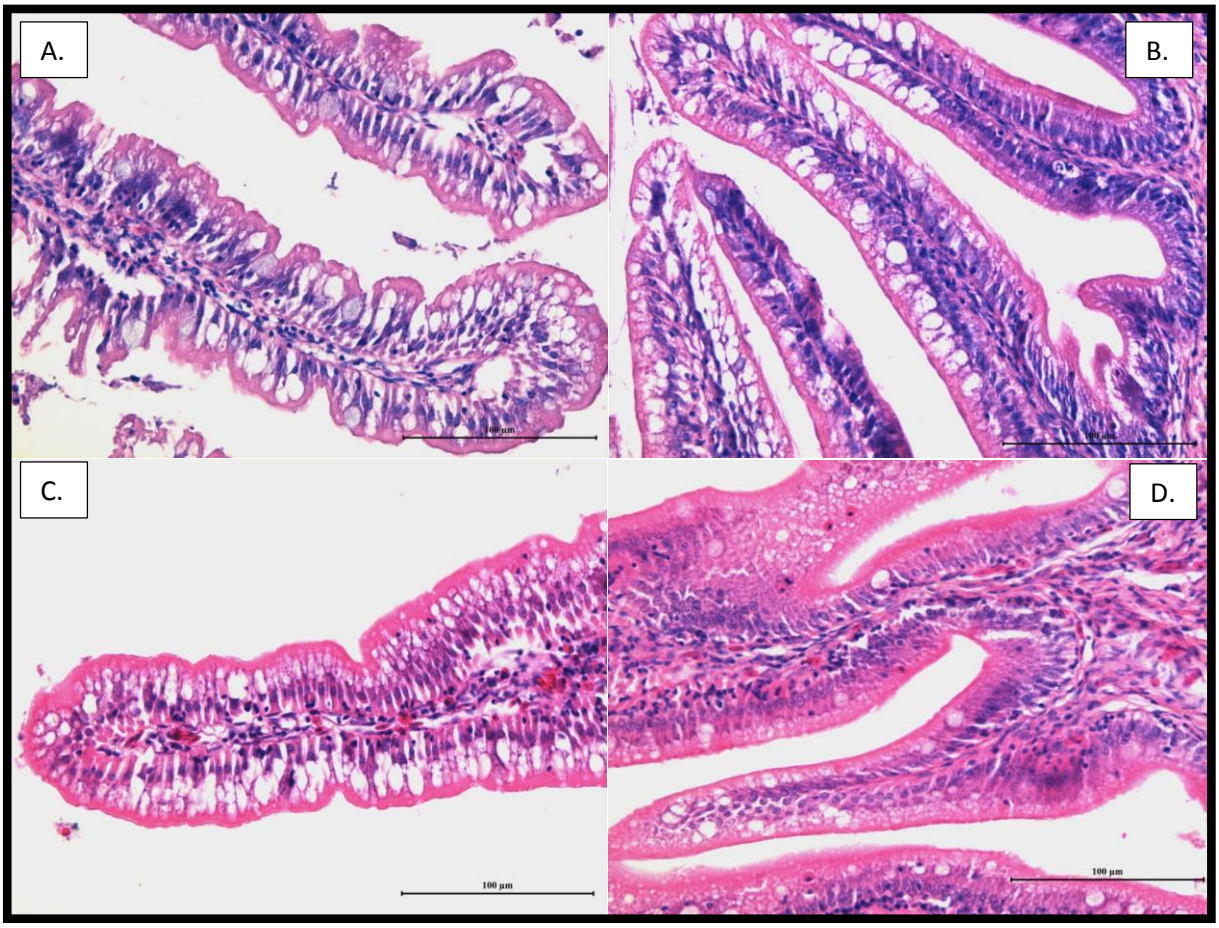

Figure 2. Examples of intestinal morphology from the SBM 0% treatment at 6 weeks (A.) and 12 weeks (C.). Panels B and D show examples of the SBM 60% treatment at 6 and 12 weeks, respectively.

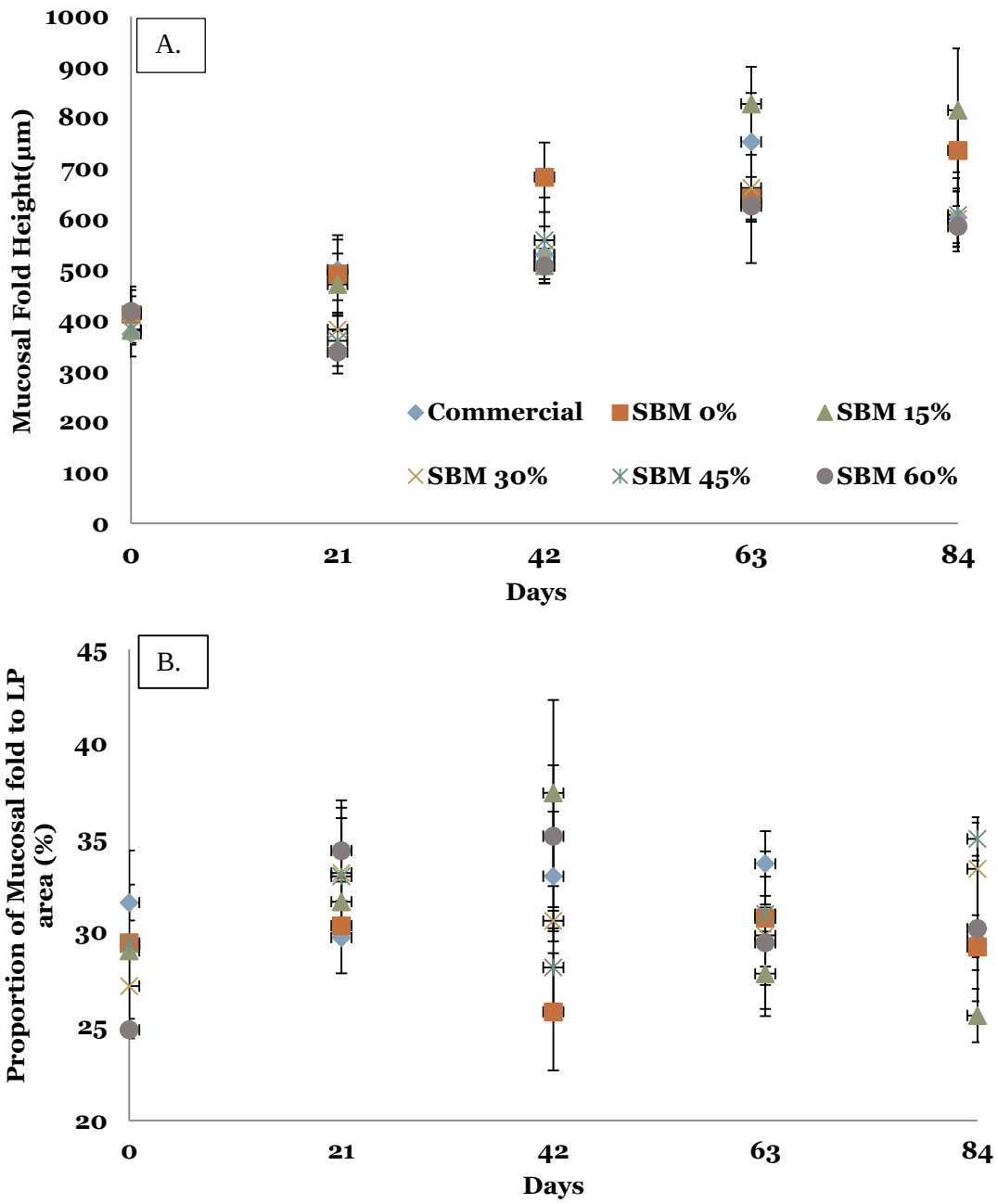

Figure 3. Mucosal fold height (µm) for each treatment throughout the course of the 12 week feeding trial (panel A) and proportion of the mucosal fold area to lamina propria area for each treatment throughout the course of the 12-week feeding trial (Panel B).

Table 11. Mucosal fold height (um) and Mucosal fold area: Lamina Propria Area (%) from distal intestine samples. Linear regression model to test for significant effect of SBM (Commercial diet excluded), $P<0.05$ indicates significant effect of SBM level.

Treatment	Mucosal Fold Height (µm)	Mucosal Fold Area: Lamina Propria Area (%)
Commercial	603.97 ± 101.91	29.70 ± 0.06
0% SBM	735.79 ± 150.50	30.33 ± 3.57
15% SBM	815.11 ± 244.16	31.61 ± 1.50
30% SBM	600.16 ± 108.93	33.14 ± 4.88
45% SBM	608.70 ± 144.57	32.95 ± 4.38
60% SBM	585.57 ± 81.24	34.32 ± 3.78
Pooled S.E.	1.623	0.0453
P	0.052	0.208

3.4 *NMR Metabolomics*

The target tissues were analyzed via PCA analysis in two ways, one to examine the time evolution (trajectory analysis) of the metabolome, and the second an analysis of the equilibrated metabolome from weeks 9-12 once the fish had acclimated to the various feeds.

Intestine Trajectory

The intestine tissue from time points T0 through T12 (thirteen time points) were used to build a PCA model (Figure 4) which has an explained variance of 47.1% in PC1 and PC2. In this figure, the sequential time points are connected with a solid line so that any time-dependent pattern would be distinguishable. The size of the error bars (± 1 standard error of the mean (SEM)) and the random nature of the trajectory paths indicate that there is very little differentiation of the different time points or the different diets. Because of the lack of definitive differentiation of the intestine tissues in this model (especially compared to the other tissues, below) it was clear that there would be no metabolic biomarkers with clear differentiation between diets and further analysis of intestine was not warranted.

Figure 4. Intestine PCA model including the three diets SBM_60, SBM_0 and HP for all sampled time points. Error bars are standard errors of the means and are meant to be representative of the errors at all time points.

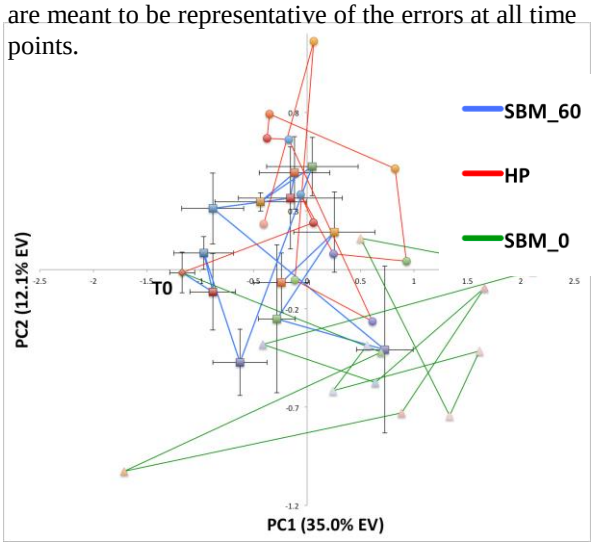

Liver Trajectory

The liver tissue from points T0 through T12 (thirteen time points) were used to build a PCA model (Figure 5) which has an explained variance of 44.1% in PC1 and PC2. In this figure, the sequential time points are connected with a solid line so that any time-dependent pattern would be distinguishable. In this model, each diet has a trajectory which progresses from the left to the right with time. The SBM_0 diet (green trajectory) moves steadily to the right for the first few weeks of the study, but from about week 5 through week 12, a stable metabolomic trajectory hovers around a locus indicating that the fish on this diet have reached some sort of homeostasis. The commercial reference (HP) diet trajectory also moves steadily to the right, although in a slower way than the SBM_0 diet. This diet seems to reach a steady homeostasis around weeks 9 through 12. Finally, the most interesting trajectory is for SBM_60 which has at least two stationary loci. In weeks 2 through 4, little discernable change is apparent indicating some metabolic stability. However, change occurs in weeks 4 and 5 as a transitory change to a stable metabolomic trajectory for weeks 6 through 12. Finally, all three diets seem to have different locations in PC-space at the end of the 12-week study. Below, we will examine this T_end difference amongst the diets to see if this trend in the liver metabolomic profiles shows consistent patterns among all the experimental diets.

Figure 5. Liver PCA model for the three diets SBM_60, SBM_0 and HP for all sampled time points. Error bars are ± 1 SEM.

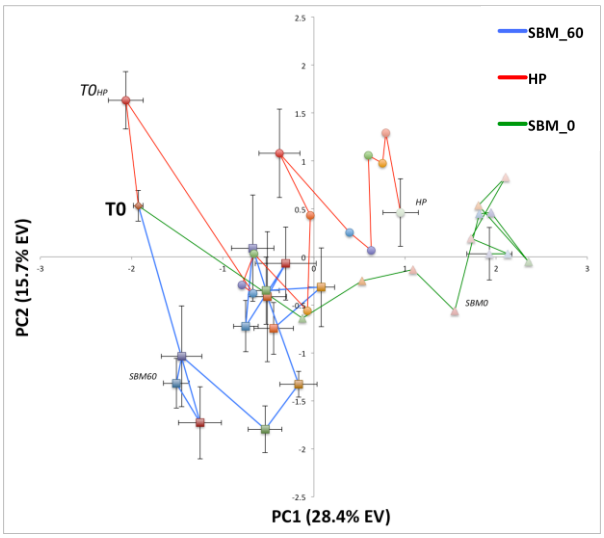

Muscle Trajectory

The muscle tissue from selected time points T0, T1, T3, T6, T9 and T12 (six time points) were used to build a PCA model (Figure 6) which has an explained variance of 60.8% in PC1 and PC2. In this figure, the sequential time points are connected with a solid line so that any time-dependent pattern would be distinguishable. In this model, each experimental diet has a trajectory which progresses from the left to the right with time, but the commercial reference diet moves to the left from the T0 point, reflecting a fundamental difference between the commercial and experimental diets in muscle tissue. For the experimental SBM diets, there is no significance in PC1 between the T9 and T12 time points, so below we will use T9 and T12, combined, as the T_end for comparison of the experimental diets at the end of the growth period.

Figure 6. Muscle PCA model for the three diets SBM_60, SBM_0 and HP for selected sampled time points (T0, T1, T3, T6, T9, T12). Error bars are ± 1 SEM.

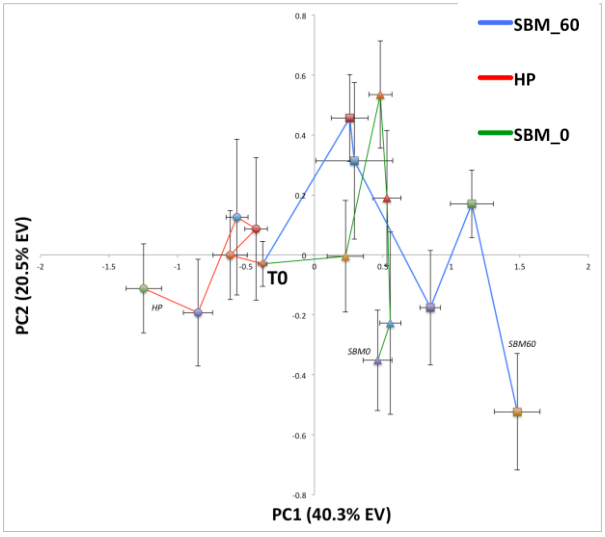

Plasma Trajectory

The plasma samples from selected time points T0, T1, T3, T6, T9 and T12 (six time points) were used to build a PCA model (Figure 7) which has an explained variance of 61.2% in PC1 and PC2. In this figure, the sequential time points are connected with a solid line so that any time-dependent pattern would be distinguishable. Much like the intestine data, the larger variability for each diet/time point obscures and makes the detection of any trends difficult. Again, there is little significant difference in PC1 for the terminal times T9 and T12, so below we will examine these two time points in a combined fashion to see if there is any difference in the final period for each of the diets.

Figure 7. Plasma PCA model for the three diets SBM_60, SBM_0 and HP for selected sampled time points (T0, T1, T3, T6, T9, T12). Error bars are ± 1 SEM.

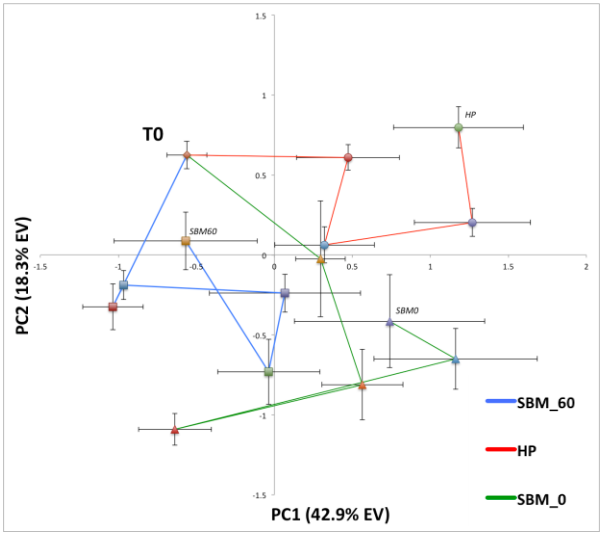

Metabolomics Endpoints.

The various tissues were analyzed at the end of the growth period via PCA analysis to examine the differences in the metabolome as a result of the experimental diets. The end point, T_end, was comprised of samples from T9, T10, T11 and T12 (N=24 samples) for intestine and liver samples, but it was comprised of only T9 and T12 (N=12 samples) for plasma and muscle since those were the time points analyzed by NMR. This was based on the observed homeostasis for all tissues after the 9 week period and was done in order to increase the numerical strength of the PCA models versus just using the T12 samples with only 6 samples per diet.

Figure 8. Intestine PCA model for all diets at T_end (combined T9, T10, T11, T12 samples) with T0 as a phenotypic anchor point. Error bars are ± 1 SEM.

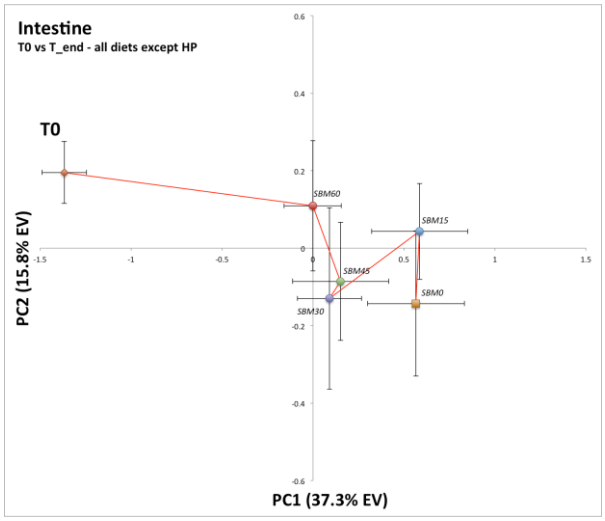

Intestine Endpoint

The intestine PCA model for the metabolomics end point was constructed using combined data from T9, T10, T11 and T12 for each diet (Figure 8) and PC1 and PC2 explain 53.1% of the variance in the data set. In this figure, the sequential diets with decreasing SBM are connected with a solid line so that any diet-dependent pattern would be distinguishable. The T0 phenotypic anchor is significantly different from all the diets in PC1, but not PC2. There is no significant difference in any of the experimental diets for PC1 or PC2 similar to the results of the time dependent trajectory analysis above (Figure 8) for intestine.

Muscle Endpoint

The muscle PCA model for the metabolomics end point was constructed using combined data from T9 and T12 for each diet (Figure 9) and PC1 and PC2 explain 67.9% of the variance in the data set. In this figure, the sequential diets with decreasing SBM are connected with a solid line so that any diet-dependent pattern would be distinguishable The T0 phenotypic anchor is significantly different from all the diets in PC1, but not PC2. There is significant difference between some of the experimental diets for PC1; for example, diets SBM_60 and SMB_45 are not significantly different from each other, but they are both significantly different from the other experimental diets, and diets SBM_0, SBM_15 and SBM_30 are not significantly different from each other in PC1. PC2 shows no significant differences between any of the diets.

Figure 9. Muscle PCA model for all diets at T_end (combined T9, T12 samples) with T0 as a phenotypic anchor point. Error bars are ± 1 SEM.

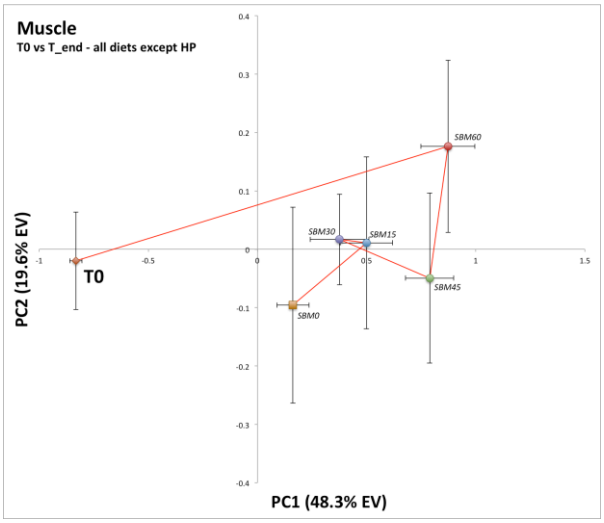

Figure 10. Plasma PCA model for all diets at T_end (combined T9, T12 samples) with T0 as a phenotypic anchor point. Error bars are ± 1 SEM.

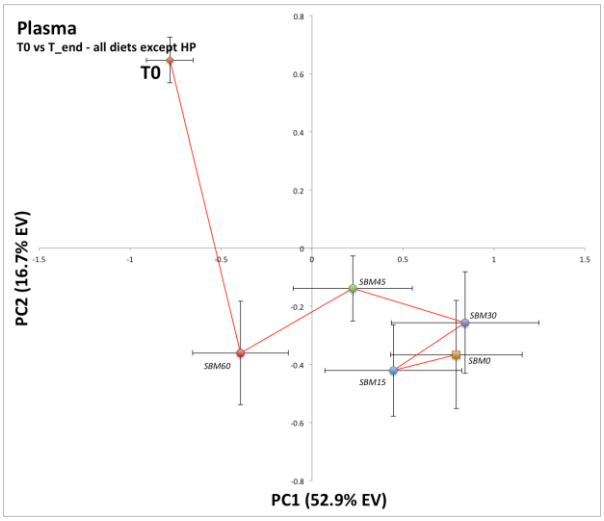

Plasma Endpoint

The plasma PCA model for the metabolomics end point was constructed using combined data from T9 and T12 for each diet (Figure 10) and PC1 and PC2 explain 69.6% of the variance in the data set. In this figure, the sequential diets with decreasing SBM are connected with a solid line so that any diet-dependent pattern would be distinguishable. The T0 phenotypic anchor is significantly different from all the diets in PC1 and PC2. Diet SBM_60 is significantly different from experimental diets SBM_15 and SBM_30 in PC1. There is no significant difference between the other experimental diets in PC1. No experimental diets show significant differences in PC2. Once again, plasma seems to be less sensitive to dietary influences in this study.

Liver Endpoint

The liver PCA model for the metabolomics end point was constructed using combined data from T9, T10, T11 and T12 for each diet (Figure 11) and PC1 and PC2 explain 52.3% of the variance in the data set. In this figure, the sequential diets with decreasing SBM are connected with a solid line so that any diet-dependent pattern would be distinguishable The T0 phenotypic anchor is significantly different from all the diets in PC1, but not significantly different in PC2. Every experimental diet is significantly different in PC1. In PC2, diets SMB_60 and SBM_45 are not significantly different, forming one group, and diets SBM_0, SBM_15 and SMB_30 are not significantly different in PC2, forming a second grouping.

Figure 11. Liver PCA model for all diets at T_end (combined T9, T10, T11, T12 samples) with T0 as a phenotypic anchor point. Error bars are ± 1 SEM.

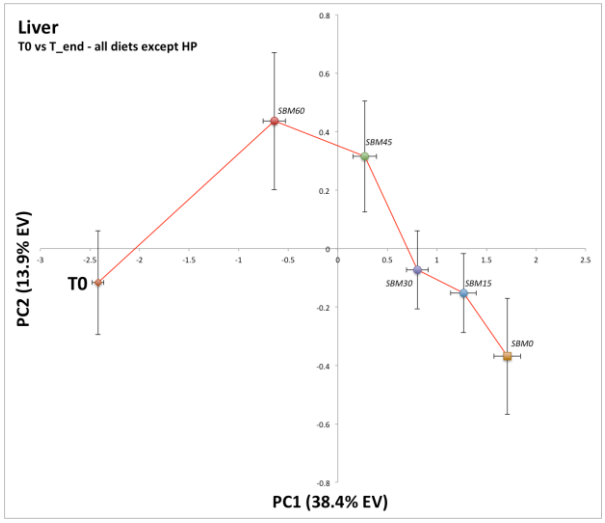

In order to assess whether the phenotypic anchor, T0, was unduly affecting this model, a new model was built excluding the T0 samples. The liver PCA model for the metabolomics end point was constructed using combined data from T9, T10, T11 and T12 for each diet while excluding the T0 samples (Figure 12). PC1 and PC2 explain 49.4% of the variance in the data set, a slightly weaker model perhaps due to the exclusion of the T0 samples. Again, every experimental diet is significantly different in PC1. In PC2, however, there is no significant difference between experimental diets.

Figure 12. Liver PCA model for all diets at T_end (combined T9, T10, T11, T12 samples). Error bars are ± 1 SEM.

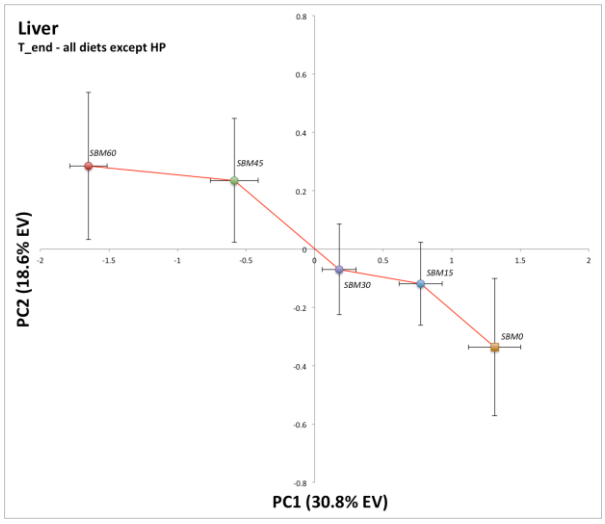

The trend in liver homeostasis at the end of the feeding trial is significant and reflects a trend based on the amount of soybean meal in the diet formulation. In order to understand this trend, we examined the loading in PC1 to identify the metabolites which lead to the variance in the samples. The intensity of a chemical shift bin in the loadings plot corresponds to that spectral feature's influence in the scores plot. For example, a positive peak in the loadings plot corresponds to a feature which will cause spectra which have that corresponding feature to shift to the right (more positive PC1 score) in the scores plots. In comparison, a loadings bin with a negative intensity will cause a spectrum to shift to the left (more negative PC1 score) when that spectrum has a corresponding feature. By analyzing the loadings plot and identifying the compounds associated with a feature, we are able to identify compounds that show important variances between the spectra.

Figure 13. Filtered PC1 loading plot for the liver PCA model. The Filtering was based on the features with absolute intensities above the 95th percentile.

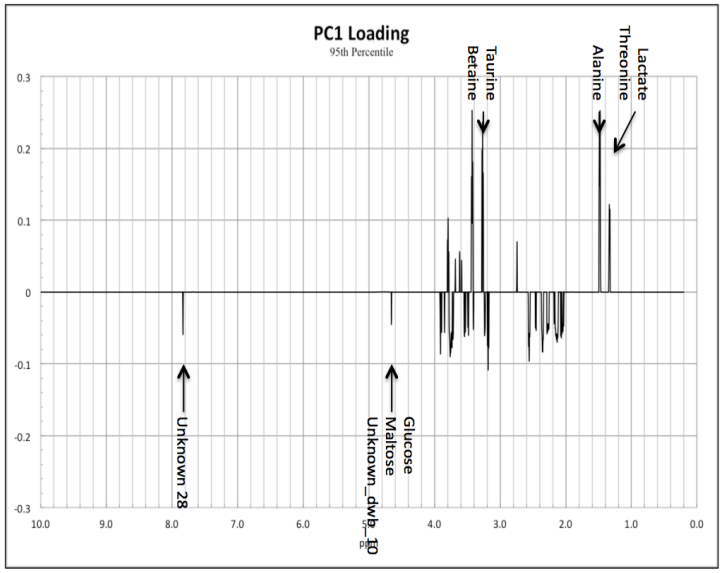

Table 22. Significant compounds in the PCA liver model for the experimental diets (Figure 12).

Putative Compound ID	Putative Compound Loading*
Alanine	Pos
b-Alanine	Neg
Betaine	Pos
Choline	Neg
Glucose	Neg
Glutamate	Neg
Glutamine	Neg
Glutathione	Neg
Glycerol	Pos
Glycogen	Neg
Lactate	Pos
Maltose	Neg
Sarcosine	Pos
Serine	Neg
Taurine	Pos
Threonine	Pos
Unknown_dwb_11a	Pos
Unknown_dwb_13	Neg
Unknown_dwb_22	Pos
Unknown_dwb_28	Neg
Unknown_dwb_31	Pos
Unknown_dwb_32b	Neg
Unknown_dwb_34	Neg
Unknown_dwb_39a	Neg
Unknown_dwb_39b	Neg

***Relative sign of loading, to be confirmed.**

For the liver PCA model (Figure 12), the most significant loadings have been identified (or enumerated if the feature could not be definitively identified) and plotted (Figure 13). The crowded region between 2.0 ppm and 4.5 ppm is shown in an expanded view (Figure 14). The list of features (Table 22) includes several features which are currently unidentified in addition to almost 20 known metabolites. The identified metabolites represent compounds that show significant variance between the experimental diet formulations, and they may be compounds that represent compounds in biochemical pathways that are modified (up or down regulated) by the diets and the organism's response to the diet, they may represent metabolic products of dietary processing or they may reflect direct dietary contributions to the metabolome.

Analysis of the biochemical interpretation of these metabolites as well as the identity of the unknowns is complex. As an example, the feature "Unknown 28" (Unknown_dwb_28 in Table 22) stands out as an unusual compound, mainly because of the peculiar ^{1}H and ^{13}C chemical shifts related to this feature. The negative sign of the feature in Figure 13 indicates that the signature pushes spectra to the left in the scores plot; this corresponds to increasing soybean meal content. Plotting the individual liver spectral features (Figure 15) shows that the mean and the variability of this spectral feature increase with increasing soybean meal content, although there is significant individual variability.

Figure 14. Expanded plot from Figure 13.

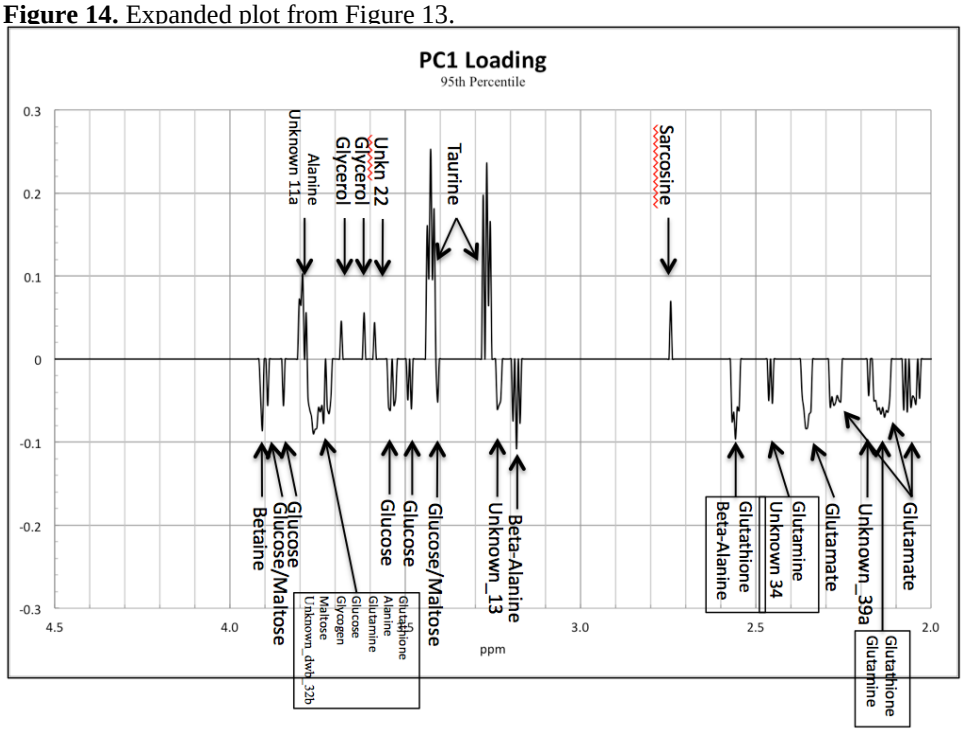

Subsequent to the development of Table 22, "Unknown 28" was identified by additional NMR experiments on a sample with a significant amount of this compound as N-formimino-L-glutamate (formiminoglutamate, FIGLU), an intermediate in the histidine degradation pathway. In fact, histidine can be metabolized via a pathway that involves the transfer of a formimine (methenimine) group from FIGLU to tetrahydrofolate (THF), thus generating glutamate. In mammals, FIGLU has been shown to accumulate in the case of folic acid deficiency or vitamin B12 deficiency. If that model also holds for fish, despite the fact that both vitamin B12 and folic acid were provided with all diets using a vitamin pre-mix, a deficiency might have been induced indirectly. As far as vitamin B12 deficiency is concerned, fish require only trace amounts of it in the diet as it is usually synthesized by microorganisms in the gut. Vitamin B12-deficiency in fish could be caused by the lack of a carrier glycoprotein in the gut called intrinsic factor (IF), which normally promotes vitamin B12 absorption. Such a scenario could be envisioned for instance if the soybean meal administered at certain levels is in some way altering the fish gut microbiome, thus disrupting normal mechanisms of nutrient absorption. Another possibility is that plant-based diets could alter the transport of folate or vitamin B12 through the intestine by causing direct cell damage or interfering with specific enzymes (i.e. formiminotransferase). These are testable hypotheses which warrant further investigation.

Figure 15. Spectral bin intensities for the liver PCA analysis. The intensities represent the amount of signal from compound formiminoglutamate in the samples. Group means and SEMs are shown as orange circles.

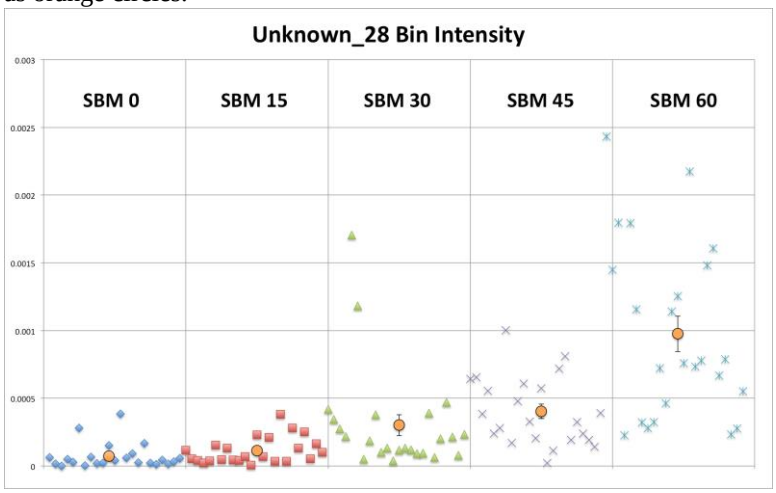

3.5 *Gene Expression Assays*

Results of the gene expression assays can be seen in the following figures. Throughout, for the first trial's results, gene expression values are shown as an average ± S.D. of the four individual livers used from each dietary treatment. Figures present each gene's expression results in a similar order; initial (T0), 0% SBM, 15% SBM, 30% SBM, 45% SBM, 60% SBM from left to right for each gene. All gene expression values for each animal are adjusted for expression of the reference gene (EF1A) and the 0% SBM is set with a reference expression level of 1 for ease of comparison throughout unless otherwise noted.

Figures 16 and 17 show the expression levels of the genes selected based on the metabolomics results discussed previously. Two weeks into the trial (Figure 16) there are no significant differences in expression of the genes when compared with the initial levels (pink bars) or as SBM level increases. For ChDh and DmgDh this changes dramatically by the conclusion of the trial (Figure 17) with significant increases in expression as SBM level increases for both. BHMT expression has also changed from the initial level, but there is no difference as SBM level increases. There does not appear to be a change in SarDh expression from initial or across increasing SBM levels. Taken together with the metabolite results, the gene expression results support the hypothesis of increased production of gluconeogenic precursors.

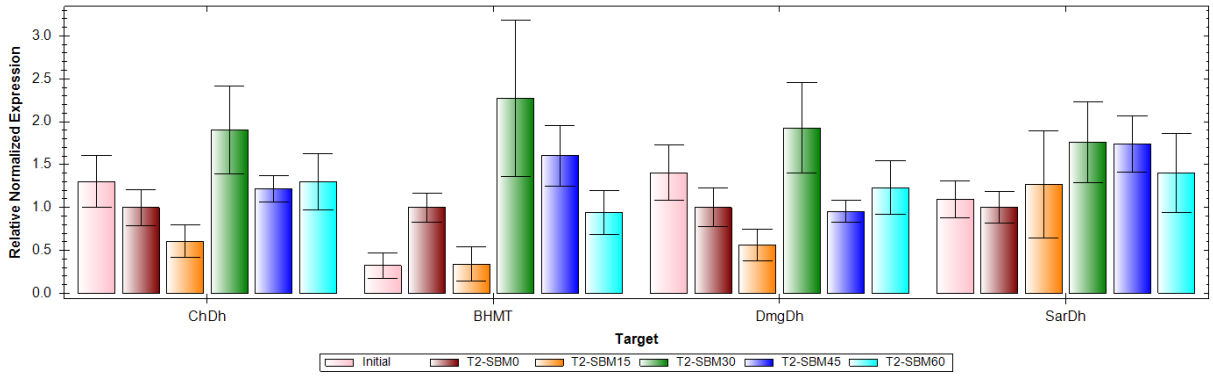

Figure 16. Liver gene expression levels (metabolomics derived genes) of graded soybean meal diets compared to initial (T0) expression levels 2 weeks into feeding trial.

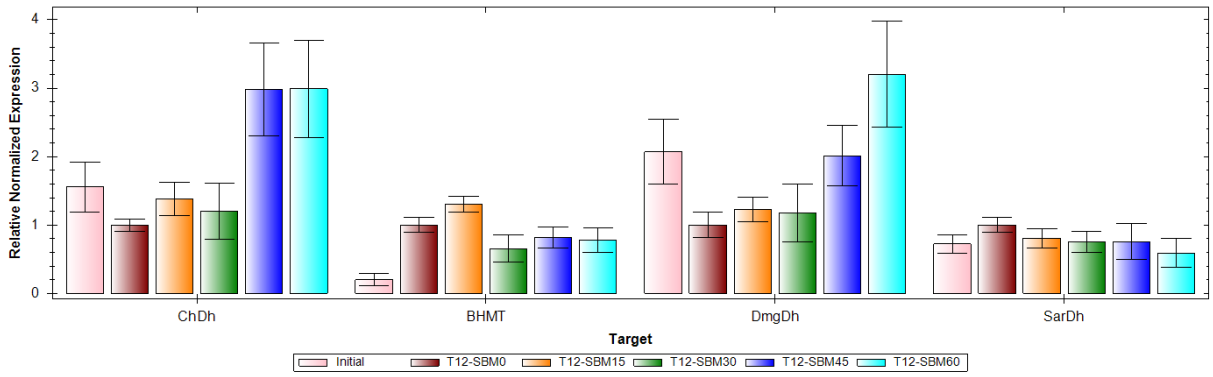

Figure 17. Liver gene expression levels (metabolomics derived genes) of graded soybean meal diets compared to initial (T0) expression levels 12 weeks into feeding trial.

Samples for the transcriptome sequencing work were taken at the week 11 sampling period, and we were curious to determine whether the gene expression in the weeks before and after that corroborated what was seen through the sequencing method. That method revealed at least a 2 fold difference in expression levels of these genes between the 0% and 60% end-point treatments of the trial. Figures 18 and 19 show the gene expression levels for the genes selected from the transcript sequencing and abundance work. Figure 18 shows the week 10 levels and figure 19 shows those from week 12. In week 10 we see statistically significant differences in all genes examined, similar to the transcript abundance work, and by week 12 all but APOA4 have maintained that difference. Interestingly, with the gene expression work, we can rapidly access the expression of the intervening SBM levels and in some cases we see a gradual drop in expression as SBM level increases; however, some genes appear to exhibit a threshold effect where as soon as the SBM level increases to a specific level (15%, 30% or 45%) we observed an immediate drop in expression for the remaining higher SBM levels.

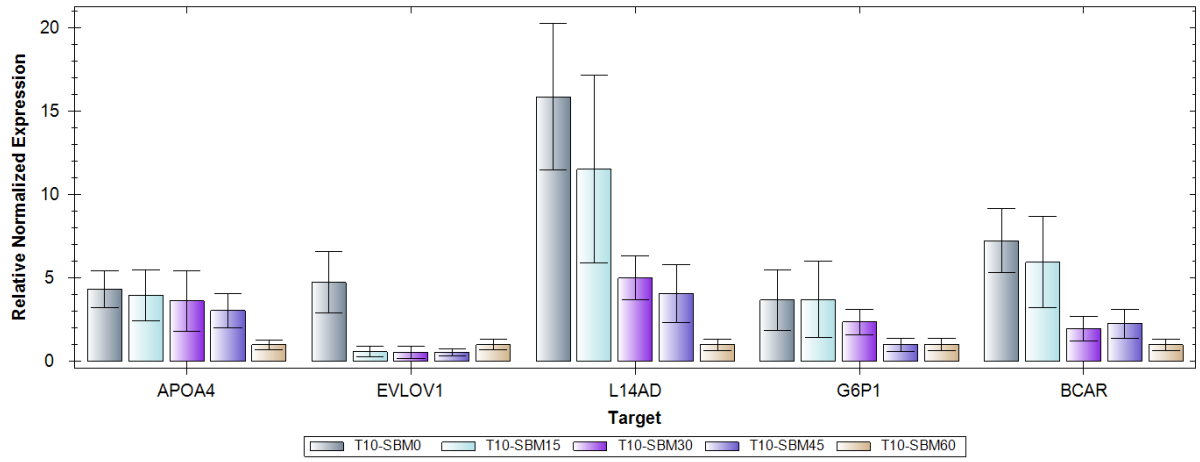

Figure 18. Liver expression of genes selected based on transcript abundance counts. Week 10 gene expression for graded SBM level diets (initial excluded).

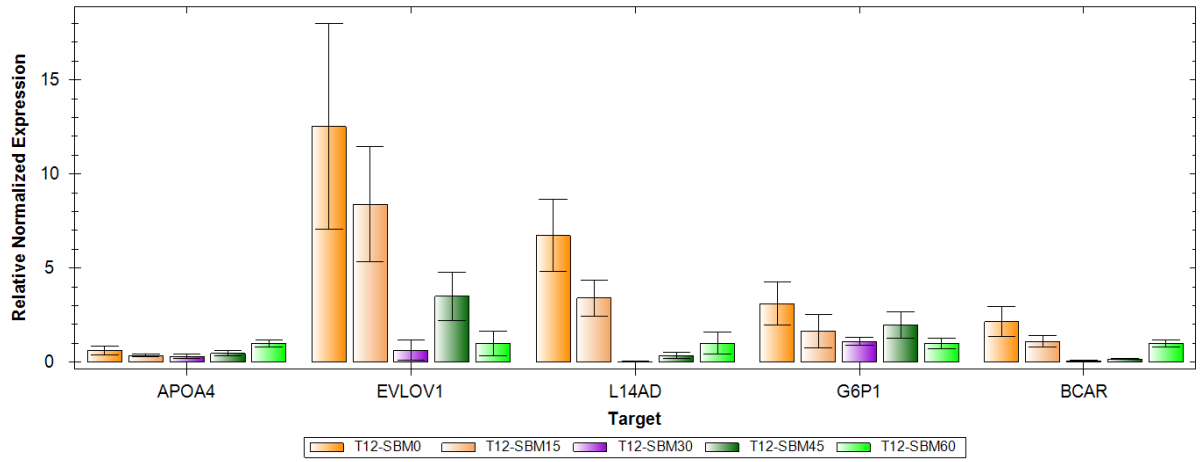

Figure 19. Liver expression of genes selected based on transcript abundance counts. Week 12 gene expression for graded SBM level diets (initial excluded).

While observing differences in multiple gene expression levels at the conclusion of the first trial with graded SBM, we were also able to examine weekly samples to determine when the changes in gene expression began to occur. Figure 20 shows the gene expression levels observed at the week 2 sampling. There does not yet appear to be strong deviations from the initial (T0) expression levels (light blue bar, far left for each gene) and there is no pattern with increasing SBM and there is high inter-animal variability in most of the measurements.

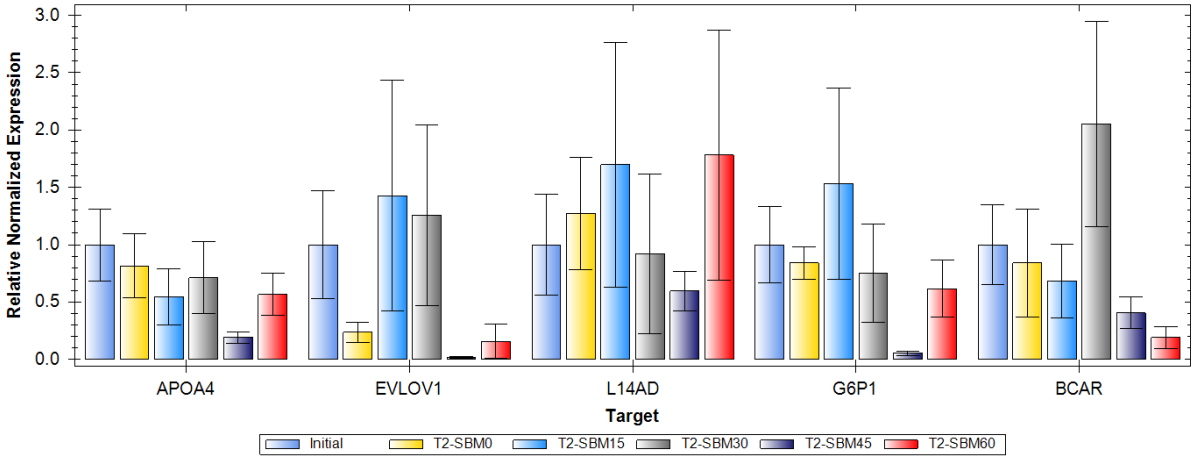

Figure 20. Gene expression in the liver two weeks into the feeding trial.

However, just two weeks later, at week 4 of the feeding trial, we begin to see significant deviations from the initial (T0) expression levels and the emergence of some of the patterns associated with SBM level that are detected throughout the trial through week 12 (Figure 21). The change in expression of L14AD is the most striking when compared to the initial expression level (Figure 22) with all SBM diets showing 18-50 fold expression differences.

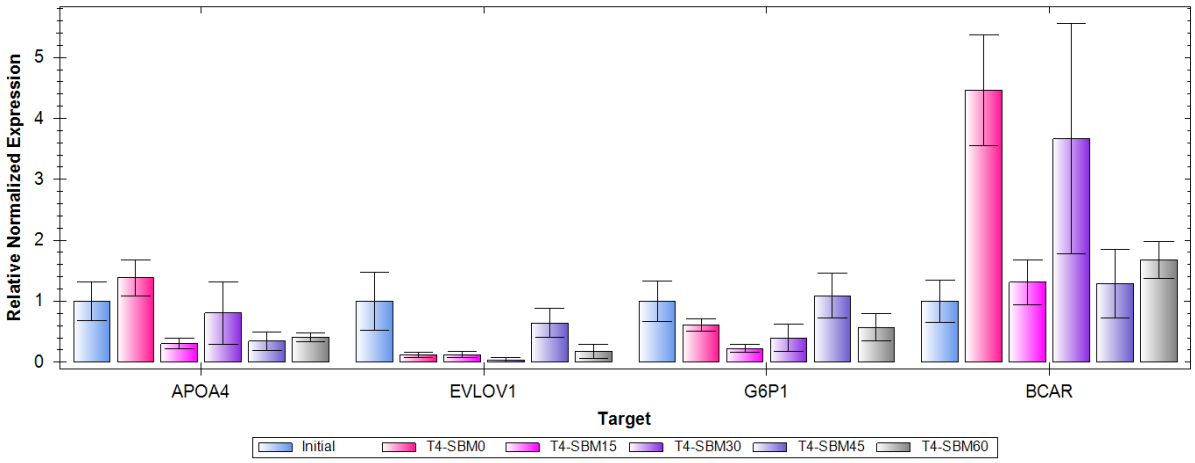

Figure 21. Gene expression in the liver four weeks into the feeding trial.

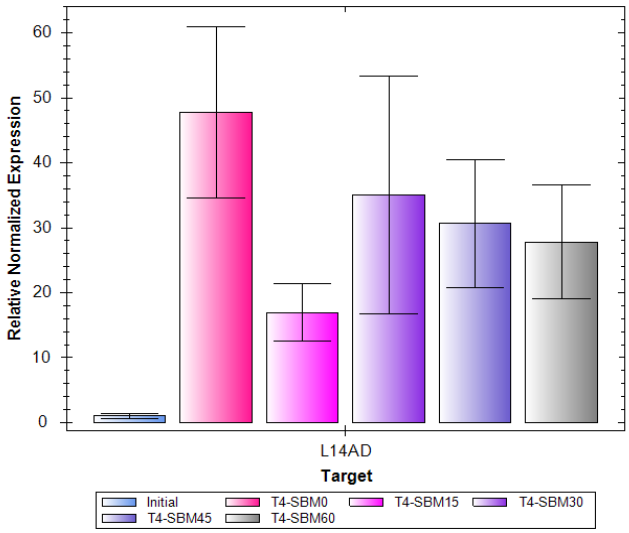

Figure 22. L14AD gene expression in the liver four weeks into the feeding trial.

4.0 Discussion of Trial #1 Results

We were able to design three sets of qPCR assays for this project, one based on genes selected from a single target pathway identified from the metabolite abundances, and two assays based on genes selected from the transcript abundance measurements. Although more description on the metabolomics process is available in that section of this report, briefly, we were able to identify a primary metabolic pathway that was most affected by soybean meal level. This pathway is the glycine, serine, threonine pathway (Figure 23) and several metabolites (choline, betaine, serine) are part of this pathway and contain a limited set of genes connecting them. Choline dehydrogenase (ChDh), Betaine homocysteine methyltransferase (BHMT), Dimethylglycine dehydrogenase (DmgDh), and Sarcosine Dehydrogenase (SarDh) were selected through this work to examine through q-PCR. These genes guide the pathway from choline through betaine aldehyde to betaine, then to dimethylglycine through sarcosine and towards glycine, a precursor for gluconeogenesis. Lactate dehydrogenase (LacDh) was also selected from this pathway since lactate was another metabolite with strong effects on the overall metabolome; however, for LacDh the gene expression assays were inconclusive from the first trial.

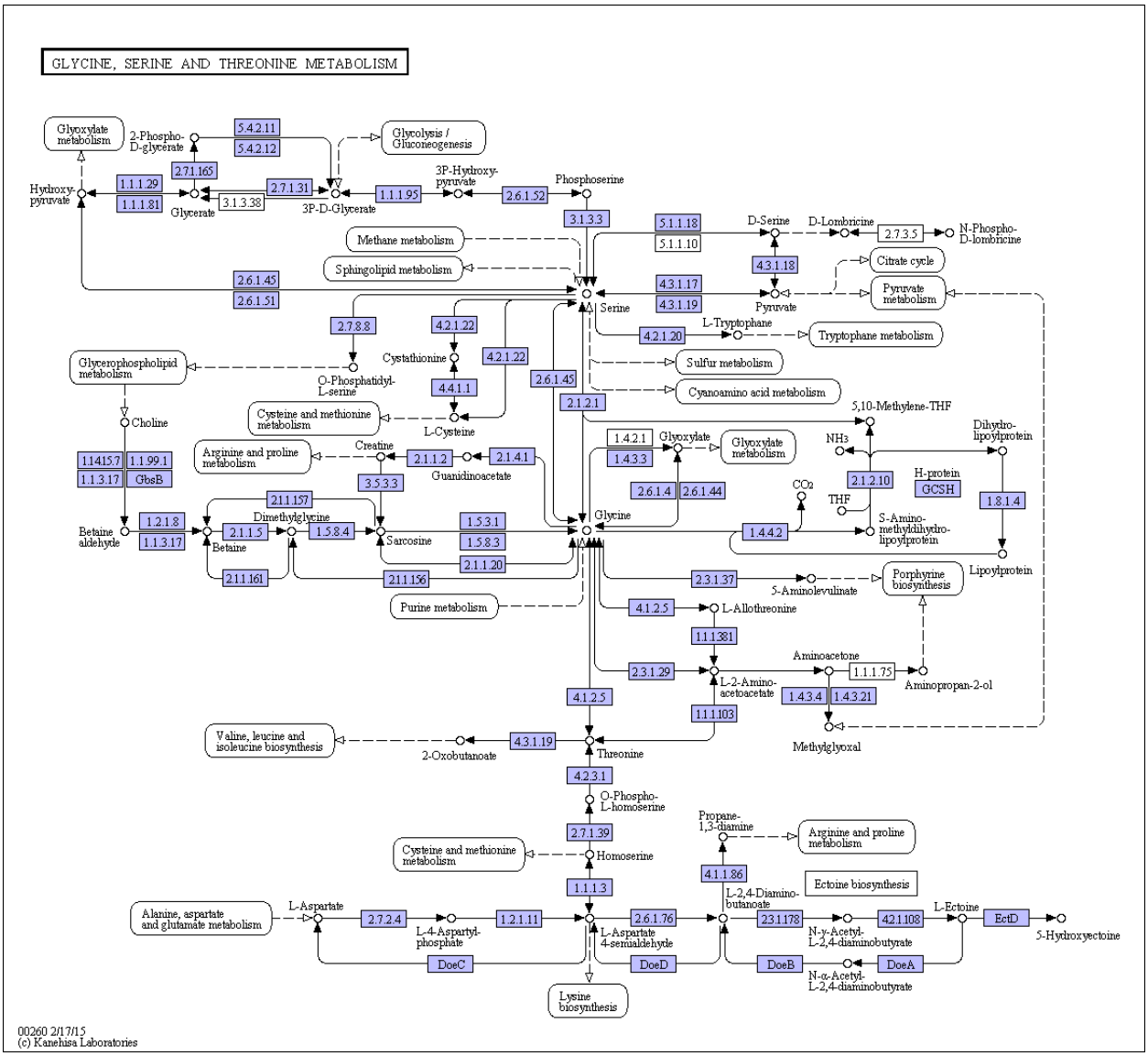

Figure 23. Glycine, serine, and threonine metabolic pathway. Numbers in purple and white boxes indicate specific genes responsible for transitions between metabolites of pathway and arrows indicate direction of reactions. From KEGG database (http://www.genome.jp/kegg/).

Unlike the genes selected through the metabolomics based approach, the genes selected from the transcript abundance dataset are not all from a common pathway. We identified over 200 unique transcripts that were found with at least a 2-fold abundance difference between the 0% SBM and 60% SBM livers. Starting with those genes with the largest fold differences and working towards the lowest fold differences, we selected a total of 8 genes that had critical functions, are the beginning steps of primary metabolic pathways, or are critical bottleneck stages of metabolic pathways. Using this approach we were also able to focus on genes from lipid metabolism. This is important to note because the specific NMR approaches used in this project only capture small polar lipids, leaving the vast majority of lipids uncharacterized. Combining these approaches has helped us get a more complete picture of potential physiological changes through the targeted gene expression assays.

Apolipoprotein a-IV (APOA4) is a lipid transport protein, elongation of very long chain fatty acids 1 (EVLOV1) is a critical gene in fatty acid synthesis, lanosterol 14-alpha demethylase (L14AD) is a critical enzyme in synthesizing cholesterol signaling pathway precursors, glucose-6-phosphate isomerase (G6PI) is involved in the transformation of glucose and fructose and is critical in carbohydrate metabolism, and breast cancer anti-estrogen resistance (BCAR) is a critical regulator of multiple signaling pathways. Thioredoxin (TXN) and lysozyme (LYZ) were selected and are important anti-oxidant and bacterial response genes; however, their expression levels were highly individual specific and had no pattern with time or dietary treatment. Squalene synthase (SQS) was also selected, however was rarely detected in our experimental samples and with no apparent pattern or relationship to diet.

Metabolomic data suggests a delayed metabolite response from what was predicted in Figure 1. Minimal differences in final weight and growth rates corroborate this assessment although there is a negative effect on performance characteristics as dietary SBM level increases. The most encouraging result from the feeding trial and growth data alone is that the performance of the commercial diet falls well within the ranges observed on the experimental feeds. This is an important finding due to the fact that all experimental diets were 100% fishmeal free, indicating the success and potential of this more sustainable aquaculture approach for juvenile red drum.

The data indicate the tissue with the strongest time-dependent trajectory with regard to the experimental diets is liver. Muscle tissue showed some weak time dependence. Intestine and plasma trajectories did not show distinct time-dependent trajectories, possibly indicating that these tissues are not as affected as other tissues by the diet in this study or that the statistical power of the study was not strong enough to detect small differences in these trajectories. It should be noted, however, that the number of samples for a tissue trajectory was rather large for a preliminary metabolomics study like this.

Interestingly, the liver trajectory results for SBM_60 indicate a short period of homeostatic equilibrium during weeks 1 through 4, then a progression over two or three weeks to a separate homeostatic equilibrium for the duration of the 13 week study. This indicates a surprisingly long period for the fish to reach an equilibrium on a high-soy diet and shows that feeding studies in this species on soy diets should not be shorter than 9 to 12 weeks of growth.

The analysis of the tissues at the endpoints (as judged from the trajectory stability noted in the trajectory analysis protocol, typically T9-T12) in liver tissue indicates a strong effect of soybean meal dietary content, with a slightly weaker effect observed in muscle tissue. There was little effect of soybean meal content on intestine or plasma. Based on the significantly varying metabolites in liver several metabolomic pathways are implicated as being affected by increasing soybean meal content, including the glycine, serine and threonine pathway and the starch and sucrose pathways. The unusual appearance of FIGLU as a significantly varying metabolite also has interesting implications for the histidine degradation pathway and a potential link to gut flora.

Metabolomic data also allowed for improvements to be made to the sampling regime employed during the second feeding trial. Plasma and intestine metabolomes do not show consistent patterns over time or between diets. This is most likely due to the high level of activity in the intestines and the presence of intestinal bacteria that are highly active metabolically. Plasma represents an interesting tissue due to the time-delayed responses of various digestive and transport activities. Since these feeding trials were designed to maximize feed consumption and growth, they were not well designed to specifically target changes in the plasma metabolome. Overlapping digestive periods occurred at the sampling point; however, once metabolites indicative of the

overall changes observed in liver and muscle (two tissues which do show significant differences over time and between all dietary treatments) are positively identified, we will be able to quantify their presence in the plasma metabolome to determine if individual metabolites indicative of the observed changes in muscle and liver are also changing in the plasma.

We also observed several specific periods within the metabolomic sampling regimes. The first few weeks after the initiation of the experimental feeds represent a period of constant change from the pre-trial feed for several weeks before trajectories indicative of stabilization of the metabolome after beginning the new feeds begins to occur. The metabolomes of each tissue and diet (where changes were observed) also appear to reach an equilibrium state at about 9 weeks after the experimental diet initiation and no significant changes were observed between weeks 9-12 for the experimental diets. We believe this represents the metabolic state that the animals reach where all physiological responses to the new feeds have stabilized at our experimental conditions (temperature, salinity) and this represents the metabolic and physiological state from which performance predictions may be most accurate. For this reason we modified the sampling regime used in the second feeding trial to capture the initial change period in weeks 2-5, and then again in weeks 9-12 to capture the equilibrium state. We also determined that acquiring the metabolomic data from intestine tissue was not informative based on the preliminary results of the first trial. Intestine was collected and preserved at all sampling points in the second trial; however, it will not be processed for metabolomics or transcriptomics unless the in-depth metabolomic analyses from trial 1 reveal new data. Although plasma also appeared to not be an optimal target tissue for the objectives of this study, due to the ease of collection and processing, it was still collected and analyzed in the second trial. It was also determined that increasing sample size of each tissue from each diet at each time point would significantly increase the precision of metabolomics assessment. With the removal of several time points and only collecting and not processing intestine samples, we were also able to increase our sample size from 6 to 12 for each tissue and time point, which improved resolution for detecting differences in the metabolome between treatments.

5.0 Methods and Materials for second trial

5.1 Diets

A one month soy-free conditioning diet was fed to all juvenile red drum prior to the start of the experiment. A 12-week feeding trial was then conducted evaluating four practical, isonitrogenous diet formulations utilizing high quantities of soy ingredients (>40 g $100g^{-1}$ diet of Hamlet Protein HP-300, Solae Pro-fine VF, or ADM SBM), a reference diet with 60% soybean meal (SBM) and a natural diet consisting of equal parts cigar minnows, squid, and shrimp. The formulations of the conditioning and experimental pelleted diets are provided in table 13. The 60% SBM formulation from the first trial was repeated in trial 2 as a negative reference and the natural diet was introduced as the positive reference. Past SCDNR studies have indicated this diet always out-performs experimental and commercial compound feeds and collaborative studies with SCDNR and NIST partners at the Hollings Marine Laboratory (HML) are on-going to understand

these differences. Wheat flour, wheat gluten meal and menhaden oil were adjusted to maintain isolipidic and isonitrogenous diets.

Table 13. Composition of experimental diets for juvenile red drum fed a range of soy products.

Grams/100 grams	Conditioning	SBM 60% (#1)	Pro-Fine (#2)	Nutrivance (#3)	Nutriferma (#4)	HP 300 (#5)
Nutrivance, Soy PC	0.00	0.00	0.00	55.35	0.00	0.00
Nutraferma, Soy PC	0.00	0.00	0.00	0.00	47.20	0.00
HP 300, Soy PC [a]	0.00	0.00	0.00	0.00	0.00	50.41
Soy protein concentrate [b]	0.00	0.00	43.10	0.00	0.00	0.00
Soybean meal [c]	0.00	59.00	0.00	0.00	0.00	0.00
Wheat flour [d]	36.42	11.38	27.93	13.48	22.42	20.32
Wheat gluten meal	0.00	5.90	3.80	5.30	4.57	4.46
Poultry by-product meal	18.10	0.00	0.00	0.00	0.00	0.00
Corn protein concentrate	18.10	0.00	0.00	0.00	0.00	0.00
Blood meal	5.00	0.00	0.00	0.00	0.00	0.00
Menhaden oil [e]	10.20	12.75	14.20	14.35	14.45	13.42
Squid meal, CSF	4.08	4.08	4.08	4.08	4.08	4.08
Lysine HCl	2.40	1.68	1.61	1.95	1.60	1.87
Methionine	0.60	0.71	0.72	0.77	0.72	0.77
Threonine	0.80	0.30	0.26	0.47	0.26	0.47
Mono-Dical phosphate	2.40	2.30	2.40	2.35	2.40	2.30
Vitamin premix [f]	1.00	1.00	1.00	1.00	1.00	1.00
Choline CL	0.60	0.60	0.60	0.60	0.60	0.60
Vitamin C [g]	0.20	0.20	0.20	0.20	0.20	0.20
Trace min premix [h]	0.10	0.10	0.10	0.10	0.10	0.10
Formulated Composition, % as-is						
Crude Protein	41.08	40.06	40.08	40.06	40.03	40.10
Lipid	14.08	15.01	15.05	15.05	15.04	15.02
Phosphorus	0.92	0.90	0.90	0.91	0.91	0.92

[a] Hamlet Protein, HP-300, 560 g/kg crude protein.

[b] Solae, Pro-Fine VF, 693 g/kg crude protein.

[c] ADM, 468 g/kg crude protein

[d] Manildra Milling, 120 g/kg crude protein.

[e] Omega Proteins Inc., Virginia Prime menhaden oil .

[f] ARS 702; contributed, per kg diet; vitamin A 9650 IU; vitamin D 6600 IU; vitamin E 132 IU; vitamin K3 1.1 gm: thiamin mononitrate 9.1 mg; riboflavin 9.6 mg; pyridoxine hydrochloride 13.7 mg; pantothenate DL-calcium 46.5 mg; cyancobalamin 0.03 mg; nicotinic acid 21.8 mg; biotin 0.34 mg; folic acid 2.5 mg; inostitol 600 mg.

[g] Contributed in mg/kg of diet; manganese 13; iodine 5; copper 9; zinc 40.

5.2 Fish and Experimental Design

Captive, wild red drum broodstock were volitionally spawned at the Marine Resources Research Institute (MRRI) in Charleston, South Carolina by South Carolina Department of Natural Resources (SCDNR). Larval fish from a single unique genetic family were transported and stocked into earthen ponds at the Waddell Mariculture Center (WMC) in Bluffton, South Carolina in the fall of 2014. Fish were harvested after a mean size of 30 mm was obtained and transported to the MRRI for continued grow out in the winter of 2014. The recirculating culture system included eight, 1,600 liter tanks utilizing a sand filter, fluidized bed filter, and protein fractionation for mechanical and biological filtration and an UV sterilizer. Fish were fed to apparent satiation twice

daily with a standard commercial feed containing 40% protein and 10% lipids and excess feed was removed from tanks after ten minutes of no visible feeding. Fish were held at 21°C and a salinity of 30-32 mg L^{-1} during the winter grow-out period before being acclimated to experimental conditions in April of 2015.

Fish were split into experimental tanks on April 1st at a density of 35 fish $tank^{-1}$ and transitioned to a conditioning diet (table 9) for one month prior to the beginning of the trial. Fish were fed twice daily to satiation during the week and once daily on the weekends. Water temperature was increased four degrees to 25°C over a two week period to minimize stress. Initial mean weight of fish at the beginning of the feeding trial was 90.56 ± 3.82g. The six diets were randomly assigned to four tanks per treatment. All tanks were batch weighed on Day 0 and three fish per tank were randomly selected and sacrificed using a lethal dose of sodium bicarbonate buffered tricaine methanesulfonate (MS-222, Argent Labs) (500 mg L^{-1}) for initial body and eviscerated weights and lengths. Using a syringe with a 22 gauge needle, 1 to 2 ml of blood from the fish caudal vasculature were collected into Li heparin collection tubes and gently inverted 8 times. The collection tubes were rapidly placed on ice. Blood samples were then centrifuged at 2000xg at 4°C for 6 min. The top layer (plasma) was transferred into 2 ml cryovials, flash frozen in liquid nitrogen and stored at -80°C. After blood was drawn fish were euthanized with an overdose of MS-222 for 3 min prior to dissection. Intestine tissue extended from just posterior to the pyloric caeca to just anterior to the anus was excised, sliced lengthwise to open, and rinsed clean with cold 3% saline solution. The entire liver was excised and similarly rinsed. These two tissues were placed into 5 ml cryovials, flash frozen in liquid nitrogen, and stored at -80°C. The fish were then fully eviscerated, weighed again for carcass weight, and the one consistent fillet removed. Muscle punch samples removed from the fillet, 4-6 per individual, were collected, placed in 5 ml cryovials, flash frozen in liquid nitrogen, and stored at -80°C. Treatments were split into 2 groups (A and B), which were alternated during sampling events to minimize handling stress. Tank batch weights and metabolomic tissue sampling from six fish per tank occurred on weeks 2-5 and 9-12 alternating the A and B groups. Weekly sampling was reduced to minimize sample processing and still allow important transitions in metabolomic profiling to be detected. Fish were fed to apparent satiation twice daily during the week and once during the weekend. Any excess fed was siphoned and removed from the system after 10 minutes of no visible feeding and water exchanges were completed after tank cleaning utilizing settled, polished seawater from the Charleston Harbor. Water temperature, dissolved oxygen, pH and salinity were recorded two times per week on a subset of tanks (n= 6 tanks/sampling) and ammonia, nitrite and nitrate measured weekly (n=6 tanks/week) using Hach spectrophotometer reagents. Additional fish were sacrificed at the conclusion of the 12-week growth trial for whole-body (n=5 fish/treatment) and fillet composition (n=5 fish/treatment). Proximate analysis on the whole body and fillets was performed by Clemson University Feed and Forage Laboratory in Clemson, South Carolina.

5.3 NMR Metabolomics Sample Preparation, Data Collection and Spectroscopy

Frozen plasma samples were thawed on ice for ~ 2 hours. 350 µl of plasma per sample were loaded onto spin filters (3 kDa molecular weight cutoff) that were previously washed in DI water overnight. Filters were then centrifuged at 10,000xg, at 4°C for 90 min and for up to two

times an additional 30 min for samples that provided less than 200 µl of filtrate. 200 µl of filtrate was transferred into Eppendorf tubes and 400 µl of NMR buffer was added to each sample to a final volume of 600 µl. The samples were then vortexed for a few seconds and centrifuged. 550 µl of the resulting solution was transferred into 5 mm NMR tubes.

The total water content of each tissue (liver, muscle, intestine) was determined prior to this experiment to determine appropriate solvent volumes. The average weights of wet tissues were used to calculate the solvent volumes used for extraction. In each extraction set, seven or eight experimental samples along with QC materials were extracted using a slightly modified Bligh-Dyer bi-phasic solvent system. The QC samples used during tissue preparation were appropriate pooled tissues: control materials and NIST SRM 1946 – Lake Superior Fish Tissue. A cold polar solvent mixture, methanol (4 mL g^{-1} wet weight, henceforth 'gww') (Honeywell) and Millipore water (1.6 mL g^{-1} ww), was added to the frozen homogenate sample in the ceramic bead tube. The tissues/polar solvents were mixed using a Precellys 24 homogenizer (Bertin Technologies) in two cycles of 15 s at 6500 rpm. The whole polar homogenate was transferred to a glass vial containing cold chloroform (4 mL g^{-1} ww) (Fisher Scientific) and Millipore water (2 mL g^{-1} ww) for a final solvent volume ratio of 2 chloroform: 2 methanol: 1.8 water. The mixture was vortexed for 30 s and incubated on ice for 10 min. The solvent phases were partitioned by centrifugation at 2000 x g at 4 °C for 5 min. The upper polar phase was collected into a 1.5 mL Eppendorf tube, and dried by vacuum centrifuge for 2 hours at room temperature (Eppendorf, Vacufuge). Dried polar extracts were re-hydrated with 600 µL of NMR buffer, and 550 µL of each sample was then transferred into 5 mm NMR tubes for analysis.

Approximately 2370 samples (5 experimental diets with various soy protein products plus a natural reference diet; liver, plasma, muscle, quality control) were prepared and analyzed by NMR. Preliminary analysis of these results advised the sample collection and analysis protocols for trial 2. In addition, NMR spectra such as ^{13}C-HSQC and TOCSY experiments were collected on selected samples to aid compound identification.

All spectra were obtained at a temperature of 298 K on a Bruker Advance II 700 MHz NMR spectrometer (Bruker Biospin, Inc., Billerica, MA) equipped with a cryoprobe (TCI 5 mm triple-resonance, z-gradient). Spectra were collected under full automation using ICON-NMR with a standard 1D pulse sequence (noesygppr1d). The NMR protocol included 10 minutes for temperature equilibration, automated shimming with on-axis and off-axis shims, automated probe tuning and pulse calibration on each individual sample. ^{1}H spectra were acquired with 65536 real data points across a spectral width of 20 ppm with 8 steady state scans, 80 transients, a 3 s relaxation delay, a 60 ms mixing period and an acquisition time of 2.34 s for a total repetition time (D1 + AQ) of 5.34 s. The spectra were Fourier transformed after multiplying the free induction decay by an exponential line broadening function of 0.3 Hz and zero-filling to 65536 complex points. The spectra were manually phased, and the baseline was automatically corrected with a fifth order polynomial. For the trial 1 samples, additional spectra were acquired under similar parameters including CPMG, 2D JRES and PURGE water suppression, giving an NMR protocol duration of approximately 60 minutes per sample.

Two-dimensional edited ^{13}C heteronuclear single quantum correlation (HSQC) spectra with adiabatic ^{13}C decoupling (hsqcedetgpsisp2.2) were collected on selected samples to enable improved metabolite identification. In general, 128 scans and 2048 data points with 512 increments

were acquired with spectral widths of 11 ppm in F2 and 180 ppm in F1 (^{13}C). A relaxation delay equal to 1.5 s was used between acquisitions, and a refocusing delay corresponding to a 145 Hz $^{1}J_{C\text{-}H}$ coupling was used. The FIDs were weighted using a shifted sine-square function in both dimensions. Manual two-dimensional phasing was applied; all spectra were referenced to the TMSP internal standard at 0.00 ppm for ^{1}H and ^{13}C.

Selected samples were also used for 2-dimensional Total Correlation Spectroscopy (TOCSY) analysis to elaborate the ^{1}H-^{1}H coupling networks for compound identification. A phase-sensitive TOCSY with a DIPSI2 mixing sequence (90 ms duration) and water suppression via pre-saturation and excitation sculpting (dipsi2esgpph) was used for this. In general, 48 scans and 2048 data points with 256 increments were acquired with spectral widths of 10 ppm in F1 and F2. A relaxation delay equal to 1.5 s was used between acquisitions. The FIDs were weighted using a shifted sine-squared function in both dimensions, and the data was Fourier transformed to 4096 by 1024 complex points by zero filling. Manual two-dimensional phasing was applied; all spectra were referenced to the TMSP internal standard at 0.00 ppm for ^{1}H.

5.4 NMR Spectral Analysis, Multivariate Analysis and Quality Control

Metabolites were identified based on 1D ^{1}H, 2D ^{1}H-^{1}H TOCSY and 2D ^{1}H-^{13}C HSQC NMR experiments. Identities were based on comparison of chemical shifts and spin-spin couplings with reference spectra and tables noted in published reports, the Human Metabolome Database (HMDB), the Biological Magnetic Resonance data bank (BMRB), an in-house compiled spectrabase and Chenomx® NMR Suite profiling software (version 8.1). Metabolite identification most often was achieved at a Level 2, putative identification level (Sumner Ref).

For multivariate analysis, the spectra were binned with a bin size of 0.005 ppm between 0.2 ppm and 10.0 ppm and certain spectral regions were excluded because of spectral artifacts due to water suppression or because of contaminants that appeared in our blank sample spectra. Spectra were checked for uniform referencing and baseline condition and normalized to constant total spectral intensity after binning and exclusions. Generally, principal component analysis (PCA) was conducted on appropriate subsets of the data with appropriate class labeling of the subsets to aid in visual pattern recognition. Pareto normalization with mean centering of the bins was used in all cases to account for the sometimes wide dynamic range of spectral feature intensity. PCA scores plots were assessed for meaningful groupings and groups were assessed for significant differences using ± 1 standard error of the mean (SEM) error bars and Student's t-tests.

Quality control materials were used during this study to ensure the reproducibility of the sample processing method. Red Drum Fillet Control Material (RD-FCM) and Liver Control Material (LCM) were prepared by pooling homogenized fillet or liver samples collected during the preliminary studies. NIST SRM 1946– Lake Superior Fish Tissue and pooled tissue control materials were extracted along with both liver and muscle test samples. Along with the test plasma samples, NIST standard reference materials SRM 1950–Human plasma and Red Drum Control Plasma (RDCP) were processed. Control plasma was prepared by pooling the extra red drum plasma samples collected during the previous studies. In addition to SRM and pooled control materials, experimental samples were prepared in triplicates or duplicates as technical replicates.

Blanks which do not contain any tissue were prepared to test for contamination during sample processing.

For the trial 2 growth trial (5 experimental diets with varying soy protein formulations, plus a positive reference diet and a pelleted reference diet), approximately 2376 samples (liver, muscle, plasma, quality reference) were prepared and analyzed by NMR. In addition, NMR spectra such as ^{13}C-HSQC and TOCSY experiments were collected on selected samples to aid compound identification. For the trial 2 samples, only an additional 2D JRES spectrum was collected resulting in an NMR protocol duration of approximately 45 minutes per sample.

5.5 Gene Expression Assays

Sub-samples of tissue from sample preparation for the metabolomics analyses were utilized for gene expression assays. These consisted of aliquots of homogenized liver stored at -80°C. Six of twelve fish sampled at each sampling point for each diet were used for gene expression analyses from the second trial and samples from all weeks where sampling occurred were analyzed. RNA was extracted via a standard phenol/chloroform extraction, dried and reconstituted in 50 µl water, and quantified using a Qbit™ fluorometer. 1000 ng of RNA from each sample was used in a reverse transcription reaction (iScript RT Supermix, Bio-Rad, Hercules, CA, USA) and diluted to 10 ng μl^{-1}. Genes selected based on the transcriptomic sequencing were analyzed in two multiplexed reaction sets using iQ Multiplex Powermix (Bio-Rad, Hercules, CA, USA) with 800 µmolar primer and 400 µmolar probe concentrations in 10 µl reaction volumes (Tables 3 and 4). Elongation factor 1-alpha (EF1A) was used as a common reference gene across all q-PCR panels. All samples were run with 10 ng total RNA in triplicate on a Bio-Rad CFX96 Touch Real Time PCR Detection system (Bio-Rad, Hercules, CA, USA). Currently all plots and statistics have been run solely within the Bio-Rad CFX manager software.

5.6 Calculations and Statistical Analyses

The standard performance parameters utilized in this feeding trial to compare treatments were:

- Weight gain, % = (final weight − initial weight) / initial weight ∗ 100
- Specific growth rate, SGR = ln (final weight − initial weight) / days ∗ 100)
- Protein efficiency ratio, PER = grams weight gained / grams protein fed
- Feed conversion ratio, FCR = grams fed / grams weight gained
- Condition factor, K = (weight (g) ∗ 100) / (length $(cm)^3$)
- Hepatosomatic index, HSI = (liver weight / body weight) * 100

The effects of experimental treatments were compared using an ANOVA with significance levels determined using Tukey's post-hoc test, with critical limits set to $P < 0.05$.

6.0 Results from second feeding trial

6.1 Diets

Proximate and mineral compositions of the experimental feeds used in the second feeding trial are shown in table 14. A commercial reference diet was not utilized in this trial, however a reference diet of equal parts fish, squid, and shrimp was used to compare the performance of the experimental feeds to the theoretical maximum performance that can be observed in this RAS under these conditions. Compositions for the components of the natural diet are shown separately.

6.2 Feeding trial

Water quality parameters during the second feeding trial are shown in table 15. All measured parameters were within optimal ranges for juvenile red drum.

Table 15. Water quality parameters during the second trial.

Parameter	Average ± S.D.
Temperature (°C)	25.1 ± 0.3
Dissolved Oxygen (mg L^{-1})	5.88 ± 0.4
Salinity (ppt)	31.67 ± 0.69
pH	7.49 ± 0.09
NH_3 (mg L^{-1})	0.11 ± 0.07
NO_2 (mg L^{-1})	0.030 ± 0.006
NO_3 (mg L^{-1})	2.7 ± 0.7

Production characteristics from the second feeding trial are shown in table 16. There was a significant difference in feed consumption between treatments (ANOVA, P=0.021) with fish consuming significantly more of the Nutraferma based diet per fish than the Pro-Fine based diet. In spite of this difference, weight gain in grams gained per fish, weight gain as a percent of initial weight, final weight, final length, feed conversion ratio, specific growth rate, and condition factor were all found to not be significantly different across treatments. The natural diet treatment was not included in these statistical analyses, however all parameters were found to significantly out-perform all experimental feeds when a separate ANOVA was run.

Proximate and mineral compositions of whole body tissue from each treatment are shown in table 17. Dry matter content was significantly lower in the whole body tissue from the SBM 60% treatment than the Nutrivance and HP 300 treatments (P=0.007). No other significant differences were observed between treatments in regards to dry matter. No significant differences were observed in whole body protein, fat, or ash between treatments. Both phosphorous and calcium exhibited similar patterns of significance between treatments with the Pro-Fine treatment being significantly lower than the HP 300 treatment with all other dietary treatments falling between those two and not significantly different from each other or the Pro-Fine and HP 300 treatments. Potassium was found to be significantly higher in the Nutraferma treatment than the Pro-Fine and HP 300 treatments. The Pro-Fine treatment was also significantly lower in potassium concentration than the Nutrivance treatment. No significant differences were observed in the other minerals (Table 17).

Proximate and mineral compositions of the fillet tissues from each dietary treatment are shown in table 18. Fillet protein was significantly higher in the Nutrivance treatment compared to all other dietary treatments, with no other significant differences between treatments. Fillet ash content was significantly lower in the Pro-Fine treatment when compared to the SBM 60% and Nutraferma treatments, but was not significantly different from the Nutrivance or HP 300 treatments. No significant differences were observed in fillet dry matter, fat or any of the minerals (Table 18).

Table 14. Proximate composition of diets for second feeding trial (Clemson University analyses).

	SBM 60% (#1)	Pro-Fine (#2)	Nutrivance (#3)	Nutraferma (#4)	HP 300 (#5)	Natural Diet Components (fed in equal parts)[1]		
						Shrimp	Squid	Fish
Crude protein (g $100g^{-1}$)	44.28	43.78	46.41	43.06	46.28	74.97	75.03	71.13
Fiber (ADF) (g $100g^{-1}$)	7.25	11.55	4.5	4.4	4.2	8.05	4.3	3.7
Crude fat (g $100g^{-1}$)	8.85	8.8	8.2	11	8.4	3.1	8.3	6.7
Ash (g $100g^{-1}$)	6.55	5.35	4.75	6.3	6.1	13.75	7.4	17.55
Dry matter (g $100g^{-1}$)	93.53	93.46	94.66	93.91	92.78	29.48	33.26	35.56
Phosphorous (g $100g^{-1}$)	9834.77	9700.33	10533.8	10024.87	9880.38	14774.75	11468.35	22808.8
Potassium (g $100g^{-1}$)	15278.5	10901.65	4266.43	14230.4	15049.45	10060.55	13537.2	9329.9
Calcium (g $100g^{-1}$)	8950.88	8057.3	10167.4	9042.37	7836.47	39988.9	1170.11	35212.85
Magnesium (g $100g^{-1}$)	2408.87	1949.94	1515.72	2243.64	2120.2	3951.18	2267.67	1424.86
Sulfur (g $100g^{-1}$)	7978.65	8076.38	8476.26	7865.62	8250.48	10531.7	16756.2	7775.53
Zinc (ppm)	125.63	119.02	138.55	129.83	139.54	61.55	86.83	74.7
Copper (ppm)	38.67	41.8	56.08	46.94	53.78	61.64	77.9	14.37
Manganese (ppm)	65.34	66.54	68.98	67.91	72.37	5.86	2.87	3.83
Iron (ppm)	428.19	406.45	480.95	394.35	396.02	89.55	63.56	115.25

[1] Dry weight basis.

Table 16. Production characteristics from the second feeding trial. ANOVA (p=0.05) to test for significant differences between dietary treatments. Natural diet feed consumption is wet weight and excluded from analysis. Values with different superscripts are significantly different from one another.

Treatment	Feed consumption (g fish)	Weight gain (g)	Weight gain (% initial)	Final weight (g)	Final length (mm)	FCR	PER	SGR	Condition factor
SBM 60% (#1)	151.98 ± 6.32[a,b]	55.31 ± 16.91	61.94 ± 19.49	144.80 ± 16.33	241.25 ± 26.13	2.99 ± 1.06	0.82 ± 0.23	0.57 ± 0.15	0.99 ± 0.12
Pro-Fine (#2)	123.29 ± 16.83[a]	73.66 ± 24.17	80.42 ± 22.31	164.00 ± 30.39	239.08 ± 22.32	1.80 ± 0.50	1.36 ± 0.32	0.70 ± 0.16	1.06 ± 0.13
Nutrivance (#3)	139.54 ± 11.60[a,b]	88.76 ± 24.23	98.18 ± 26.56	179.05 ± 25.41	257.50 ± 16.20	1.64 ± 0.35	1.37 ± 0.29	0.81 ± 0.15	1.08 ± 0.06
Nutraferma (#4)	157.15 ± 16.32[b]	83.52 ± 39.09	90.00 ± 42.41	176.74 ± 38.52	247.33 ± 27.39	2.20 ± 0.94	1.23 ± 0.46	0.74 ± 0.27	1.03 ± 0.05
HP 300 (#5)	137.32 ± 12.65[a,b]	75.18 ± 18.51	83.21 ± 21.12	165.68 ± 18.18	255.25 ± 14.40	1.91 ± 0.46	1.18 ± 0.28	0.71 ± 0.14	1.05 ± 0.07
Natural	1201.33 ± 2.62	308.04 ± 27.53	344.87 ± 36.03	397.52 ± 27.73	318.67 ± 17.72	1.30 ± 0.13[1]	1.05 ± 0.09[1]	1.78 ± 0.09	1.21 ± 0.05
P	0.021	0.449	0.505	0.432	0.169	0.117	0.174	0.479	0.150

[1] FCR and PER for natural diet calculated using dry weight of natural feed items (assuming 67% water content – derived from average weight of oven dried natural feed items).

Table 17. Proximate analyses for whole body. ANOVA (p=0.05) to test for significant differences between dietary treatments (Natural diet excluded). Values with different superscripts are significantly different from one another.

Treatment	Dry matter (%)	Protein (%)	Fat (%)	Ash (%)	P (ppm)	K (ppm)	Ca (ppm)	Mg (ppm)	Zn (ppm)	Cu (ppm)	Mn (ppm)	Fe (ppm)	S (ppm)	Na (ppm)
SBM 60% (#1)	24.35 ± 0.01[a]	73.18 ± 2.07	7.43 ± 2.29	16.53 ± 2.47	27248.54 ± 2686.37[a,b]	12656.48 ± 369.66[a,b,c]	49795.66 ± 4815.17[a,b]	1514.30 ± 149.48	48.37 ± 2.95	24.63 ± 12.91	20.09 ± 4.03	53.61 ± 10.66	9461.03 ± 906.18	6003.10 ± 662.84
Pro-Fine (#2)	25.73 ± 0.01[a,b]	70.85 ± 4.29	9.77 ± 1.11	14.05 ± 1.58	24391.99 ± 1383.31[a]	12022.51 ± 528.24[a]	43140.97 ± 4483.05[a]	1430.14 ± 81.86	43.85 ± 3.65	12.04 ± 4.54	16.59 ± 2.50	44.69 ± 5.91	9585.42 ± 329.34	5478.61 ± 298.88
Nutrivance (#3)	26.13 ± 0.01[b]	76.35 ± 6.43	8.46 ± 1.85	15.54 ± 1.26	26772.07 ± 1686.83[a,b]	12890.83 ± 497.26[b,c]	46089.07 ± 4697.63[a,b]	1495.94 ± 57.91	48.19 ± 3.05	18.30 ± 9.71	15.06 ± 1.69	46.21 ± 6.75	10205.53 ± 432.78	5476.36 ± 342.56
Nutraferma (#4)	25.08 ± 0.00[a,b]	76.69 ± 5.47	8.41 ± 1.26	15.05 ± 1.48	26112.27 ± 2417.67[a,b]	13203.18 ± 674.12[c]	45082.10 ± 6403.01[a,b]	1434.61 ± 99.39	46.49 ± 5.38	15.67 ± 3.18	18.92 ± 2.59	49.81 ± 12.89	10330.56 ± 354.00	5845.36 ± 307.29
HP 300 (#5)	26.03 ± 0.01[b]	70.88 ± 3.43	10.61 ± 1.52	15.96 ± 2.47	29465.62 ± 2044.92[b]	12366.92 ± 571.30[a,b]	52471.67 ± 6586.25[b]	1591.48 ± 122.83	49.24 ± 2.85	16.61 ± 5.81	15.46 ± 3.60	50.79 ± 9.85	9654.05 ± 548.50	5564.45 ± 655.61
Natural	28.15 ± 0.00	66.49 ± 2.84	12.34 ± 1.26	15.74 ± 1.00	29011.18 ± 1742.87	11069.51 ± 581.88	49799.30 ± 4068.58	1542.40 ± 67.05	43.64 ± 2.73	15.48 ± 6.76	6.67 ± 0.92	37.86 ± 5.24	8294.88 ± 422.20	4221.23 ± 214.70
P	0.007	0.059	0.059	0.316	0.006	0.001	0.041	0.080	0.175	0.176	0.059	0.450	0.055	0.364

Table 18. Proximate analyses for fillets. ANOVA (p=0.05) to test for significant differences between dietary treatments (Natural diet excluded). Values with different superscripts are significantly different from one another.

Treatment	Dry matter (%)	Protein (%)	Fat (%)	Ash (%)	P (ppm)	K (ppm)	Ca (ppm)	Mg (ppm)	Zn (ppm)	Cu (ppm)	Mn (ppm)	Fe (ppm)	S (ppm)	Na (ppm)
SBM 60% (#1)	24.62 ± 0.04	87.59 ± 1.31[a]	1.00 ± 0.12	4.77 ± 0.21[a]	9397.88 ± 275.81	19106.02 ± 347.55	784.50 ± 407.80	1366.14 ± 66.26	28.43 ± 4.36	50.11 ± 100.86	1.99	64.28 ± 107.15	11705.66 ± 425.94	1697.27 ± 467.22
Pro-Fine (#2)	22.79 ± 0.04	87.56 ± 2.07[a]	1.10 ± 0.27	4.55 ± 0.21[b]	7311.08 ± 3445.98	14346.02 ± 6904.60	541.67 ± 249.51	1068.73 ± 501.61	20.36 ± 9.66	6.15 ± 5.53	< 1.00	25.38 ± 19.00	8413.74 ± 3934.68	1232.76 ± 586.49
Nutrivance (#3)	24.31 ± 0.06	95.41 ± 1.72[b]	0.62 ± 0.22	5.14 ± 0.17[a,b]	9956.84 ± 564.13	18726.50 ± 652.09	875.67 ± 261.84	1473.23 ± 72.20	29.17 ± 4.20	7.59 ± 2.99	1.27 ± 0.13	41.8 ± 13.4	11769.99 ± 1164.30	1752.88 ± 114.88
Nutraferma (#4)	21.93 ± 0.05	86.65 ± 2.07[a]	0.82 ± 0.04	5.20 ± 0.19[a]	10029.12 ± 534.83	19157.50 ± 503.60	1613.42 ± 1245.41	1432.95 ± 91.52	30.23 ± 10.12	13.48 ± 6.57	1.41 ± 0.01	53.64 ± 24.18	12555.00 ± 189.65	1928.65 ± 415.81
HP 300 (#5)	23.89 ± 0.02	86.36 ± 1.12[a]	1.02 ± 0.28	5.56 ± 1.58[a,b]	9524.85	18335.50	438.38	1278.50	22.25	9.13	2.10	71.13	10765.10	1338.16
Natural	23.82 ± 0.01	85.86 ± 2.18	1.60 ± 0.58	5.16 ± 0.18	9540.31 ± 257.37	17673.32 ± 719.88	910.85 ± 725.53	1252.87 ± 37.21	21.60 ± 3.63	16.04 ± 6.32	2.62 ± 1.63	63.41 ± 36.80	10668.36 ± 381.58	1275.99 ± 174.31
P	0.865	0.0001	0.588	0.011	0.274	0.328	0.132	0.273	0.259	0.727	n/a	0.867	0.143	0.267

Table 19 shows the eviscerated body weights (g) and hepatosomatic index (HSI) for each treatment at the conclusion of the 12-week trial (n=12 per dietary treatment). There was no significant difference between treatments for eviscerated body weight (ANOVA, *P*=0.183). Hepatosomatic index was significantly different between treatments (ANOVA, *P*=0.002). The Pro-Fine dietary treatment resulted in a significantly higher HSI than the SBM 60%, Nutrivance, and Nutraferma treatments but was not significantly different than the HP 300 treatment.

Table 19. Eviscerated fish weight (g) and hepatosomatic index (HSI) at final sampling. ANOVA (p=0.05) to test for significant differences between dietary treatments (Natural diet excluded).

Treatment	Eviscerated Weight (g)	Hepatosomatic Index
SBM 60% (#1)	132.50 ± 52.64	0.94 ± 0.23[a]
Pro-Fine (#2)	137.17 ± 46.93	1.38 ± 0.44[b]
Nutrivance (#3)	170.33 ± 32.22	1.04 ± 0.22[a]
Nutraferma (#4)	147.33 ± 49.42	1.01 ± 0.21[a]
HP 300 (#5)	161.17 ± 31.13	1.25 ± 0.26[a,b]
Natural	366.00 ± 71.37	1.14 ± 0.18
P	0.183	0.002

6.3 NMR Metabolomics

The target tissues were analyzed via PCA analysis in two ways, one to examine the time evolution (trajectory analysis) of the metabolome, and the second an analysis of the equilibrated metabolome from weeks 9-12 once the fish had acclimated to the various feeds.

Liver Trajectories

The liver tissue samples from points T0 through T12 (nine time points: T0, T2, T3, T5, T9, T10, T11, T12) were used to build PCA models for each of the five experimental diets and the natural diet (CUT), with the latter used as a positive control (Figure 24). The total explained variance in PC1 and PC2 was approximately 70% for all models. In this figure, the sequential time points are connected with a solid line so that any time-dependent pattern would be distinguishable. It can be observed that the natural diet displays a clear trajectory that progresses from the left to the right of the score plot with time. This trajectory moves steadily to the right for the first few weeks of the study (T2-T4), but starting from about week 5 and until week 12, the metabolomic trajectory stabilizes around a single point indicating that the fish on this diet have reached some sort of metabolic equilibrium. The experimental diets (#1-5) similarly move steadily to the right, although less rapidly compared with the natural diet, requiring 3-4 weeks to develop an intermediate metabolic profile, which significantly differs from the initial state as represented by T0. These diets seem to reach a final homeostasis around weeks 9 through 12. Below, we will focus on differences amongst the six diets at the end points (T9-T12) to investigate whether this trend in the liver metabolomic profiles shows consistent patterns among all the experimental diets.

Muscle Trajectories

The muscle tissue samples from nine time points (T0, T2, T3, T5, T9, T10, T11, T12) were used to generate PCA scores plots for each of the five experimental diets (diets #1-5) and the natural diet (CUT) (Figure 25). The total explained variance in PC1 and PC2 was approximately 60%-70% for all models. In this figure, the sequential time points are connected with a solid line so that any time-dependent pattern would be distinguishable. In the case of the natural diet the explained variance in PC1 alone is 65.6% and appears to be dominated by the difference in metabolic profiles between the T0 state on one hand and the time points T2-T12 on the other. As far as the five experimental diets are concerned, a trajectory which progresses with time from one side of the plot to the opposite side (the direction of the trajectory is not relevant since the sign is arbitrary) reflect metabolome differences between the reference diet and the experimental diets in the context of the muscle tissue. In general, for the experimental diets there is no significant difference along PC1 among time points T9-T12, once again indicating that a stable metabolic state is reached passed week 9, thus justifying our use of the combined T9, T10, T11 and T12 as the end point (T_end) of the trajectory for comparison of the experimental diets at the end of the growth period.

Plasma Trajectory

Plasma samples from nine time points (T0, T2, T3, T5, T9, T10, T11, T12) were used to generate PCA scores plots for each of the five experimental diets (diets #1-5) and the reference diet (natural) (Figure 26). The total explained variance in PC1 and PC2 was approximately 60% for all models. In this figure, the sequential time points are connected with a solid line so that any time-dependent pattern would be distinguishable. Larger variability for each diet/time point obscures and makes the detection of any significant trends difficult. Nonetheless, there is little significant difference in PC1 for the terminal times T9-T12, therefore, T9, T10, T11 and T12 were combined as the end point (T_end) of the trajectory to investigate possible differences in the end point of the metabolic trajectory for each of the diets.

Figure 24. Liver PCA models for the 5 soy-based experimental diets (diet#1-5) and the natural diet (reference) for all sampled time points. Error bars represent the mean ± 1 SEM.

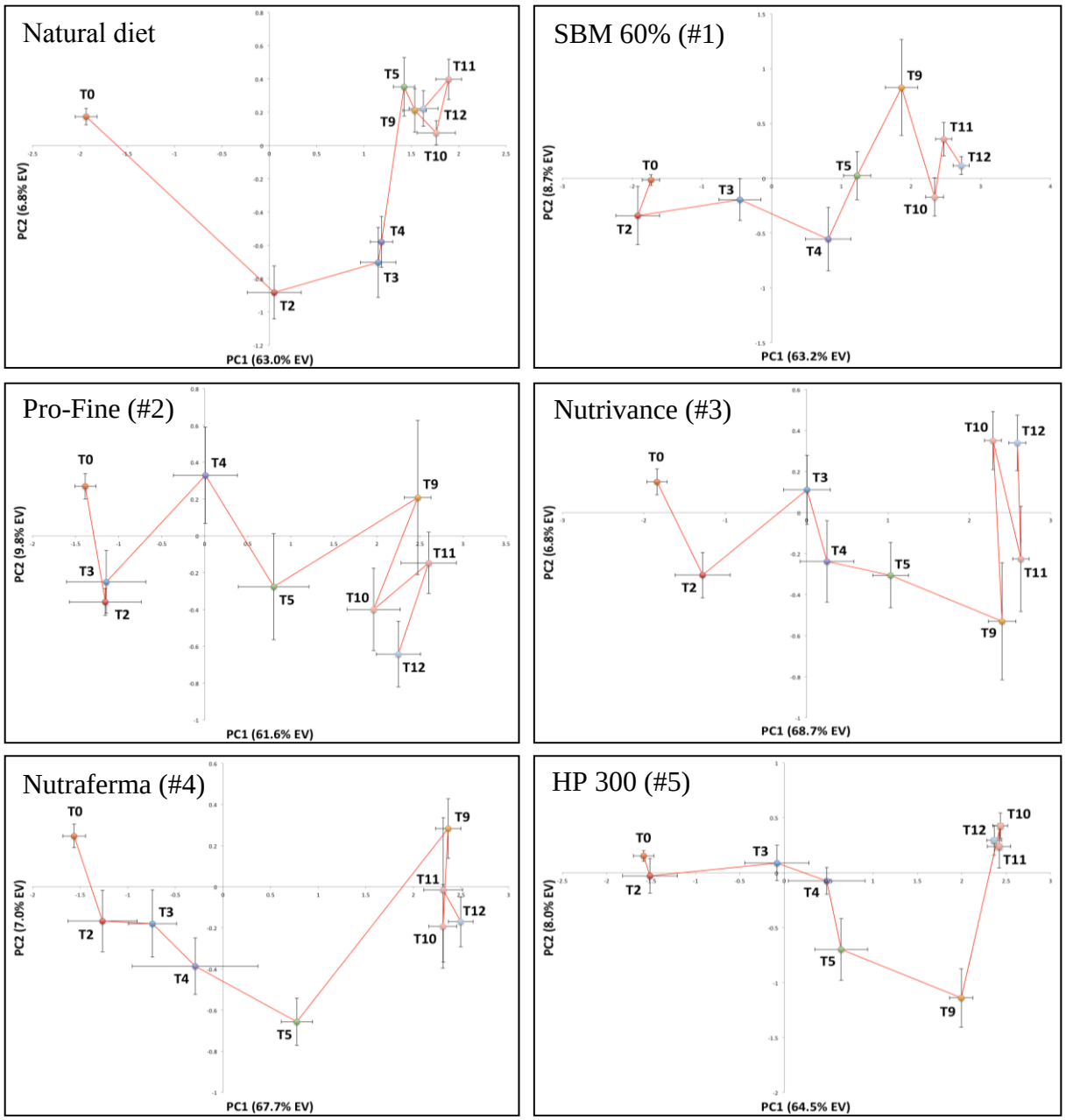

Figure 25. Muscle PCA models for the 5 soy-based experimental diets (diet #1-5) and the natural diet (reference) for all sampled time points. Error bars represent the mean ± 1 SEM.

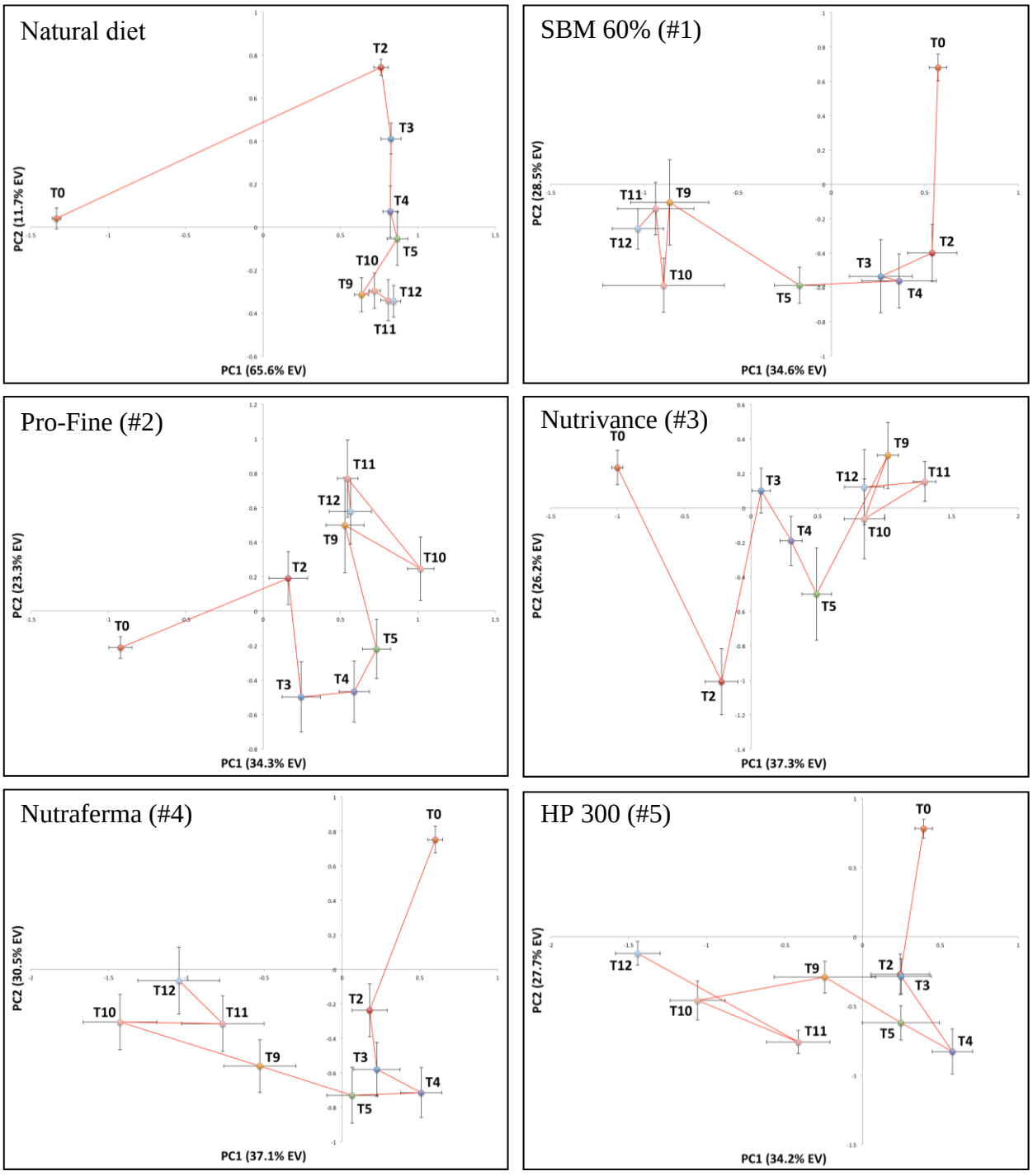

Figure 26. Plasma models for the 5 soy-based experimental diets (diet #1-5) and the natural diet (reference) for all sampled time points. Error bars represent the mean ± 1 SEM.

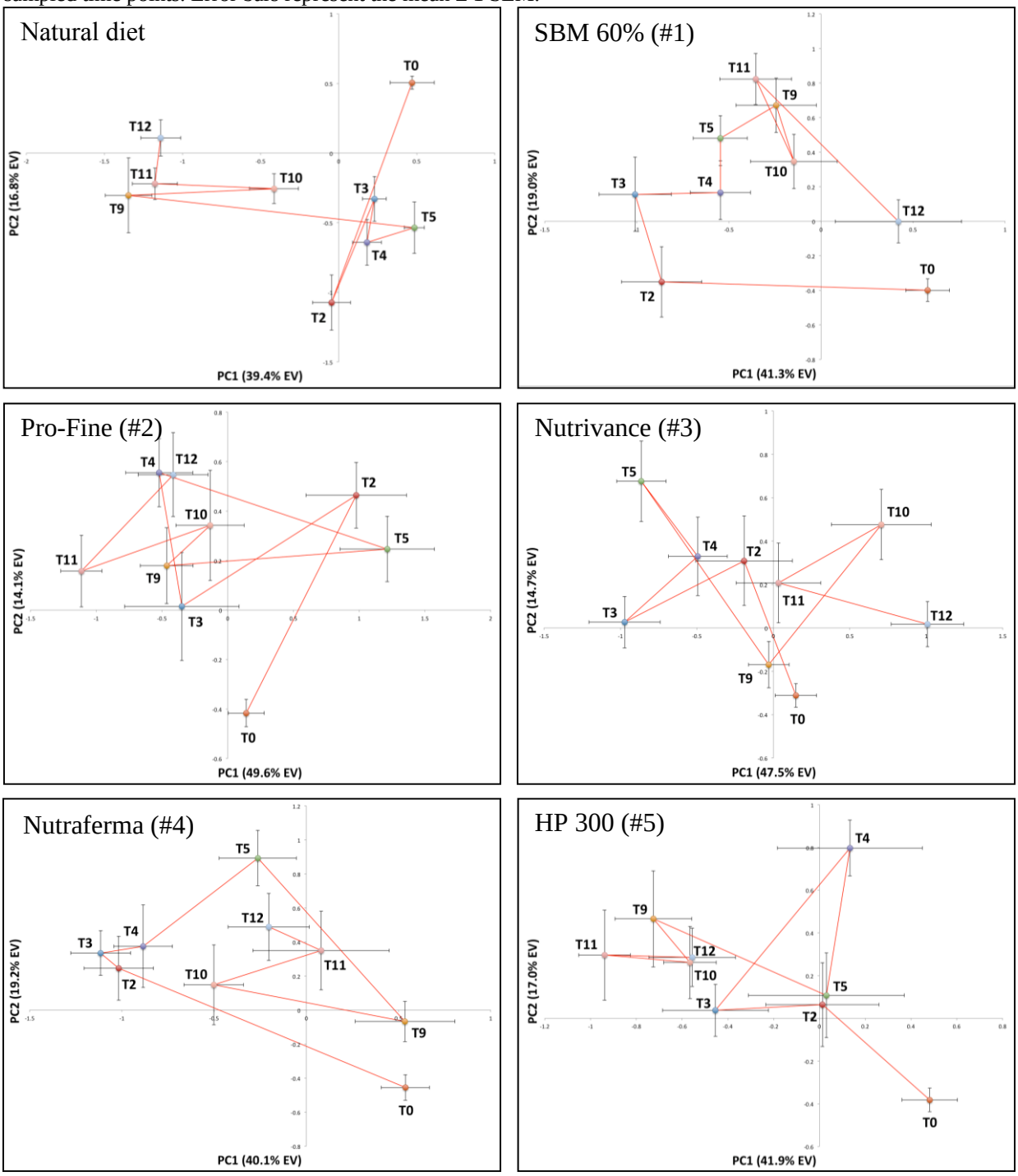

Metabolomics Endpoints.

The various tissues were analyzed at the end of the growth period via PCA to examine the time course of metabolic changes as a result of the soy-based experimental diets compared with the natural diet (reference). The end point, T_end, was comprised of samples from T9, T10, T11 and T12 for liver, muscle and plasma samples. Combining these time points was justified based on the observed homeostasis for all tissues after the 9-week period and it allowed an increase in the number of samples for the analysis and consequently in the numerical strength of the PCA models.

Liver Endpoint

The liver samples show a significant difference in the metabolic profiles between the natural diet (CUT, reference) on the left side of the PCA scores plot and the experimental diets (diet #1-5) on the right side, along PC1 (Figure 27). The total explained variance in PC1 and PC2 is approximately 46.5%. Additionally, this model indicates some differences among the different experimental diets, in particular diet #2 is significantly different from the other four experimental diets (#1, 3, 4 and 5).

Figure 27. Liver end point (T_end) PCA scores plots for the 5 experimental diets and the natural diet (CUT). Error bars represent the means ± 1 SEM.

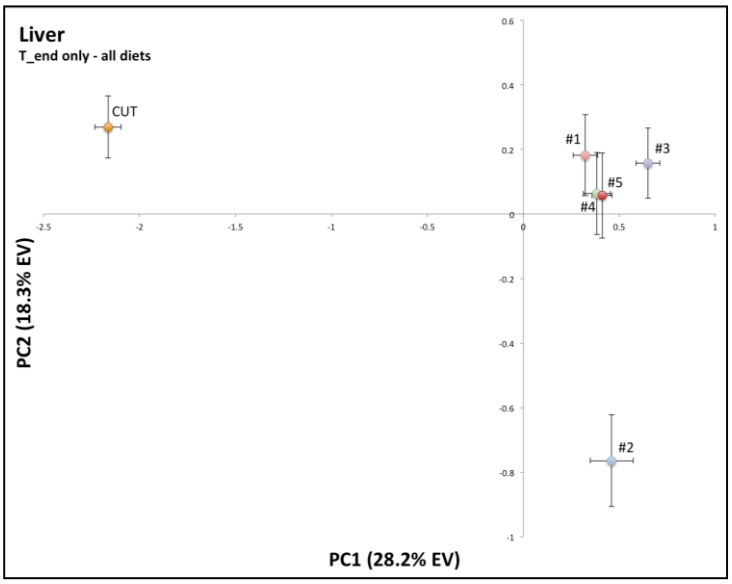

Figure 28. Liver end point (T_end) PCA scores plots for the 5 experimental diets (diet #1-5). The natural (CUT) diet was not included. Error bars represent the means ± 1 SEM.

An additional PCA model was generated, which excluded the natural diet samples, thus focusing on the differences among the five experimental diets (Figure 28). This new model has a total explained variance in PC1 and PC2 of 41.9% and shows a significant difference between diet #2 and the other four experimental diets (#1, 3, 4 and 5) along PC1.

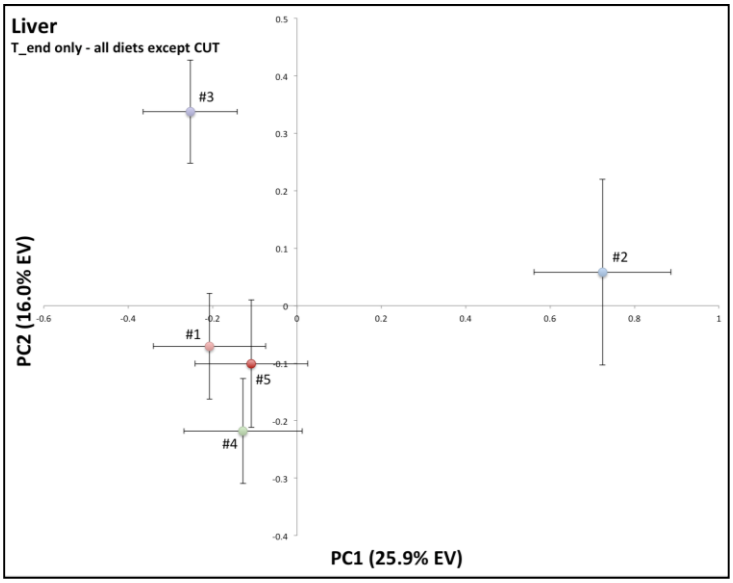

Muscle Endpoint

Similar to the liver samples, the muscle tissue samples show a significant difference in the metabolic profiles between the natural diet (CUT, reference) on the left side of the PCA scores plot and the experimental diets (diet #1-5) on the right side, along PC1 (Figure 29). The total explained variance in PC1 and PC2 is 63.8%. Once again, this model indicates that among the various soy formulations, diet #2 is significantly different from the other four soy-based diets (#1, 3, 4 and 5).

Figure 29. Muscle end point (T_end) PCA scores plots for the 5 experimental diets (diet #1-5) and the natural diet (reference). Error bars represent the means ± 1 SEM.

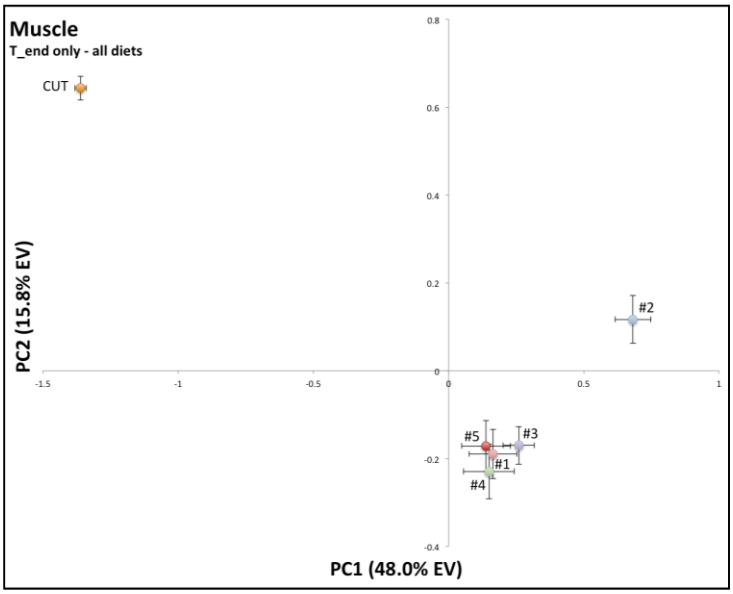

An additional PCA model was generated, which excluded the natural diet samples, thus focusing on the differences among the five experimental diets (Figure 30). This new model has a total explained variance in PC1 and PC2 of 63.7% and shows a significant difference between diet #2 and the other four soy-based diets (#1, 3, 4 and 5) along PC1.

Figure 30. Muscle end point (T_end) PCA scores plots for the 5 experimental diets (diet #1-5). The natural diet was not included. Error bars represent the means ± 1 SEM.

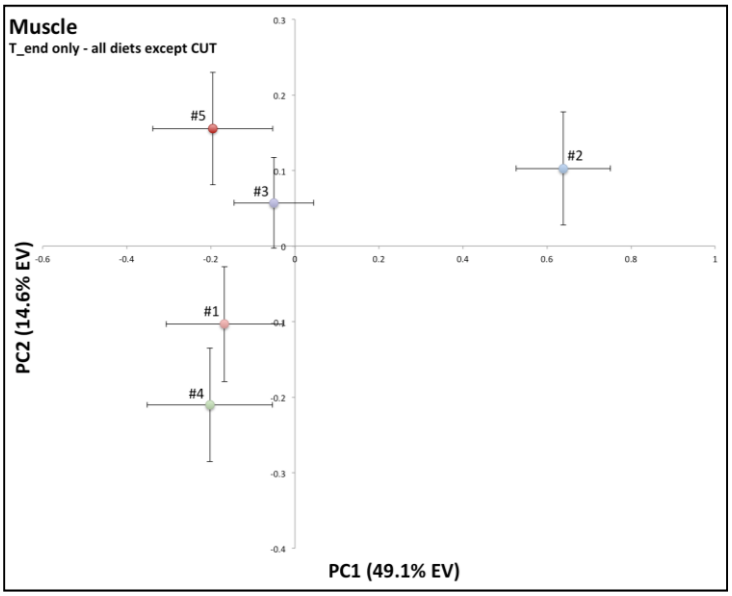

Plasma Endpoint

The plasma samples do not display the same differences in the metabolic profiles observed in the other two tissues, liver and muscle. Differences between the natural diet (CUT, reference) and the experimental diets (diet #1-5) are clearly less pronounced (Figure 31). In our calculated model the total explained variance in PC1 and PC2 is 56.9%. There is not a significant difference between the natural diet and diet #5, and diet #3 is significantly different from the other diets, but diets #2 and 4 are not significantly different along PC1. Once again, our results indicate that plasma does not reflect the variations observed in the other tissues and therefore might not be suitable as a model for the purpose of our metabolomics feed study.

Figure 31. Plasma end point (T_end) PCA scores plots for the five experimental diets (diet #1-5) and the natural diet (reference). Error bars represent the means ± 1 SEM.

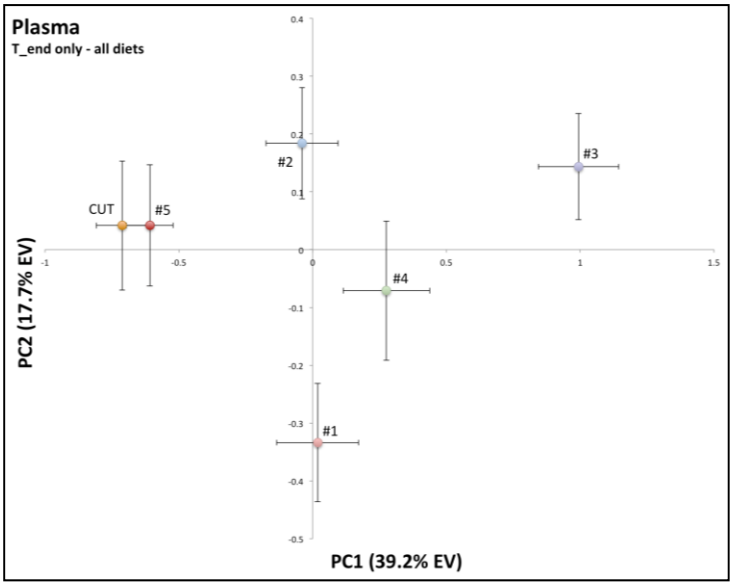

PC1 loadings analysis and metabolite identification.

Based on the results from the PCA models for the end-point differences, we proceeded with the analysis of corresponding loadings in order to correlate the observed differences in metabolic profiles among the various diets with specific metabolites. Furthermore, due to the well-defined metabolic trajectories observed for the liver samples and the similarities between liver and muscle samples, we focused subsequent analyses on the liver and muscle PCA loadings analysis.

Liver PC1 loadings analysis

The PC1 loadings plot derived from the model in Figure 27 were analyzed in an attempt to identify the specific metabolites that drive the separation along PC1 between the soy-based diets (diet #1- 5) and the natural diet. The 95th percentile was used as an arbitrary threshold to select approximately 100 NMR spectral features (signals), which represent the metabolites that significantly change in one direction or the other.

Figure 32. PC1 loadings plot (95th percentile) for the five soy-based diets (diets #1-5) and the natural diet. Loadings with a positive sign indicate metabolites that are higher in fish fed the soy-based diets and lower in the ones fed the natural diet, and vice versa.

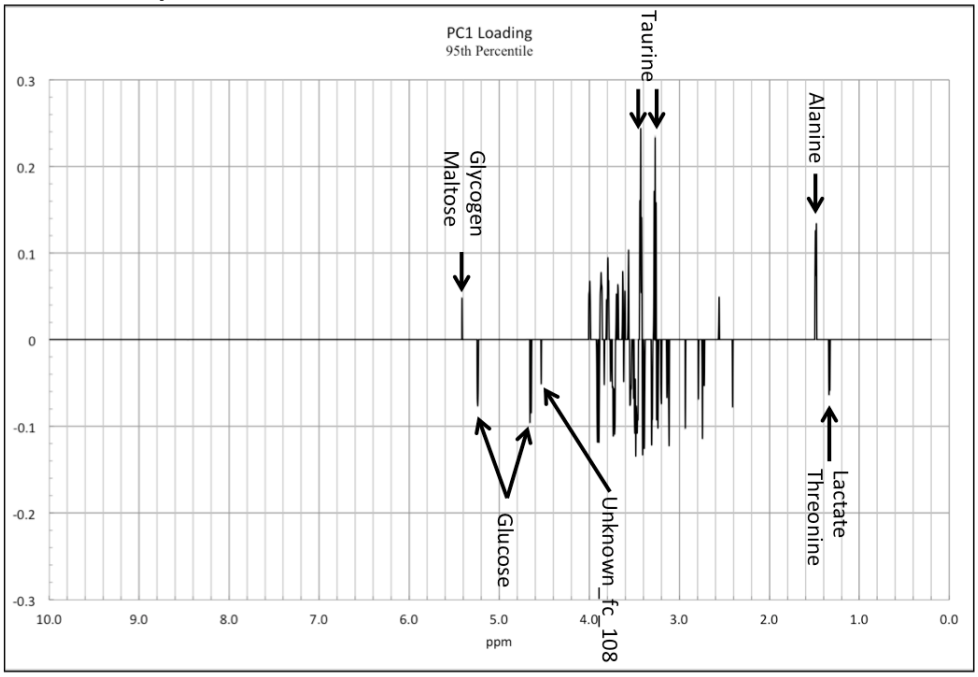

An expanded view of the loadings plot is also displayed, which focuses on the most crowded region (Figure 33).

Figure 33. PC1 loadings plot (95th percentile) expanded view of the region 2.0-4.5 ppm. Loadings with a positive sign indicate metabolites that are higher in fish fed the soy-based diets and lower in the ones fed the natural diet, and vice versa.

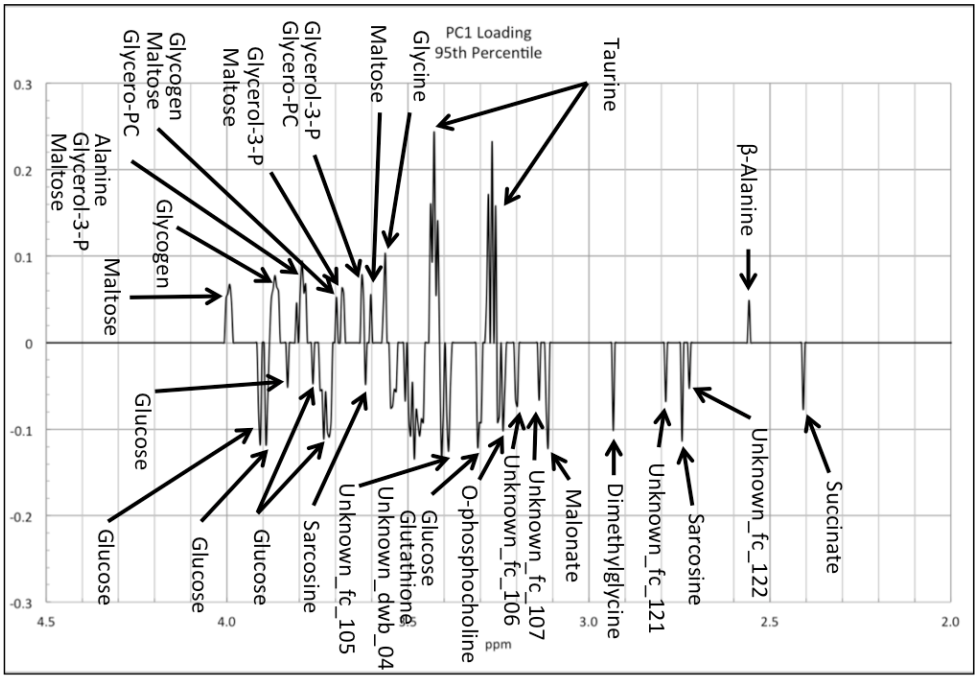

Our results show that red drum fed the soy-based experimental diets, when compared to the natural diet, generally display high levels of glycine, β-alanine, alanine, taurine, glycerophosphocholine (glycero-PC), glycerol 3-phosphate (glycerol 3-P), glycogen and maltose, whereas they show lower levels of metabolites such as dimethylglycine, sarcosine, malonate, oxidized glutathione, glucose, O-phosphocholine (phosphorylcholine), succinate, lactate, and threonine. A list of the metabolites is displayed in Table 20.

Subsequently, we removed the natural diet and generated a PC1 loadings plot from the model in Figure 34 in an attempt to identify the compounds responsible for the separation along PC1 between diet #2 and the other four experimental diets (diet #1, 3, 4 and 5) (Figure 34).

Table 20. List of metabolites identified in the PCA liver model that change significantly between the experimental diets (diets #1-5) and the natural diet (reference).

Putative Compound ID	Putative Compound Loading*
Alanine	Pos
Beta-Alanine	Pos
Dimethylglycine	Neg
Glucose	Neg
Oxidized glutathione	Neg
Glycerol 3-phosphate	Pos
Glycerophosphocholine	Pos
Glycine	Pos
Glycogen	Pos
Lactate	Neg
Malonate	Neg
Maltose	Pos
O-phosphocholine (Phosphorylcholine)	Neg
Sarcosine	Neg
Succinate	Neg
Threonine	Neg
Taurine	Pos
Unknown_dwb_04	Neg
Unknown_fc_105	Neg
Unknown_fc_106	Neg
Unknown_fc_107	Neg
Unknown_fc_108	Neg
Unknown_fc_121	Neg
Unknown_fc_122	Neg

***Relative sign of loading, to be confirmed.**

Figure 34. PC1 loadings plot (95th percentile) for the five experimental diets (diet #1-5). The natural diet was not included. Loadings with a negative sign indicate metabolites that are lower in diet #2 samples and higher for diets #1, 3, 4, and 5 and vice

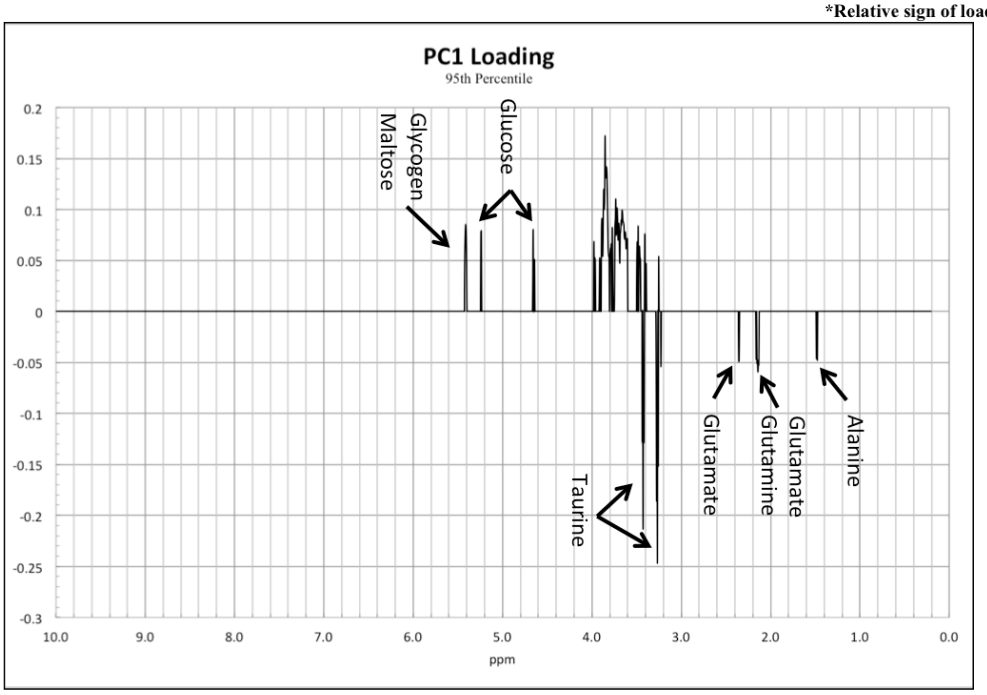

An expanded view of region 2.0-4.5 ppm of the loadings plot is also shown (Figure 35). Our results reveal that fish fed soy formulation #2 generally display higher levels of metabolites such as glucose, glycerol 3-phosphate (glycerol 3-P), glycogen, maltose and serine, whereas they

show lower concentrations of alanine, glutamate, glutamine, glutathione, O-phosphocholine and taurine. A list of the detected metabolites is also shown in Figure 35.

Figure 35. PC1 loadings plot (95th percentile), expanded view of the region 2.0-4.5 ppm. On the right a table summarizing the most significantly changing metabolites with the respective signs for the loadings.

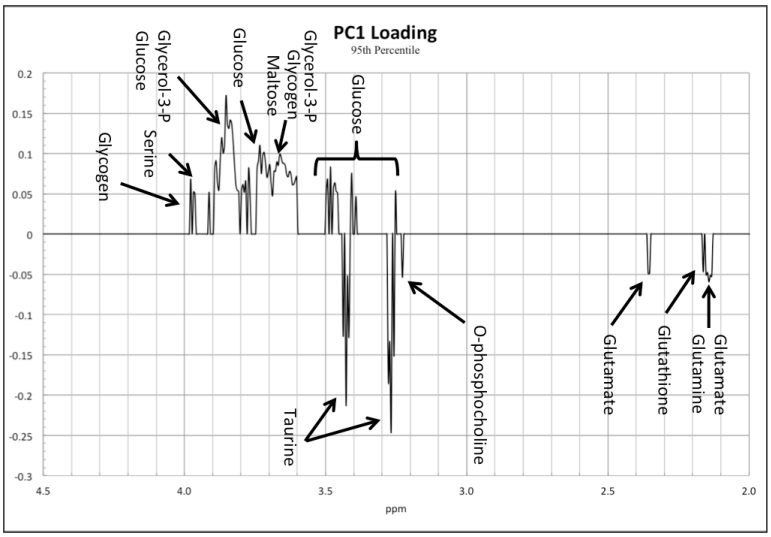

Putative Compound ID	Putative Compound Loading*
Alanine	Neg
Glucose	Pos
Glutamate	Neg
Glutamine	Neg
Glutathione	Neg
Glycerol-3-phosphate	Pos
Glycogen	Pos
Maltose	Pos
O-phosphocholine	Neg
Serine	Pos
Taurine	Neg
Unknown_dwb_33	Pos
Unknown_fc_70	Pos
Unknown_fc_79	Pos

***Relative sign of loading, to be confirmed.**

Muscle PC1 loadings analysis

The PC1 loadings plot derived from the model in Figure 30 were analyzed in an attempt to identify the specific metabolites that drive the separation along PC1 between the natural diet (CUT, reference) and the experimental soy-based diets (diet #1-5) (Figure 36).

Figure 36. PC1 loadings plot (95th percentile) for the five experimental diets (diets #1-5) and the natural diet (reference). Loadings with a positive sign indicate metabolites that are higher in fish fed the soy-based diets (#1-5) and lower in fish fed the natural diet and vice

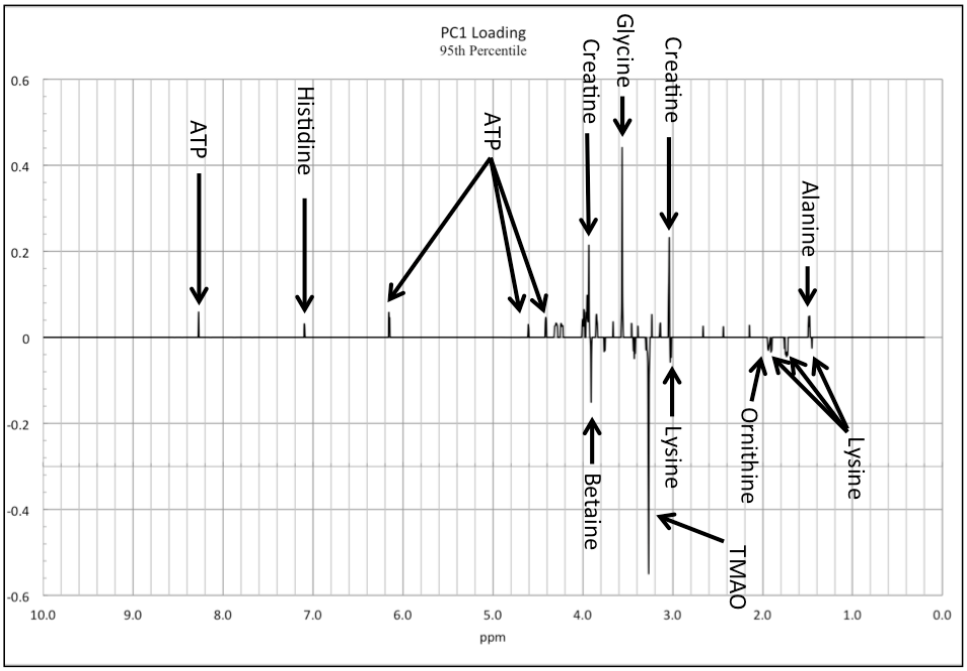

A close-up view of the loadings plot is also displayed, which focuses on the most crowded region (Figure 37).

Figure 37. PC1 loadings plot (95th percentile) for the five experimental diets (diets #1-5) and the natural diet (reference). Expanded view of the region 2.0-4.5 ppm.

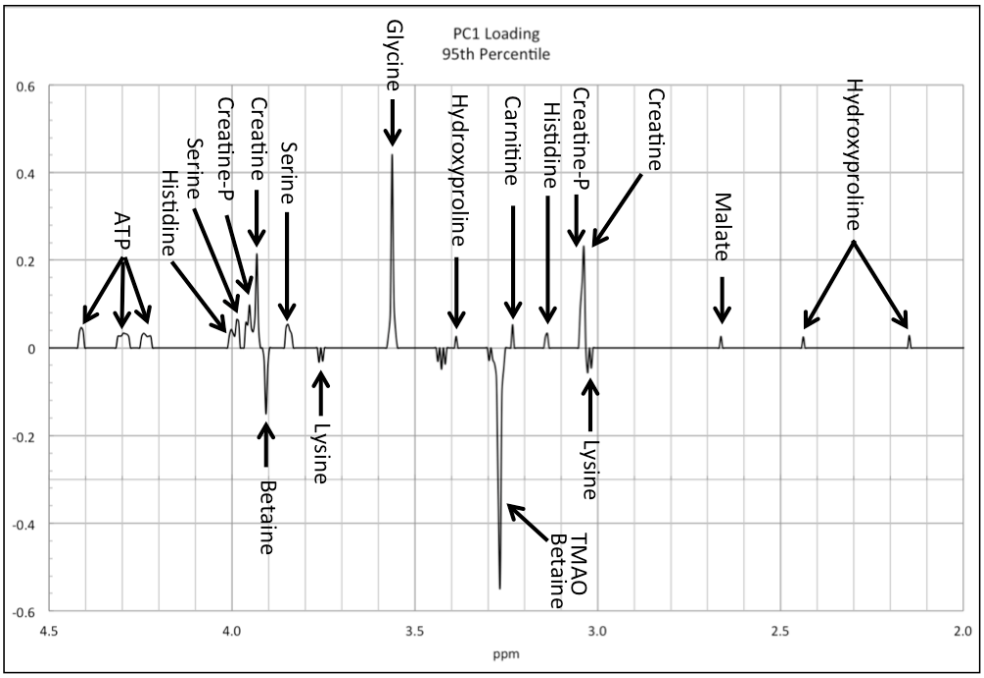

Our results show that red drum fed the soy-based experimental diets (#1-5) show higher levels of metabolites such as glycine, malate, carnitine, 4-hydroxyproline, alanine, ATP, histidine, creatine, creatine phosphate, serine and glycerophosphocholine and lower concentrations of trimethylamine-N-oxide (TMAO), lysine, ornithine and betaine. The complete list of metabolites is displayed in Table 21.

Table 21. List of metabolites identified in the PCA muscle model that change significantly between the experimental diets (diets #1-5) and the natural diet (reference).

Putative Compound ID	Putative Compound Loading*
Alanine	Pos
ATP	Pos
Betaine	Neg
Creatine	Pos
Creatine phosphate	Pos
Carnitine	Pos
Glycine	Pos
Histidine	Pos
Hydroxyproline	Pos
Lysine	Neg
Malate	Pos
Ornithine	Neg
Serine	Pos
TMAO	Neg

***Relative sign of loading, to be confirmed.**

Subsequently we removed the natural diet and generated a PC1 loadings plot from the model in 30 in an attempt to identify the metabolites responsible for the separation along PC1 between diet #2 and the other four soy-based diets (diet #1, 3, 4 and 5) (Figure 38). An expanded view of region 2.0-4.5 ppm of the loadings plot is also shown (Figure 39).

Figure 38. PC1 loadings plot (95th percentile) for the five experimental diets (diet #1-5). The natural diet was not included. Loadings with a positive sign indicate metabolites that are higher in diet #2 samples and lower for diets #1, 3, 4, and 5 and vice versa.

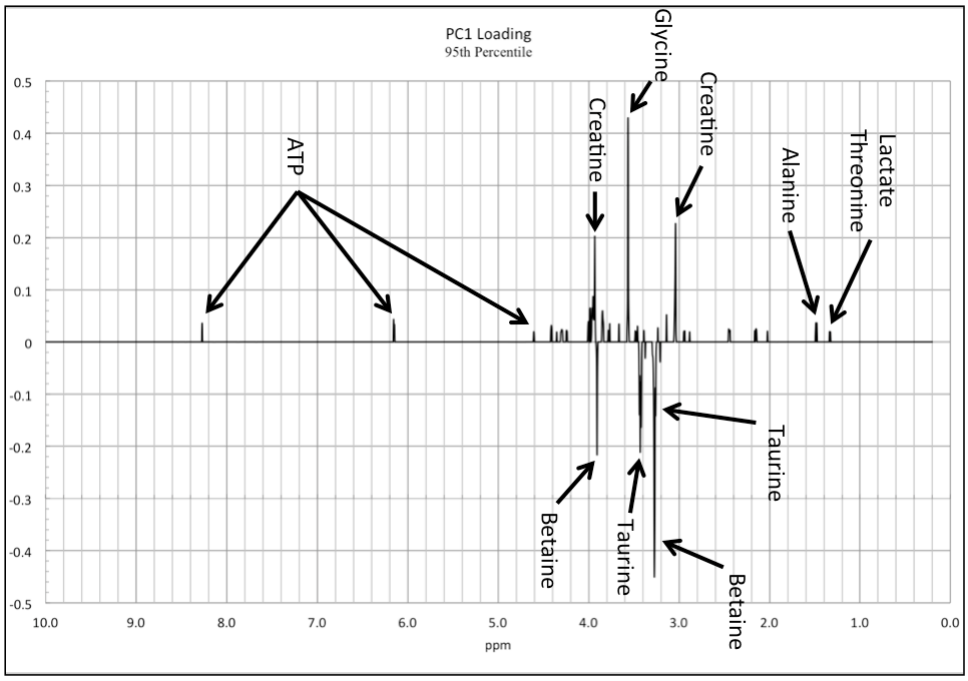

Figure 39. PC1 loadings plot (95th percentile), expanded view of the region 2.0-4.5 ppm.

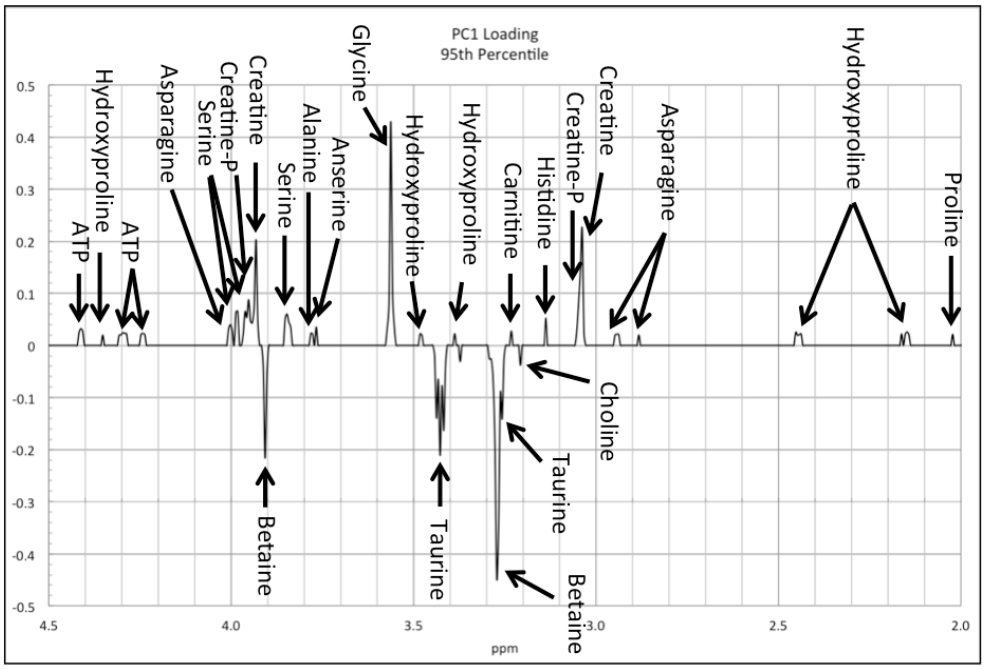

Our results reveal that red drum fed diet #2 generally show higher levels of metabolites such as glycine, ATP, 4-hydroxyproline, creatine, creatine phosphate, carnitine, anserine, serine, histidine, alanine, lactate, asparagine, proline, and threonine, whereas they show lower concentrations of betaine, taurine and choline. A list of the detected metabolites is provided in Table 22.

Table 22. List of metabolites identified in the PCA muscle model that change significantly between diet #2 and diets #1,3,4,5.

Putative Compound ID	Putative Compound Loading*
Alanine	Pos
Anserine	Pos
Asparagine	Pos
ATP	Pos
Betaine	Neg
Choline	Neg
Creatine	Pos
Creatine phosphate	Pos
Carnitine	Pos
Glycine	Pos
Histidine	Pos
Hydroxyproline	Pos
Lactate	Pos
Proline	Pos
Serine	Pos
Taurine	Neg
Threonine	Pos

***Relative sign of loading, to be confirmed.**

6.3 Gene Expression Assays

Our growth and metabolomics results from the second feeding trial indicated very few differences between the four experimental soy based feeds, with the exception of diet #2 having a significantly different metabolome in the liver and muscle than the other soy diets. We wanted to examine the gene expression of the transcript abundance of selected genes during the second trial to see if similar potential effects on lipid metabolism were evident at the gene expression level. Figures 40 and 41 show the results of these analyses from week 2 and week 12, respectively. In accordance with the growth and metabolomics results, and similar to the other gene expression assays, we do not see any emerging differences at the 2 week sampling (Figure 40). Interestingly, and confirming the results from the first trial that there appears to be an interaction between soy protein level and lipid metabolism, figure 41 shows no major differences between diets or from the initial expression levels (Conditioning diet, far left green bar for each gene) for the genes examined, with a few exceptions. During the second trial, we ran a natural diet (CUT) of fish, squid, and shrimp and by week 12 there are significant differences in expression between that diet and the others for all genes except LYZ. Again LYZ and TXN, which were not shown for the first trial, showed high inter-animal variability and diets #1 and #2 had significantly higher expression than all other diets. LYZ however is not related to lipid metabolism.

Overall, both gene selection methods, transcript abundance and metabolomic profile based, revealed potential targets for use as transcriptomic biomarkers. ChDh, DmgDh, EVLOV1, G6PI, BCAR, and L14AD all responded within several weeks of trial initiation and all had consistent patterns with increasing SBM level for each gene. In addition to this, the metabolomics findings potentially indicate an increase in gluconeogenic precursors as SBM level increases. Although more work is required to pin-point the SBM level at which these animals cross over into that non-growth optimal metabolic process, the metabolites, metabolite levels, and target gene expression levels can be used to help guide the maximum amount of SBM this species can tolerate. Since metabolic processes are fairly similar across many fish species, these same techniques can rapidly be applied to other species in aquaculture. This process can also be used to examine the effects of other ingredients like soy oil, or to better understand how physiology changes and affects growth when some fishmeal is added back to these currently fishmeal free formulations.

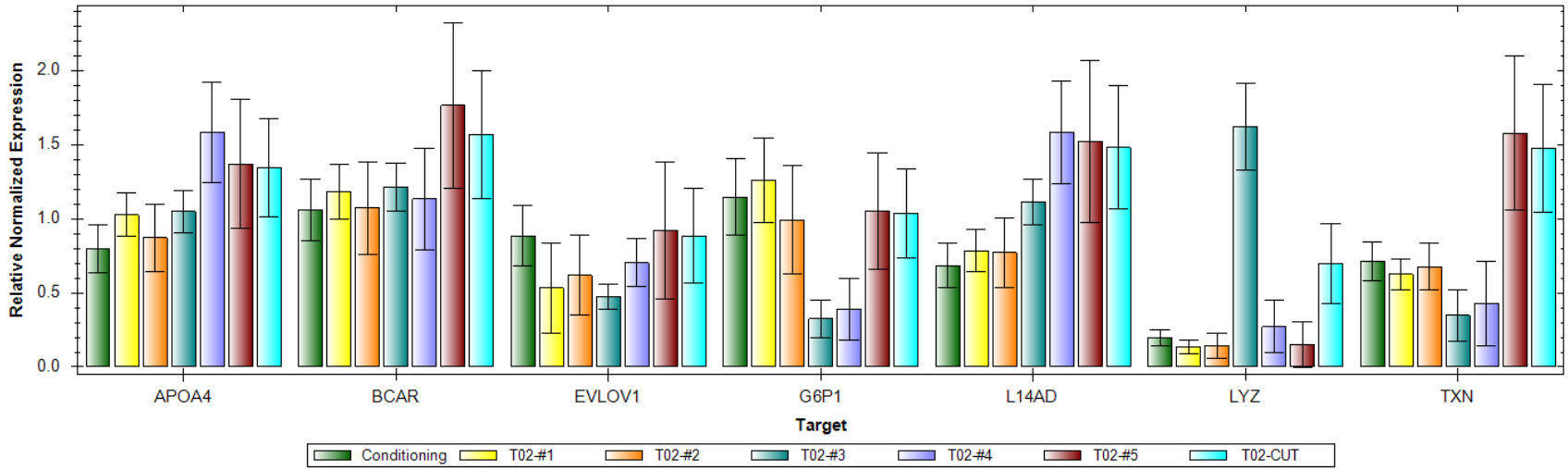

Figure 40. Gene expression of transcript abundance selected genes from week 2 of the second trial with different commercially available soy protein products at high levels (45-55%).

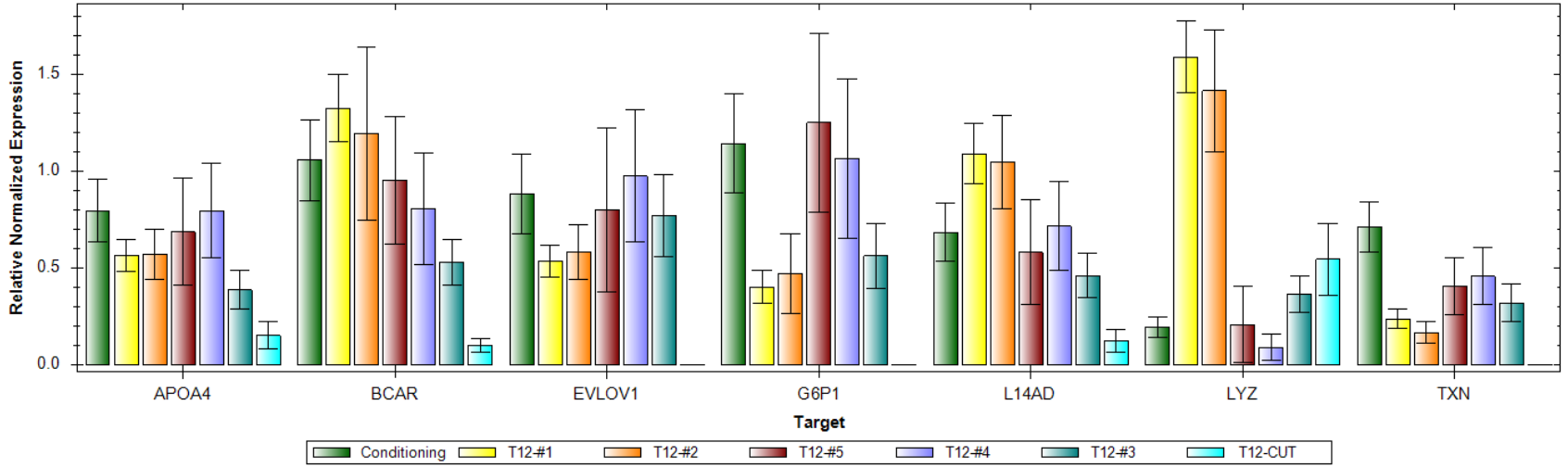

Figure 41. Gene expression of transcript abundance selected genes from week 12 of the second trial with different commercially available soy protein products at high levels (45-55%).

7.0 Discussion of trial #2 results

The second feeding trial evaluated several commercially available soy protein products as potential protein sources in feeds for juvenile red drum. Based on the high tolerance to soybean meal observed in the first trial, evidenced by histological similarities across all treatments and minimal performance differences from 0-60% SBM, we included several soy protein concentrate ingredients in separate diets at relatively high inclusion levels, 40-55 g 100^{-1} g in the diet. Although all of the experimental soy-based feeds in the second trial performed at less than 50% of the performance of their theoretical maximum (the natural diet utilized as a positive reference) in this RAS and under these experimental conditions, several encouraging results were observed. Feed conversion ratios for three of the four experimental feeds were below 2, indicating no issues with digestibility or absorption of nutrients from the feeds. The ability of the fish to retain consumed protein from the feeds, their protein efficiency ratio for the experimental feeds were all higher than that calculated for the natural diet, also an indicator that the fish were readily able to digest and utilize the available protein in the diets. The biggest factor causing the lower performance observed in the experimental high soy diets, was feed consumption. Adjusting for the wet weight of the natural feed items as compared to the dry weight of the pelleted feeds, feed consumption was just under 50% for the experimental feeds, similar to the other performance metrics. This indicates that the biggest concern and area for improvement with these high soy-based feeds is palatability.

Unlike the first feeding trial, the evaluation of diets containing commercial sources of soy proteins did result in a noteworthy difference in fillet composition. The Nutrivance diet resulted in a significantly higher fillet protein level than the other feeds, however this also resulted in a lower lipid level in these fillets. Although no explanation for this is immediately apparent, the metabolomics results may help in explaining this difference. There was also a significant difference observed in the hepatosomatic index resulting from the experimental diets with the Pro-Fine treatment being higher than three of the other pelleted feeds (60% SBM, Nutrivance and Nutraferma), however all HSI's were relatively low (~1% bw), typically an indicator of healthy, but not atrophied livers.

Collectively, our data indicate that among the three types of tissues analyzed, liver, muscle and plasma, the liver samples from fish fed the five soy-based experimental diets and the natural diet display strong time-dependent metabolic trajectories followed by muscle tissue. In the case of the plasma, larger variability for each diet/time point was observed that does not allow for the detection of any significant trends.

Interestingly, based on the liver trajectories, while fish fed the natural diet undergo rapid metabolic changes, which are already detectable at week 2 of the 12-week trial, a longer period of time of 3-4 weeks is required for the fish fed soy-based diets to be able to detect significant differences. Additionally, for all soy-based diets a metabolic equilibrium is reached around week 9 and remains stable until week 12, therefore suggesting that short-term feed studies on fish fed soy-based diets should not be shorter than 9 to 12 weeks of growth.

PCA analysis of the three tissues at the endpoints (combined T9, T10, T11 and T12) shows that there is a significant difference between the natural diet (reference), which reproduces the fish natural diet and the five formulations of soy-containing experimental diets. Furthermore, both in

the liver and in the muscle tissue, metabolic differences have been identified that allow distinguishing diet #2 from the other soy-based diets. Based on the loadings plots, a number of metabolites have been identified that are responsible for this metabolic difference. Compounds such as glycerophosphocholine and glycerol 3-phosphate constitute intermediates of glycerophospholipid metabolism. These metabolites have been detected at higher levels in liver samples from red drum fed the experimental soy-based diets compared with the natural diet, thus suggesting that lipid catabolism is upregulated in these fish. A number of free amino acids (e.g. alanine, glycine, serine and histidine) are present at higher concentrations in muscle samples of fish fed the soy-based formulations compared with the reference diet, therefore indicating that protein catabolism is also upregulated in the same groups of fish. These catabolic pathways are important because they provide intermediates of gluconeogenesis, ultimately leading to increased ATP production. These differences are even more pronounced in the case of diet #2. Overall, our results indicate that among the metabolic pathways impacted by the different dietary regimes are pathways related to energy metabolism and gluconeogenesis suggesting that red drum fish fed any of the soy-based experimental diets are in a sub-optimal metabolic state compared with fish fed on the reference diet, thus suggesting that improvements are still required in the development of soy-based formulations as alternative feeds to fishmeal. Additionally, our results indicate that plasma does not reflect the changes observed in the other tissues and differences among the experimental diets and the reference diet are less pronounced, thus leading us to conclude that this biofluid might not be a suitable model for the purpose of this metabolomics feed study.

Red drum appear to be highly tolerant to SBM inclusion, performing equivalently to a commercial diet from 0-60% inclusion levels in the first trial. The formulations for this study were also 100% fishmeal free, in itself a major step forward for increasing the sustainability and viability of aquaculture. The only drawback to the study appears to be lower than optimal feed consumption and subsequent growth rates in the second trial evaluating practical formulations containing commercially available soy protein ingredients. Although feed consumption and growth were low, feed conversion ratios were acceptable to good, indicating that more success may be observed simply by improving the palatability of feeds that contain such high levels of plant ingredients.

Both the metabolomics and gene expression assay work identified candidate biomarkers for soy exposure, and further work with these datasets and tools that have been developed will assist in identifying the maximum amount of soy red drum can tolerate and will assist in identifying specific metabolites and dietary components that can be supplemented to prevent red drum from entering into the non-growth optimal gluconeogenic processes observed here at very high soy inclusion levels.

8.0 References Cited

Chikwati, E.M., Sahlmann, C., Holm, H., Penn, M.H., Krogdahl, Å., Bakke, a. M., 2013. Alterations in digestive enzyme activities during the development of diet-induced enteritis in Atlantic salmon, Salmo salar L. Aquaculture 402-403, 28–37.

Core, T.R., 2013. R: A language and environment for statistical computing.

Duarte, I.F., Diaz, S.O., Gil, A.M., 2013. NMR metabolomics of human blood and urine in disease research. J. Pharm. Biomed. Anal. 1–10.

Knolhoff, A.M., Nautiyal, K.M., Nemes, P., Kalachikov, S., Morozova, I., Silver, R., Sweedler, J. V, 2013. Combining small-volume metabolomic and transcriptomic approaches for assessing brain chemistry. Anal. Chem. 85, 3136–43.

Lilleeng, E., Frøystad, M.K., Vekterud, K., Valen, E.C., Krogdahl, Å., 2007. Comparison of intestinal gene expression in Atlantic cod (Gadus morhua) fed standard fish meal or soybean meal by means of suppression subtractive hybridization and real-time PCR. Aquaculture 267, 269–283.

Luo, Y., Ai, Q., Mai, K., Zhang, W., Xu, W., Zhang, Y., 2012. Effects of dietary rapeseed meal on growth performance, digestion and protein metabolism in relation to gene expression of juvenile cobia (Rachycentron canadum). Aquaculture 368-369, 109–116.

Martinez, I., Bathen, T., Standal, I.B., Halvorsen, J., Aursand, M., Gribbestad, I.S., Axelson, D.E., 2005. Bioactive compounds in cod (*Gadus morhua*) products and suitability of 1H NMR metabolite profiling for classification of the products using multivariate data analyses. J. Agric. Food Chem. 53, 6889–95.

Sahlmann, C., Sutherland, B.J.G., Kortner, T.M., Koop, B.F., Krogdahl, A., Bakke, A.M., 2013. Early response of gene expression in the distal intestine of Atlantic salmon (Salmo salar L.) during the development of soybean meal induced enteritis. Fish Shellfish Immunol. 34, 599–609.

Samuelsson, L.M., Björlenius, B., Förlin, L., Larsson, D.G.J., 2011. Reproducible (1)H NMR-based metabolomic responses in fish exposed to different sewage effluents in two separate studies. Environ. Sci. Technol. 45, 1703–10.

Samuelsson, L.M., Larsson, D.G.J., 2008. Contributions from metabolomics to fish research. Mol. Biosyst. 4, 974–979.

Schock, T.B., Duke, J., Goodson, A., Weldon, D., Brunson, J., Leffler, J.W., Bearden, D.W., 2013. Evaluation of Pacific white shrimp (Litopenaeus vannamei) health during a superintensive aquaculture growout using NMR-based metabolomics. PLoS One 8, e59521.

Schock, T.B., Newton, S., Brenkert, K., Leffler, J., Bearden, D.W., 2012. An NMR-based metabolomic assessment of cultured cobia health in response to dietary manipulation. Food Chem. 133, 90–101.

Solanky, K.S., Burton, I.W., MacKinnon, S.L., Walter, J. a, Dacanay, A., 2005. Metabolic changes in Atlantic salmon exposed to Aeromonas salmonicida detected by 1H-nuclear magnetic resonance spectroscopy of plasma. Dis. Aquat. Organ. 65, 107–14.

Sumner LW, Amberg A, Barrett D, Beale MH, Beger R, Daykin CA, et al. Proposed minimum reporting standards for chemical analysis. Metabolomics. 2007;3(3):211-21. doi: 10.1007/s11306-007-0082-2.

Teets, N.M., Peyton, J.T., Ragland, G.J., Colinet, H., Renault, D., Hahn, D. a, Denlinger, D.L., 2012. Combined transcriptomic and metabolomic approach uncovers molecular mechanisms of cold tolerance in a temperate flesh fly. Physiol. Genomics 44, 764–77.

Urán, P.A., Gonçalves, A.A., Taverne-Thiele, J.J., Schrama, J.W., Verreth, J.A.J., Rombout, J.H.W.M., 2008. Soybean meal induces intestinal inflammation in common carp (Cyprinus carpio L.). Fish Shellfish Immunol. 25, 751–760.

Venold, F.F., Penn, M.H., Thorsen, J., Gu, J., Kortner, T.M., Krogdahl, A., Bakke, A.M., 2013. Intestinal fatty acid binding protein (fabp2) in Atlantic salmon (Salmo salar): Localization and alteration of expression during development of diet induced enteritis. Comp. Biochem. Physiol. A. Mol. Integr. Physiol. 164, 229–40.

Wacyk, J., Powell, M., Rodnick, K., Overturf, K., Hill, R. a., Hardy, R., 2012. Dietary protein source significantly alters growth performance, plasma variables and hepatic gene expression in rainbow trout (Oncorhynchus mykiss) fed amino acid balanced diets. Aquaculture 356-357, 223–234.

WHO, 2013. Real-time RT-PCR Protocol for the Detection of Avian Influenza A (H7N9) Virus.